(12) INTERNATIONAL APPLICATION PUBLISHED UNDER THE PATENT COOPERATION TREATY (PCT)

(19) World Intellectual Property Organization
International Bureau

(43) International Publication Date
25 March 2021 (25.03.2021)

WIPO | PCT

(10) International Publication Number
WO 2021/051256 A1

(51) International Patent Classification:
C12N 5/071 (2010.01) *A61K 35/39* (2015.01)
C12N 5/07 (2010.01) *A61K 9/50* (2006.01)

(21) International Application Number:
PCT/CN2019/106093

(22) International Filing Date:
17 September 2019 (17.09.2019)

(25) Filing Language: English

(26) Publication Language: English

(71) Applicant: **CENTER FOR EXCELLENCE IN MOLECULAR CELL SCIENCE, CHINESE ACADEMY OF SCIENCES** [CN/CN]; Building 35, 320 Yueyang Road, Xuhui District, Shanghai 200031 (CN).

(72) Inventors: **ZENG, Yi**; 319 Yue Yang Road, Shanghai 200031 (CN). **WANG, Daisong**; 319 Yue Yang Road, Shanghai 200031 (CN).

(74) Agent: **SHANGHAI PATENT & TRADEMARK LAW OFFICE, LLC**; 435 Guiping Road, Shanghai 200233 (CN).

(81) Designated States *(unless otherwise indicated, for every kind of national protection available)*: AE, AG, AL, AM, AO, AT, AU, AZ, BA, BB, BG, BH, BN, BR, BW, BY, BZ, CA, CH, CL, CN, CO, CR, CU, CZ, DE, DJ, DK, DM, DO, DZ, EC, EE, EG, ES, FI, GB, GD, GE, GH, GM, GT, HN, HR, HU, ID, IL, IN, IR, IS, JO, JP, KE, KG, KH, KN, KP, KR, KW, KZ, LA, LC, LK, LR, LS, LU, LY, MA, MD, ME, MG, MK, MN, MW, MX, MY, MZ, NA, NG, NI, NO, NZ, OM, PA, PE, PG, PH, PL, PT, QA, RO, RS, RU, RW, SA, SC, SD, SE, SG, SK, SL, SM, ST, SV, SY, TH, TJ, TM, TN, TR, TT, TZ, UA, UG, US, UZ, VC, VN, ZA, ZM, ZW.

(84) Designated States *(unless otherwise indicated, for every kind of regional protection available)*: ARIPO (BW, GH, GM, KE, LR, LS, MW, MZ, NA, RW, SD, SL, ST, SZ, TZ, UG, ZM, ZW), Eurasian (AM, AZ, BY, KG, KZ, RU, TJ, TM), European (AL, AT, BE, BG, CH, CY, CZ, DE, DK, EE, ES, FI, FR, GB, GR, HR, HU, IE, IS, IT, LT, LU, LV, MC, MK, MT, NL, NO, PL, PT, RO, RS, SE, SI, SK, SM, TR), OAPI (BF, BJ, CF, CG, CI, CM, GA, GN, GQ, GW, KM, ML, MR, NE, SN, TD, TG).

Published:
— *with international search report (Art. 21(3))*
— *with sequence listing part of description (Rule 5.2(a))*

WO 2021/051256 A1

(54) Title: PANCREATIC PRO-ENDOCRINE PROGENITOR CELLS AND USE THEREOF

(57) Abstract: Provided herein are pro-endocrine progenitor cells and organoids derived from adult islets in vitro, as well as methods for making and using the same. The compositions are useful for treating or preventing diabetes, other diseases or disorders characterized by impaired islet function, and symptoms thereof.

PANCREATIC PRO-ENDOCRINE PROGENITOR CELLS AND USE THEREOF

BACKGROUND

The pancreas consists of three main cellular components: endocrine islets, exocrine acini, and ducts. Pancreatic β-cells of the islets of Langerhans are the only cells that produce insulin in humans as well as in almost all other vertebrates. In the mouse, the islet is organized into spherical structures in which β-cells form a core surrounded by a mantle of α-, δ- and pancreatic polypeptide (PP)-cells. These cells produce insulin, glucagon, somatostatin and pancreatic polypeptide (PP; Ppy) respectively (Pan and Wright, 2011). β-cells have a limited capacity for regeneration, a predisposing factor for the development of diabetes (Hardikar, 2016).

Cell therapy is considered as a potential therapeutic alternative to traditional treatments of diabetes. Islet- and whole pancreas transplantations can restore glucose homeostasis by replenishing β cells (Lysy et al., 2013). Limitations in availability of donors have led to a search for strategies for generating β-cells in vitro. Besides the use of embryonic stem cell (ES)/ induced pluripotent stem cell (iPSCs)-based technologies for the generation of transplantable β-cells (Cheng et al., 2012; Pagliuca et al., 2014; Rezania et al., 2014; Sneddon et al., 2012), organoids directly derived from the tissue of interest have been investigated. However, it has so far proven difficult to produce new β-cells in culture from embryonic or adult pancreas, while the closely related enteroendocrine cells of the gut are readily generated in such organoids (Gehart et al., 2019).

Mouse embryonic pancreas progenitors, cultured in three-dimensional (3D), reflect exocrine and endocrine cell differentiation in vitro, yet does not support long-term expansion of pancreas cells (Greggio et al., 2013; Sugiyama et al., 2013). Tissue culture strategies using adult duct (Bonner-Weir et al., 2000; Gao et al., 2005; Huch et al., 2013; Jin et al., 2013; Ramiya et al., 2000; Rovira et al., 2010; Yatoh et al., 2007), acinar (Minami et al., 2005), and insulin^{low} (Seaberg et al., 2004; Smukler et al., 2011) cells have only been marginally effective for expanding and differentiating putative progenitor cells into β-like cells.

Thus, a need exists for methods and compositions for in vitro production and long-term expansion of β-cells.

SUMMARY

In one aspect, provided herein is a method of obtaining pro-endocrine progenitor cells, comprising: contacting, *in vitro*, adult islet cells with an anti-Procr antibody or antigen-binding fragment thereof; and isolating a Procr^{+} pro-endocrine progenitor cell that binds to the anti-Procr antibody or fragment thereof, preferably using fluorescence assisted cell sorting (FACS).

Also provided herein is a method of producing a pancreatic organoid *in vitro*, comprising: providing a pro-endocrine progenitor cell isolated from adult islet cells; and 3D culturing *in vitro* the pro-endocrine progenitor cell in an organoid medium under conditions suitable to produce a pancreatic organoid comprising functional β-cells and/or β-like cells, wherein preferably the organoid medium further comprises a three-dimensional matrix such as Matrigel™. In some embodiments, the pro-endocrine progenitor cell expresses Procr.

In some embodiments, the adult islet cells are from human. In one embodiment, the organoid medium comprises DMEM/F12 supplemented with one or more of: 1-5% (e.g., 2%) B27, 0.1-5% (e.g., 1%) ITS, 10-200 (e.g., 50) ng ml^{-1} EGF, 0.1-5 (e.g., 2) μg ml^{-1} heparin, 1-50 (e.g., 10) ng ml^{-1} FGF2, 1-10 (e.g., 3) μM Wnt agonist such as CHIR99021, 1-100 (e.g., 30) ng/ml Wnt surrogate such as NGS, 1-10 (e.g., 2) μM TGF-beta pathway inhibitors such as SB431542 or A83-01A83-01, 10-500 (e.g., 100) ng ml^{-1} Bmp inhibitor such as Noggin, 1-50 (e.g., 10) μM Rock inhibitor such as Y27632.

In some embodiments, the adult islet cells are from mouse. In some embodiments, the 3D culturing comprises co-culturing with a plurality of endothelial cells, and wherein the pro-endocrine progenitor cell expresses one or more of, preferably all of, Procr, Rspo1, Fgf1, Upk3B, and Hoxa5. In one embodiment, the culture medium comprises DMEM/F12 supplemented with one or more of: 1-5% (e.g., 2%) B27, 0.1-5% (e.g., 1%) ITS, 10-200 (e.g., 50) ng ml^{-1} EGF, 0.1-5 (e.g., 2) μg ml^{-1} heparin, 1-50 (e.g., 10) ng ml^{-1} FGF2, and 1-20 (e.g., 5) ng ml^{-1} VEGFa.

In some embodiments, the co-culturing step comprises culturing until the pro-endocrine progenitor cell forms a colony of about 100-200 μm in diameter, and continuously culturing the colony to form the mouse pancreatic organoid of about 150-500 μm in diameter.

Another aspect relates to a method of obtaining pancreatic organoids *in vitro*, comprising: (a) enriching endocrine cells from adult pancreas, preferably by one or more of the following methods: (1) staining dissociated adult pancreas cells with TSQ (6 - methoxy - 8 - *p* - toluenesulfonamido - quilone), followed by FACS; (2) contacting, *in vitro*, dissociated adult mouse islet cells with an anti-Procr antibody or antigen-binding fragment thereof, followed by FACS; and (3) hand-picking and dissociating islets from adult pancreas; and (b) 3D culturing the enriched endocrine cells in an organoid medium under conditions suitable to produce a pancreatic organoid comprising functional β-cells and/or β-like cells, wherein preferably the organoid medium further comprises a three-dimensional matrix.

In some embodiments, the organoid medium comprises Matrigel™ and DMEM/F12 supplemented with one or more of: 1-5% (e.g., 2%) B27, 0.1-5% (e.g., 1%) ITS, 10-200 (e.g., 50) ng ml^{-1} EGF, 0.1-5 (e.g., 2) μg ml^{-1} heparin, 1-50 (e.g., 10) ng ml^{-1} FGF2, 1-10 (e.g., 3) μM Wnt agonist such as CHIR99021, 1-100 (e.g., 30) ng/ml Wnt surrogate such as NGS, 1-10 (e.g., 2)

μM TGF-beta pathway inhibitors such as SB431542 or A83-01A83-01, 10-500 (e.g., 100) ng ml^{-1} Bmp inhibitor such as Noggin, 1-50 (e.g., 10) μM Rock inhibitor such as Y27632.

In some embodiments, the pancreatic organoid is about 50-500 or about 100-300 μm in diameter.

In some embodiments, the method can further include expanding the organoid through passaging for at least 10 times, at least 20 times, or at least 30 times. In some embodiments, the method can further include culturing the expanded organoids for about 1-4 weeks to generate mature organoids. In some embodiments, the mature organoid senses glucose and produces and secretes insulin in response to glucose.

A further aspect relates to a composition comprising a plurality of pro-endocrine progenitor cells isolated from adult islet cells, a culture medium and optionally a plurality of endothelial cells. In some embodiments, the pro-endocrine progenitor cells express Procr. In some embodiments, when the adult islet cells are derived from mouse, the pro-endocrine progenitor cells express one or more of Procr, Rspo1, Fgf1, Upk3B, and Hoxa5. In some embodiments, the culture medium further comprises a three-dimensional matrix, preferably Matrigel™. In some embodiments, the adult islet cells are from mouse and wherein the culture medium comprises DMEM/F12 supplemented with one or more of: 1-5% (e.g., 2%) B27, 0.1-5% (e.g., 1%) ITS, 10-200 (e.g., 50) ng ml^{-1} EGF, 0.1-5 (e.g., 2) μg ml^{-1} heparin, 1-50 (e.g., 10) ng ml^{-1} FGF2, and 1-20 (e.g., 5) ng ml^{-1} VEGFa. In some embodiments, the adult islet cells are from human and wherein the culture medium comprises DMEM/F12 supplemented with one or more of: 1-5% (e.g., 2%) B27, 0.1-5% (e.g., 1%) ITS, 10-200 (e.g., 50) ng ml^{-1} EGF, 0.1-5 (e.g., 2) μg ml^{-1} heparin, 1-50 (e.g., 10) ng ml^{-1} FGF2, 1-10 (e.g., 3) μM Wnt agonist such as CHIR99021, 1-100 (e.g., 30) ng/ml Wnt surrogate such as NGS, 1-10 (e.g., 2) μM TGF-beta pathway inhibitors such as SB431542 or A83-01A83-01, 10-500 (e.g., 100) ng ml^{-1} Bmp inhibitor such as Noggin, 1-50 (e.g., 10) μM Rock inhibitor such as Y27632.

Another aspect relates to a pancreatic organoid comprising functional β-cells and/or β-like cells differentiated in vitro from pro-endocrine progenitor cells, wherein the pro-endocrine progenitor cells are isolated from adult islet cells. In some embodiments, the organoid senses glucose and produces and secretes insulin in response to glucose. In some embodiments, the organoid is about 50-500 or about 100-300 μm in diameter.

A further aspect relates to the culture media disclosed herein, for in vitro expansion and/or differentiation of pro-endocrine progenitor cells and pancreatic organoids.

Use of the organoid disclosed herein is also provided, for treating or preventing diabetes, or for screening in vitro an agent for treating or preventing diabetes.

BRIEF DESCRIPTION OF THE DRAWINGS

FIGs. 1A-1M illustrate single cell RNAseq analysis reveals a novel pancreatic cell population with EMT properties. FIG. 1A includes graphs depicting distributions of the number of unique molecular identifiers (UMIs) per cell (left) and the number of genes detected per cell (right) are shown for pancreatic single cell (sc) RNAseq data. FIG. 1B includes dot-plots illustrating the reproducibility between three biological replicates. Average gene expression values (Log2(TPM+1)) across all cells of three sc RNAseq experiments are used for the calculation (r = Pearson correlation coefficient). FIG. 1C includes t-SNE plots of three independent sc RNAseq experiments. Cell counts of each experiment and indicated cell type are labeled in brackets. Throughout the figures, unless indicated otherwise, "Mesen" denotes mesenchymal; "Endo." denotes endothelial. "New pop" denotes new population. FIG. 1D is a series of t-SNE plots of marker genes expression for endocrine or exocrine cells. For FIGs. 1D, 1E, and 1I, post hoc cluster interpretation was based on the expression of known cell type markers; and the different clusters represent the same cell types as shown in FIG. 1C. FIG. 1E is a series of t-SNE plots of marker genes expression for cell lineages other than endocrine and exocrine. FIG. 1F is a t-SNE plot of 7,160 pancreatic single cell (sc) RNAseq profiles (points) and annotated post hoc. The new population (new pop.) is. Cell counts of indicated cell types are in parentheses. Cells are pooled together from three biological replicates. FIG. 1G is a series of tSNE plots and accompanying Vlin plots illustrating gene expression for different pancreatic cell types. The different clusters represent the same cell types as shown in FIG. 1F. FIG. 1H is a series of tSNE plots and accompanying Vlin plots illustrating gene expression for different pancreatic cell types. The different clusters represent the same cell types as shown in FIG. 1F. FIG. 1I includes t-SNE plots of marker genes expression for the new population of cells. FIG. 1J is a heat map of cell type-enriched genes. Each column represents a single cell and each row represents one signature gene. The shading ranging from dark shading to brighter shading, which indicate low to high relative gene expression levels, respectively. FIG. 1K is a dot plot for signature genes of each cluster. The shadings denote average expression levels and the sizes of dots denote fractional expression. FIG. 1L is graph of selected gene ontology (GO) terms of upregulated genes (1536 genes are selected with p value $< 5x10^{-3}$) in the new population. FIG. 1M includes tSNE plots and Vlin plots illustrating expression levels of epithelial and mesenchymal markers are projected onto t-SNE plots. The Vlin plot under the t-SNE plot shows the expression level (Log2(TPM+1)) of the indicated gene in each cell type. The new population (circled) express both epithelial and mesenchymal markers, indicating the EMT properties.

FIGs. 2A-2I illustrate that the new population in adult islets aligns with a subpopulation

of embryonic endocrine cells. FIG. 2A is a tSNE plot showing two different single cell RNAseq datasets containing E14.5 Ngn3- expressing endocrine precursors integrated with the presently disclosed adult single cell RNAseq dataset and annotated post hoc. Both the aligned (left) and split (right) view are shown. Cell counts of each dataset and the new population (new pop.) are in parentheses. FIG. 2B includes tSNE plots that show expression levels of pancreatic endocrine and exocrine marker genes for each indicated cell type. The color bar and Log2(TPM+1) value for each indicated gene are shown. FIG. 2C includes t-SNE plots of expression levels of epithelial and mesenchymal markers for E14.5 Ngn3-expressing endocrine precursors. The color bar and Log2(TPM+1) value for each indicated gene are shown. Similar to the adult new population, the new sub-cluster (circled) of E14.5 Ngn3-expressing endocrine precursors express both epithelial and mesenchymal markers, indicating the EMT properties. FIG. 2D includes t-SNE plots showing expression levels of Ngn3. FIG. 2E includes t-SNE plots showing Rspo1 and Procr expression in the new population. The color bar and Log2(TPM+1) value for each indicated gene are shown. E14.5 $Ngn3^+$ new pop. cells (circled) express Rspo1 and Procr at the similar levels as adult new pop. cells, while adult new pop. cells lose their Ngn3 expression. FIG. 2F is a dot plot showing the expression signatures of the new population across three datasets. FIG. 2G includes t-SNE plots that show expression levels of marker genes in the new population. Three datasets are shown separately for comparison. The color bar and Log2(TPM+1) value for each indicated gene are shown. Within each dataset, cells are separated as new pop and others. The shadings denote average expression levels and the sizes of dots denote fractional expression. FIG. 2H includes graphs showing the developmental trajectory of the adult new population of cells and alpha, beta, delta, and PP cells (4,986 cells used) produced by Monocle2. The colors in left panel denote cell types. The cell counts for the indicated cell types are labeled in brackets. Pseudotime (arbitrary units) is depicted from dark to light blue (right panel). FIG. 2I is a gene branched Heat map depicting the expression of genes along each branch in pseudotime. An independent expression pattern is calculated across the entire pseudotime trajectory for each branch. Therefore, the portion of the trajectory before the branch point is displayed for each branch separately. Genes are clustered based on expression pattern across pseudotime, selected genes with differential expression along the branches are labeled on the right.

FIGs. 3A-3L characterize the isolated new islet population using the Procr surface marker. FIG. 3A includes graphs depicting the FACS analysis gating strategy for unstained control islet Procr-expressing cells. Doublets were excluded based on forward scatter and trigger pulse width. Lin^+ cells are excluded by CD31, CD45, and Ter119 antibodies staining. $Procr^+$ cells are analyzed in the $EpCAM^+$ islet epithelial cells. FIG. 3B includes graphs depicting the

FACS analysis gating strategy for antibody stained samples of islet Procr-expressing cells. Doublets were excluded based on forward scatter and trigger pulse width. Lin^+ cells are excluded by CD31, CD45, and Ter119 antibodies staining. $Procr^+$ cells are analyzed in the $EpCAM^+$ islet epithelial cells. For FIGs. 3A and 3B, one of three similar biological replicates is shown. FIG. 3C include graphs summarizing the FACS analysis of Procr-expressing cells in hand-picked mouse islets. The Lin^+ and non-epithelial cells are gated out based on Lin (including CD31, CD45, and Ter119) and EpCAM antibodies staining. Within the Lin^- $EpCAM^+$ islet epithelial compartment $1.02 \pm 0.14\%$ cells are $Procr^+$. Data are pooled from five biological replicates and presented as mean ± s.e.m. FIG. 3D includes graphs that show the expression levels of new population signature genes in each isolated cell populations (i.e., the FACS-sorted islet or non-islet $Procr^+$ and $Procr^-$ pancreatic cells) as measured by qPCR. Islet Procr+ cells are the enriched new population with high levels of the new population markers expression. n=3 biological replicates. For each replicate, cells were isolated from four mice. Data are presented as mean ± s.e.m. FIG. 3E includes graphs of the FACS analysis of $Procr^+$ cells in Ngn3-Cre;Rosa26-tdTomato pancreatic islets. Islet epithelial cells are marked by Lin^-, $EpCAM^+$. The majority of $Procr^+$ cells are $tdTomato^+$ ($tdTom^+$). One of three similar biological replicates is shown. FIG. 3F is a diagram of a double-reporter allele of Procr with a membrane GFP (mGFP)-2A-LacZ cassette inserted after the ATG start codon of Procr. FIG. 3G is a diagram illustrating a targeting strategy to generate the ProcrmGFP-2A-LacZ knock-in double reporter mouse. Designs of southern blot probe and genotyping primers are as indicated. FIG. 3H includes images of Southern blot analysis with a 5' external probe of BamHI-digested DNA from mouse embryonic stem cells that show an 8.5 kb band in addition to the 9.9 kb WT band (left) and an image of a Southern blot analysis with a 3' external probe of SacI-digested DNA from mouse embryonic stem cells that shows a 5.6 kb band in addition to the 6.9 kb WT band (right) in clones that have undergone homologous recombination at the Procr locus. FIG. 3I is a gel image of genotyping PCR reaction products, which indicate that pups #2, 3, 5, 7 were heterozygotes. One of three similar experiments are shown. FIG. 3J includes images of whole-mount X-gal staining that shows individual LacZ-expressing ($Procr^+$) cells within ProcrmGFP-2A-LacZ islets. The wildtype negative control is shown on the right. Scale bar denotes 20 μm. A similar distribution pattern was observed using in three mice. FIG. 3K includes a graph of a FACS analysis of $Procr^+$ and $Procr^-$ cells (image) and a graph illustrating the overlap of $Procr^+$ cells and $mGFP^+$ cells, which validates the ProcrmGFP-2A-LacZ knock-in report mouse. The islet $Procr^+$ or $Procr^-$ cells were FACS sorted and validated by mGFP immunostaining. The overlapping of sorted $Procr^+$ and $mGFP^+$ cells are quantified. The ProcrmGFP-2A-LacZ knock-in mice recapitulate the Procr expression in islets. n=3 biological replicates. Data are presented

as mean ± s.e.m. Scale bar denotes 20 μm. FIG. 3L includes representative confocal images of ProcrmGFP-2A-LacZ islets whole mount immunostaining, which indicate that mGFP+ cells (Procr+ cells, allow) do not overlap with the mature β-cells (Ins^+), α-cells (Gcg^+), δ-cells (Sst^+) or PP-cells (Ppy^+). Scale bar denotes 20 μm. Similar results are confirmed by n=3 mice. FIG. 3M includes representative confocal image of pancreas section immunostaining that show that the $mGFP^+$ cell ($Procr^+$ cell, arrow) expresses both epithelial marker EpCAM and mesenchymal marker Col1a1. Scale bar denotes 20 μm. Sections are stained and analyzed from n=3 mice.

FIGs. 4A and 4B characterize pancreatic organoids at 7 days and 28 days of culture. FIG. 4A includes bright field images of freshly isolated primary islet cells cultured after 7 days. $Procr^+$ or $Procr^-$ islet cells are FACS sorted from ICR mice and cultured respectively. Only $Procr^+$ cells form colonies. Experiments were performed for n=3 biological replicates. For each replicate, cells are sorted from at least 5 mice. Scale bar denotes 50 μm. FIG. 4B is a scatterplot showing the size per islet organoid cultured for 7 or 28 days, with or without endothelial cells. Experiments were performed for 3 biological replicates. One of three similar results are shown. The average sizes are shown as mean ± s.e.m.

FIGs. 5A-5N demonstrate that islet organoids derived from single $Procr^+$ islet progenitor cells can express insulin. FIG. 5A illustrates the FACS analysis of $Procr^+$ and $Procr^-$ cells sorted (from ICR or FVB mice) and co-cultured with $CD31^+$ endothelial cells (from Actin-DsRed), respectively. FACS analysis of Procr). Bright field/fluorescence representative images are presented of freshly isolated primary islet cells cultured after 5 or 8 days. The red fluorescence indicating where $CD31^+$ endothelial cells are. Only $Procr^+$ cells form islet organoids under this culture condition. n=5 biological replicates. For each replicate, cells are sorted from at least 5 mice. Scale bar denotes 50 μm. FIG. 5B includes bright field (left) and whole mount immunofluorescence images (right) of $Procr^+$ cell-derived islet organoids cultured for 28 days. Both $Procr^+$ cells and $CD31^+$ endothelial cells are sorted from ICR mice. The endothelial cells are labeled by CD31 antibody staining in red color. n=3 biological replicates. For each replicate, cells are sorted from at least 5 mice. "Org." denotes organoid. Scale bar denotes 50 μm. FIG. 5C is a scatter plot showing the size per islet organoid cultured for 7 or 28 days. n=3 biological replicates, one of three similar results are shown. The average organoid sizes are presented as mean ± s.e.m. FIG. 5D includes representative confocal images of whole mount insulin immunostaining in fresh islets or organoids cultured for 7 or 28 days, with or without glucose challenge. Scale bar denotes 20 μm. "hi glucose" denotes high glucose. FIG. 5E is a scatterplot showing the percentage of $insulin^+$ (highly-expressed) cells per organoid under each indicated condition. n=3 biological replicates, one of three similar results is shown. The average percentages are presented as mean ± s.e.m. "d7" denotes day 7; "hi glu" denotes high

glucose. FIG. 5F includes graphs showing expression levels of beta cells marker genes under each indicated condition are detected by qPCR. n= 3 biological replicates. Data are presented as (mean + min)/max. FIG. 5G includes graphs showing representative population measurements of dynamic normalized Fluo-4 fluorescence intensity for primary day 28 islet organoids challenged sequentially with 2, 20, 2, 20, 2, and 20 mM glucose and 30 mM KCl. The x axis represents time. n=3 biological replicates are shown separately. FIG. 5H includes electron microscopy images and quantification (e) of granules within sectioned cells for each indicated culture condition. A fresh islet β-cells sample is shown. Increasing numbers of crystallized insulin granules are found in day 28 organoids after glucose challenge, indicating maturation of the β-cells. n=3 biological replicates. One of three similar quantification results is shown. Scale bar denotes 1 μm. "d7" denotes day 7; "d28" denotes day 28; "hi glu." denotes high glucose; "org." denotes organoid. FIG. 5I is a scatterplot quantifying the results observed in FIG. 5H. FIG. 5J is a graph of ELISA measurements of secreted insulin from day 28 islet organoids challenged sequentially with 2, 20, 2, 20, 2, and 20 mM glucose, with a 30-minute incubation for each condition. n= 3 biological replicates. Data are presented as mean ± s.e.m. FIG. 5K includes images of whole mount immunostaining of α-cells marker Gcg, δ-cells marker Sst or PP-cells marker Ppy expressed by cells in fresh islets. FIG. 5L is a graph quantifying the results observed in FIG. 5K. FIG. 5M includes images of whole mount immunostaining of α-cells marker Gcg, δ-cells marker Sst or PP-cells marker Ppy expressed by cells in day 28 organoids. FIG. 5N is a graph quantifying the results observed in FIG. 5M. For FIGs. 5K-5N, the existence of different types of hormone-expressing cells within organoids is validated based on n=3 biological replicates. One of three similar quantification results is shown. n=3 mice are used for the quantification of fresh islets. Scale bar denotes 20 μm. Data are presented as mean ± s.e.m

FIGs. 6A-6N illustrate that $Procr^+$ cells-derived organoids can be expanded *in vitro*. FIG. 6A includes representative images of cultured organoids from different passages. All passage experiments were performed for n=3 biological replicates. Scale bar denotes 50 μm. FIG. 6B is a graph showing the sizes of the cultured organoids from FIG. 6A. One of three similar quantification results are shown. Average sizes of organoids are shown as mean ± s.e.m. FIG. 6C is an expansion curve of islets organoids (derived from primary mouse islet Procr+ cells) followed from passage 1 to passage 20. n=3 biological replicates. Data are presented as mean ± s.e.m. FIG. 6D is an illustration of an organoid expansion/maturation model. FIG. 6E includes representative images of whole mount immunostaining of β-cells marker Ins, α-cells marker glucagon (Gcg), δ-cells marker somatostatin (Sst), and PP-cells marker pancreatic polypeptide (Ppy) in 15th passaged day 30 organoids after glucose challenge. Scale bar denotes 20 μm. FIG. 6F is a graph quantifying the whole mount immunostaining described in FIG. 6E. n=3

biological replicates. One of three similar quantification results are shown. The average percentages are shown as mean ± s.e.m. FIG. 6G includes representative images of whole mount immunostaining of β-cells marker Ins, α-cells marker glucagon (Gcg), δ-cells marker somatostatin (Sst), and PP-cells marker pancreatic polypeptide (Ppy) in 7th passaged day 30 organoids after glucose challenge. Scale bar denotes 20 μm. FIG. 6H is a graph quantifying the whole mount immunostaining described in FIG. 6G. n=3 biological replicates. One of three similar quantification results are shown. The average percentages are shown as mean ± s.e.m. FIG. 6I includes graphs showing representative population measurements of dynamic normalized Fluo-4 fluorescence intensity for 15th passaged day 30 islet organoids challenged sequentially with 2, 20, 2, 20, 2, and 20 mM glucose and 30 mM KCl. The x axis represents time. n=3 biological replicates are shown separately. FIG. 6J includes electron microscopy images of granules within sectioned cell. Crystallized insulin granules are found in 15th day 30 organoids after glucose challenge, indicating the maturation of β-cells. n=3 biological replicates. Scale bar denotes 1 μm. FIG. 6K is a graph depicting ELISA measurements of secreted insulin from 15th passaged day 30 islet organoids challenged sequentially with 2, 20, 2, 20, 2, and 20 mM glucose, with a 30-minute incubation for each concentration. n= 3 biological replicates. Data are presented as mean ± s.e.m. FIG. 6L includes electron microscopy images of granules within sectioned cell. Crystallized insulin granules are found in 7th day 30 organoids after glucose challenge. n=3 biological replicates. Scale bar denotes 1 μm. FIG. 6M is a graph depicting ELISA measurements of secreted insulin from 7th passaged day 30 islet organoids challenged sequentially with 2, 20, 2, 20, 2, and 20 mM glucose, with a 30-minute incubation for each condition. n= 3 biological replicates. Data are presented as mean ± s.e.m. FIG. 6N includes graphs depicting representative population measurements of dynamic normalized Fluo-4 fluorescence intensity for 7th passaged day 30 islet organoids challenged sequentially with 2, 20, 2, 20, 2, and 20 mM glucose and 30 mM KCl. The x axis represents time. n=3 biological replicates are shown separately.

FIGs. 7A-7N demonstrate that long-term cultured organoids restore insulin-dependent glucose homeostasis in streptozotocin (STZ)-induced T1D mice. FIG. 7A is a graph showing blood glucose levels after engrafting. The immunodeficient mice are made diabetic with streptozotocin (STZ) 7 days before engrafting. Random fed blood glucose levels are routinely checked. The blood glucose decreases to a normal level after engrafting of 1,000 7th or 15th passaged islet organoids, similar to the controls engrafting mouse 300 islets. Unengrafted diabetics remained hyperglycemic. Groups are indicated by colored lines and numbers of mice measured per group are labeled in parentheses. Data are presented as mean ± s.e.m. FIG. 7B is a graph showing body weight of mice after engrafting. The immunodeficient mice were made

diabetic with streptozotocin (STZ) 7 days before engrafting. Body weight changes are routinely checked. The body weight loss of the diabetics can be rescued by engrafting of 1,000 7th or 15th passage islet organoids, similar to the controls engrafting 300 islets. The body weight of unengrafted diabetics continuously decreased. Groups are indicated by colored lines and numbers of mice measured per group are labeled in parentheses. Data are presented as mean ± s.e.m. FIG. 7C is a graph of a glucose tolerance test (GTT) administered 1 month after engrafting that indicates significantly improved glucose tolerance in both organoids engrafted and islets engrafted groups. Groups are indicated by colored lines and numbers of mice analyzed per group are labeled in parentheses. Data are presented as mean ± s.e.m. FIG. 7D is a graph showing ELISA measurements of serum insulin for each indicated group before and after glucose injection (15 minutes after glucose injection). The number of mice used per group are the same as in FIGs. 7A and 7C. Data are presented as mean ± s.e.m. FIG. 7E is representative images of immunofluorescence staining of β-cells marker Ins, α-cells marker Gcg, δ-cells marker Sst or PP-cells marker Ppy on regenerated tissues engrafted organoids for 1 month. n=3 mice. Scale bar denotes 20 μm. "Org." denotes organoid. FIG. 7F is a graph quantifying the different hormone-expressing cells in regenerated tissues engrafted organoids for 1 month. n=3 mice. FIG. 7G includes electron microscopy images of granules within sectioned cell. The organoid cells are isolated 1 month after engrafting. Crystallized insulin granules indicating maturation of the β-cells. n=3 mice. Scale bar denotes 1 μm. FIG. 7H includes t-SNE2 plots of 2,129 engrafted hormone-expressing single cells RNAseq profiles (points). Organoids cells are isolated 1 month after engrafting. Data are shown by aligning with the primary single cell RNAseq dataset described above and colored by cluster assignment and annotated post hoc (left), or colored by cell source (right). The engrafted cells were pooled from n=3 mice. FIG. 7I is a graph showing the distributions of the number of UMIs per cell (left) and the number of genes detected per cell (right) for the engrafted single cell (sc) RNAseq dataset. FIG. 7J includes t-SNE plots of Sc RNAseq profiles (points) of engrafted or primary samples in split view, colored by cluster assignment and annotated post hoc. Cell counts of indicated samples and cell types are labeled in parentheses. "Mesen." denotes mesenchymal; "Endo." denotes endothelial; "New pop." denotes new population. FIG. 7K is a heat map for signature genes of endocrine cell types. Each column represents a single cell and each row represents one signature gene. To compare the similarities, engrafted or primary cells are shown separately. The shading ranging from dark shading to lighter shading indicate low to high relative gene expression levels, respectively. FIG. 7L includes Vlin plots showing the comparable expression levels (Log2(TPM+1)) of α- or β-cell marker genes between primary and engrafted cells. FIG. 7M is a dot plot for signature genes of endocrine cell types. Engrafted or primary cells are separately shown for comparison. The

shadings denote average expression levels and the sizes of dots denote fractional expression. FIG. 7N includes Vlin plots showing the comparable expression levels (Log2(TPM+1)) of delta or PP cells markers between primary and engrafted cells.

FIGs. 8A and 8B illustrate that $Procr^+$ cells that are devoid of endocrine marker expression are found in human islets. FIG. 8A includes representative confocal images for endocrine hormones (shown in green) and PROCR (shown in red) staining on human pancreas sections from indicated donors. Islets are outlined. Similar to mouse, human islet $PROCR^+$ cells do not overlap with the hormone-expressing cells. Scale bar denotes 20 μm. FIG. 8B includes representative confocal images for PROCR (shown in red) staining on human pancreas sections from indicated donors. PROCR is also expressed in the exocrine compartment of human pancreas. Scale bar denotes 20 μm.

FIGs. 9A-9C illustrate the isolation of human islet single cells by FACS. FIG. 9A includes a representative FACS profile for TSQ staining in Hu0124 donor. Three different levels of TSQ staining are gated. FIG. 9B includes representative confocal images for the endocrine markers INS/GCG or exocrine markers AMY/KRT19 staining (shown in red) in each indicated cell population sorted from Hu0124 donor. TSQ-high cells are enriched for the islet hormone-expressing cells while the exocrine cells are TSQ-low or TSQ-neg. Scale bar denotes 20 μm. FIG. 9C includes FACS profiles for TSQ staining in different donors.

FIGs. 10A-10D illustrate screening for factors that promote growth of human islet organoids. FIG. 10A includes representative bright field images of organoids annotated to show the number of organoids cultured from donor Hu1021 under each indicated condition and a graph quantifying organoid size. FIG. 10B includes representative bright field images of organoids annotated to show the number of organoids cultured from donor Hu1130 under each indicated condition and a graph quantifying organoid size. FIG. 10C includes a graph quantifying organoid size that is annotated to show the number of organoids cultured from donor Hu0228 under each indicated condition. Data for FIGs. 10A-10C are presented as mean ± s.e.m. FIG. 10D is a representative confocal image for the endocrine markers INS (shown in red) and GCG (shown in green) staining in organoid from Hu1130 donor. Scale bars for FIGs. 10A, 10B, and 10D denote 20 μm.

FIGs. 11A-11D depict establishing a 3D culture system to expand human islet organoids. FIG. 11A is a graph showing the number of primary passage organoids formed per 10,000 TSQ-high pancreas cells from 3 different donors. FIG. 11B include representative bright field images for islet organoids from Hu0228 donor, culture days are labeled in parentheses. Representative ductal organoid with distinguished hollow structure is also shown for comparison. Scale bar denotes 100 μm. FIG. 11C includes graphs showing the sizes and growth curve of islet

organoids (derived from primary Hu0408 donor) followed from passage 1 to passage 7. Data are presented as mean ± s.e.m. FIG. 11D includes representative bright field images for islet organoids (Org) of each indicated passage cultured from Hu0408 donor. Culture days are in parentheses. Scale bar denotes 100 μm.

FIGs. 12A-12E illustrate that human islet organoids can express insulin, respond to glucose stimulation, and contain different endocrine cell types. FIG. 12A includes representative confocal images for insulin staining in islet organoids (Org) of indicated passages (culture days are in parentheses) from donor Hu0228. FIG. 12B includes representative confocal images for insulin staining in islet organoids (Org) of indicated passages (culture days are in parentheses) from donor Hu0408. For FIGs. 12A and 12B, Insulin $(INS)^+$ β-like cells dominate in islet organoids, while glucagon $(GCG)^+$ α-like cells occur at lower frequencies. No SOX9 (duct cell marker) expression was detected in islet organoids. Scale bar denotes 20 μm. FIG. 12C is a representative confocal image of SOX9 staining in ductal organoid. Scale bar denotes 20 μm. FIG. 12D is a graph showing representative population measurements of dynamic normalized Fluo-4 fluorescence intensity for the 1st islet organoids (from Hu0228 donor) challenged sequentially with 2, 20, 2, 20, 2, and 20 mM glucose. The x axis represents time. FIG. 12E includes representative confocal images for INS staining in 3rd and 6th passage islet organoids from Hu0228 or Hu0408 donors. Scale bar denotes 20 μm.

FIGs. 13A-13C demonstrate that $PROCR^+$ cells in organoids are highly proliferative. FIG. 13A includes representative confocal images for EdU staining 3rd and 6th passage islet organoids from Hu0228 or Hu0408 donors. Scale bar denotes 20 μm. FIG. 13B is a graph of a FACS analysis of $PROCR^+$ cells percentage in the 1st islet organoids culture from Hu0228 donor. FIG. 13C includes representative confocal images for EdU staining and quantification of EdU^+ cell percentages in PROCR+/PROCR- cells sorted from the islet organoids. $PROCR^+$ organoid cells are significantly more proliferative than PROCR- organoid cells. Scale bar denotes 20 μm.

DETAILED DESCRIPTION

It has generally proven challenging to produce functional β-cells *in vitro*. The present disclosure is based on the discovery of a novel cell population in adult mouse and human pancreatic islets that express Protein C receptor (Procr). These $Procr^+$ cells do not express differentiation markers and feature epithelial-to-mesenchymal transition (EMT) characteristics. $Procr^+$ cells comprise approximately 1-3% of islet cells, and Procr expression allows sorting of these cells from islets. Isolated mouse $Procr^+$ cells can robustly form islet-like organoids when cultured at clonal density with endothelial cells (ECs), while human islet cells do not require

ECs to form organoids. Exponential expansion can be maintained *in vitro* over long-time periods by serial passaging, and differentiation can be induced at any time point in culture. β-cells are predominant in Procr$^+$ progenitor cell-derived differentiated islet organoids, while α-, δ-, and pancreatic polypeptide (PP) cells occur at lower frequencies. The Procr$^+$ progenitor cell-derived organoids are glucose-responsive and insulin-secreting. Upon transplantation in diabetic subjects, these organoids reverse disease. The findings disclosed herein demonstrate that the adult pancreas islet contains a population of Procr$^+$ pro-endocrine cells with progenitor-like capacity.

Definitions

For convenience, certain terms employed herein, in the specification, examples and appended claims are collected here. Unless defined otherwise, all technical and scientific terms used herein have the meaning commonly understood by a person skilled in the art to which this invention belongs. The following references provide one of skill with a general definition of many of the terms used in this invention: Singleton et al., Dictionary of Microbiology and Molecular Biology (2nd ed. 1994); The Cambridge Dictionary of Science and Technology (Walker ed., 1988); The Glossary of Genetics, 5th Ed., R. Rieger et al. (eds.), Springer Verlag (1991); and Hale & Marham, The Harper Collins Dictionary of Biology (1991). As used herein, the following terms have the meanings ascribed to them below, unless specified otherwise.

Unless specifically stated or obvious from context, as used herein, the term "or" is understood to be inclusive. Unless specifically stated or obvious from context, as used herein, the terms "a", "an", and "the" are understood to be singular or plural.

Unless specifically stated or obvious from context, as used herein, the term "about" is understood as within a range of normal tolerance in the art, for example within 2 standard deviations of the mean. "About" can be understood as within 10%, 9%, 8%, 7%, 6%, 5%, 4%, 3%, 2%, 1%, 0.5%, 0.1%, 0.05%, or 0.01% of the stated value. Unless otherwise clear from context, all numerical values provided herein are modified by the term about.

"Procr" and "PROCR" are used interchangeably and refer to protein C receptor, with "Procr" generally referring to the gene or mRNA and "PROCR" the protein product unless otherwise noted. It should be understood that the terms include the complete gene, the cDNA sequence, the complete amino acid sequence, or any fragment or variant thereof.

An "antibody," as used herein is a protein consisting of one or more polypeptides comprising binding domains that bind to a target epitope. The term antibody includes monoclonal antibodies comprising immunoglobulin heavy and light chain molecules, single heavy chain variable domain antibodies, and variants and derivatives thereof, including chimeric

variants of monoclonal and single heavy chain variable domain antibodies. Binding domains are substantially encoded by immunoglobulin genes or fragments of immunoglobulin genes, wherein the protein immunospecifically binds to an antigen. The recognized immunoglobulin genes include the kappa, lambda, alpha, gamma, delta, epsilon and mu constant region genes, as well as myriad immunoglobulin variable region genes. Light chains are classified as either kappa or lambda. Heavy chains are classified as gamma, mu, alpha, delta, or epsilon, which in turn define the immunoglobulin classes, IgG, IgM, IgA, IgD and IgE, respectively. For most vertebrate organisms, including humans and murine species, the typical immunoglobulin structural unit comprises a tetramer that is composed of two identical pairs of polypeptide chains, each pair having one "light" (about 25 kD) and one "heavy" chain (about 50-70 kD). "V_L" and "V_H" refer to the variable domains of these light and heavy chains respectively. "C_L" and "C_H" refer to the constant domains of the light and heavy chains. Loops of β-strands, three each on the V_L and V_H are responsible for binding to the antigen, and are referred to as the "complementarity determining regions" or "CDRs". The "Fab" (fragment, antigen-binding) region includes one constant and one variable domain from each heavy and light chain of the antibody, i.e., V_L, C_L, V_H and C_H1.

Antibodies include intact immunoglobulins as well as antigen-binding fragments thereof. The term "antigen-binding fragment" refers to a polypeptide fragment of an antibody which binds antigen or competes with intact antibody (i.e., with the intact antibody from which they were derived) for antigen binding (i.e., specific binding). Antigen binding fragments can be produced by recombinant or biochemical methods that are well known in the art. Exemplary antigen-binding fragments include Fv, Fab, Fab', $(Fab')_2$, CDR, paratope and single chain Fv antibodies (scFv) in which a V_H and a V_L chain are joined together (directly or through a peptide linker) to form a continuous polypeptide.

Another class of antibodies known as heavy chain antibodies (HCA, also referred to as two-chain or two-chain heavy chain antibodies) have been reported in camelids such as dromedary camels, Bactrian camels, wild Bactrian camels, llamas, alpacas, vicuñas, and guanacos (Hamers-Casterman et al., Nature, 363, 446-448 (1993); Wesolowski et al., Med. Microbiol. Immunol (2009) 198:157-174; see also U.S. Pat. No. 5,759,808; U.S. Pat. No. 5,800,988; U.S. Pat. No. 5,840,526; and U.S. Pat. No. 5,874,541). Compared with conventional four-chain immunoglobulins of IgG-type, which are also produced by camelids, these antibodies lack the light chains and CH1 domains of conventional immunoglobulins, and their variable domains are sometimes designated "V_HH". V_HH can include four framework regions or "FR", FR1, FR2, FR3 and FR4. The framework regions are interrupted by three CDRs, CDR1, CDR2 and CDR3. One of the salient features of these naturally occurring heavy chain antibodies is the

predominant presence of Glu, Arg and Gly at VL interface positions 44, 45 and 47 (Kabat numbering), respectively, of their V_HH. The same positions in the VH of conventional four-chain antibodies (are almost exclusively occupied by Gly, Leu and Trp. These differences are thought to be responsible for the high solubility and stability of camelid HCA variable domain (V_HH), as compared with the relative insolubility of VH domain of the conventional four-chain antibodies. Two more salient features of camelid V_HH domains are their comparatively longer CDR3 and high incidence of cysteine pairs in CDRs. It appears that cysteine pairs mediate the formation of a disulfide bridge and are therefore involved in modulating the surface topology of the antibody combining site. In the crystal structure of a camel sdAb-lysozyme complex, a rigid loop protruding from the sdAb and partly stabilized by a CDR disulfide linkage extends out of the combining site and penetrates deeply into the lysozyme active site (Desmyter et al., Nature Struct. Biol., 3, 803-811 (1996)).

Antibodies also include variants, chimeric antibodies and humanized antibodies. The term "antibody variant" as used herein refers to an antibody with single or multiple mutations in the heavy chains and/or light chains. In some embodiments, the mutations exist in the variable region. In some embodiments, the mutations exist in the constant region. "Chimeric antibodies" refers to those antibodies wherein one portion of each of the amino acid sequences of heavy and light chains is homologous to corresponding sequences in antibodies derived from a particular species or belonging to a particular class, while the remaining segment of the chains is homologous to corresponding sequences in another. Typically, in these chimeric antibodies, the variable region of both light and heavy chains mimics the variable regions of antibodies derived from one species of mammals, while the constant portions are homologous to the sequences in antibodies derived from another. One clear advantage to such chimeric forms is that, for example, the variable regions can conveniently be derived from presently known sources using readily available hybridomas or B cells from non-human host organisms in combination with constant regions derived from, for example, human cell preparations. While the variable region has the advantage of ease of preparation, and the specificity is not affected by its source, the constant region being human, is less likely to elicit an immune response from a human subject when the antibodies are injected than would the constant region from a non-human source. However, the definition is not limited to this particular example. "Humanized" antibodies refer to a molecule having an antigen-binding site that is substantially derived from an immunoglobulin from a non-human species and the remaining immunoglobulin structure of the molecule based upon the structure and/or sequence of a human immunoglobulin. The antigen-binding site may comprise either complete variable domains fused onto constant domains or only the complementarity determining regions (CDRs) grafted onto appropriate framework

regions in the variable domains. Antigen binding sites may be wild type or modified by one or more amino acid substitutions, e.g., modified to resemble human immunoglobulin more closely. Some forms of humanized antibodies preserve all CDR sequences (for example, a humanized mouse antibody which contains all six CDRs from the mouse antibodies). Other forms of humanized antibodies have one or more CDRs (one, two, three, four, five, or six) which are altered with respect to the original antibody, which are also termed one or more CDRs "derived from" one or more CDRs.

An "anti-PROCR antibody" is an antibody that immunospecifically binds to PROCR (e.g., its extracellular domain). The antibody may be an isolated antibody. Such binding to PROCR exhibits a K_d with a value of, e.g., no greater than 1 μM, no greater than 100 nM or no greater than 50 nM. Kd can be measured by any methods known to a skilled in the art, such as a surface plasmon resonance assay or a cell binding assay. An anti-PROCR antibody may be a monoclonal llama antibody, e.g., GS5, GS4, GS2, HD13, HD21, HD44, HD58 or HD61 disclosed in PCT/CN2017/115198, or antigen-binding fragments thereof. Exemplary anti-PROCR antibodies inhibit PROCR binding with protein C. The anti-PROCR antibody may also be the "RCR-252" antibody, which refers to the monoclonal antibody having clone number RCR-252 as first described in Ye et al., "The endothelial cell protein C receptor (EPCR) functions as a primary receptor for protein C activation on endothelial cells in arteries, veins, and capillaries," Biochem Biophys Res Commun 1999, 259: 671. RCR-252 is a rat anti human PROCR antibody, and is commercially available from multiple sources, such as Abcam under Catalog No. ab81712 and Sigma under Product No. E6280. In some embodiments, an anti-PROCR antibody can be those disclosed in US20190045758 or PCT/CN2017/115198, incorporated herein by reference in their entirety. Other commercially available anti-PROCR antibodies can also be used, including those disclosed herein.

As used herein, the term "adult cell" refers to a cell found throughout the body after embryonic development.

The term "pancreas" refers to a glandular organ that secretes digestive enzymes and hormones. In humans, the pancreas is a yellowish organ about 7 in. (17.8 cm) long and 1.5 in. (3.8 cm) wide. It lies beneath the stomach and is connected to the small intestine, muscular hoselike portion of the gastrointestinal tract extending from the lower end of the stomach (pylorus) to the anal opening. Most of the pancreatic tissue consists of grapelike clusters of cells that produce a clear fluid (pancreatic juice) that flows into the duodenum through a common duct along with bile from the liver. Pancreatic juice contains three digestive enzymes: tryptase, amylase, and lipase, that, along with intestinal enzymes, complete the digestion of proteins, carbohydrates, and fats, respectively. Scattered among the enzyme-producing cells of the

pancreas are small groups of endocrine cells, called the islets of Langerhans, that secrete two hormones, insulin and glucagon. The pancreatic islets contain several types of cells: α cells, which produce the hormone glucagon; β cells (also referred to herein as "pancreatic β cells"), which manufacture the hormone insulin; and δ- cells, which produce the regulatory agent somatostatin. These hormones are secreted directly into the bloodstream, and together, they regulate the level of glucose in the blood. Insulin lowers the blood sugar level and increases the amount of glycogen (stored carbohydrate) in the liver; glucagon has the opposite action. Failure of the insulin-secreting cells to function properly results in diabetes or diabetes mellitus.

The terms "progenitor" and "precursor" cell are used interchangeably herein and refer to cells that have a cellular phenotype that is more primitive (i.e., is at an earlier step along a developmental pathway or progression than is a fully differentiated cell) relative to a cell which it can give rise to by differentiation. Often, progenitor cells also have significant or very high proliferative potential. Progenitor cells can give rise to multiple distinct differentiated cell types or to a single differentiated cell type, depending on the developmental pathway and on the environment in which the cells develop and differentiate.

The terms "pancreatic pro-endocrine progenitor", "pancreatic endocrine progenitor", and "$Procr^+$ pro-endocrine progenitor" are used interchangeably herein and refer to a progenitor cell which is capable of becoming a pancreatic hormone expressing cell or capable of forming pancreatic endocrine cells. In some embodiments, such progenitor cells are isolated from adult islets and are $Procr^+$, i.e., expressing Procr mRNA and/or protein.

As used herein, the term "insulin-producing cell" refers to a cell differentiated from a pancreatic pro-endocrine progenitor, or precursor thereof, which secretes insulin. An insulin-producing cell includes pancreatic β cells as that term is described herein, as well as pancreatic β-like cells (i.e., insulin-positive, endocrine cells) that synthesize (i.e., transcribe the insulin gene, translate the proinsulin mRNA, and modify the proinsulin mRNA into the insulin protein), express (i.e., manifest the phenotypic trait carried by the insulin gene), or secrete (release insulin into the extracellular space) insulin in a constitutive or inducible manner. A population of insulin-producing cells e.g. produced by differentiating insulin-positive, endocrine cells or a precursor thereof into β cells according to the methods of the present disclosre can be pancreatic β cells or β-like cells (e.g., cells that have at least one, or at least two) characteristic of an endogenous β cell and exhibit a GSIS response that resembles an endogenous adult β cell. The novelty of the present composition and methods is not negated by the presence of cells in the population that produce insulin naturally (e.g., β cells). It is also contemplated that the population of insulin-producing cells, e.g. produced by the methods as disclosed herein can comprise mature pancreatic β cells, and can also contain non-insulin-producing cells (i.e. cells of

β cell like phenotype with the exception they do not produce or secrete insulin).

In the context of cell ontogeny, the adjective "differentiated", or "differentiating" is a relative term meaning a "differentiated cell" is a cell that has progressed further down the developmental pathway than the cell it is being compared with. Thus, stem cells can differentiate to lineage-restricted precursor cells (such as a mesodermal stem cell), which in turn can differentiate into other types of precursor cells further down the pathway (such as a cardiomyocyte precursor), and then to an end-stage differentiated cell, which plays a characteristic role in a certain tissue type, and may or may not retain the capacity to proliferate further.

The term "cell culture medium" (also referred to herein as a "culture medium" or "medium") as referred to herein is a medium for culturing cells containing nutrients that maintain cell viability and support proliferation. The cell culture medium may contain any of the following in an appropriate combination: salt(s), buffer(s), amino acids, glucose or other sugar(s), antibiotics, serum or serum replacement, and other components such as peptide growth factors, etc. Cell culture media ordinarily used for particular cell types are known to those skilled in the art. An exemplary basal medium used herein include DMEM/F-12 (Dulbecco's Modified Eagle Medium/Nutrient Mixture F-12; available from Thermo Fisher Scientific). A basal medium can be supplemented with one or more of: suitable buffer (e.g., HEPES (4-(2-hydroxyethyl)-1-piperazineethanesulfonic acid)), chemically-defined supplements such as N2 (0.1-10%, e.g., 1%) and B27 (0.1-10%, e.g., 1%) serum-free supplements (available from Thermo Fisher Scientific), antibiotics such as penicillin/streptomycin (0.1-10%, e.g., 1%), MEM non-essential amino acids (Eagle's minimum essential medium (MEM) which is composed of balanced salt solutions, amino acids and vitamins that are essential for the growth of cultured cells, which, when supplemented with non-essential amino acids, makes MEM non-essential amino acid solution), glucose (0.1-10%, e.g., 0.30%), L-glutamine (e.g., GlutaMAX™), ascorbic acid, and/or DAPT (N-[N-(3,5-difluorophenacetyl)-l-alanyl]-S-phenylglycine t-butyl ester). Factors for inducing differentiation such as Wnt agonist such as CHIR99021 or Wnt surrogate such as NGS, TGF-beta pathway inhibitors such as SB431542 or A83-01, Rho-ROCK pathway inhibitor such as Y27632, Bmp inhibitor such as Noggin, EGF (epidermal growth factor), insulin transferrin selenium mixture (ITS, available from Sigma), FGF2 (fibroblast growth factor 2), Heparin, Y27632 and B27 as disclosed herein can also be added to the medium.

The term "cell line" refers to a population of largely or substantially identical cells that has typically been derived from a single ancestor cell or from a defined and/or substantially identical population of ancestor cells. The cell line may have been or may be capable of being maintained in culture for an extended period (e.g., months, years, for an unlimited period of

time). It may have undergone a spontaneous or induced process of transformation conferring an unlimited culture lifespan on the cells. Cell lines include all those cell lines recognized in the art as such. It will be appreciated that cells acquire mutations and possibly epigenetic changes over time such that at least some properties of individual cells of a cell line may differ with respect to each other. In some embodiments, a cell line comprises a Procr$^+$ pro-endocrine progenitor described herein.

By "organoid" is meant a three-dimensional multicellular *in vitro* construct that mimics, to some extent, an *in vivo* organ. For example, a pancreatic organoid comprises cells that mimic the function of islet cells. "Mature organoid" as used herein refers to an organoid that been cultured in a differentiation medium. Mature organoids, in some embodiments, have gene expression signatures similar or identical to the organ that they mimic.

The terms "isolated," "purified," or "biologically pure" refer to material that is free to varying degrees from components which normally accompany it as found in its native state. "Isolate" denotes a degree of separation from original source or surroundings. "Purify" denotes a degree of separation that is higher than isolation. A "purified" or "biologically pure" protein is sufficiently free of other materials such that any impurities do not materially affect the biological properties of the protein or cause other adverse consequences.

The term "isolated cell" as used herein refers to a cell that has been removed from an organism in which it was originally found or a descendant of such a cell. Optionally the cell has been cultured in vitro, e.g., in the presence of other cells. Optionally the cell is later introduced into a second organism or re-introduced into the organism from which it (or the cell from which it is descended) was isolated.

The term "isolated population" with respect to an isolated population of cells as used herein refers to a population of cells that has been removed and separated from a mixed or heterogeneous population of cells. In some embodiments, an isolated population is a substantially pure population of cells as compared to the heterogeneous population from which the cells were isolated or enriched from.

The term "substantially pure", with respect to a particular cell population, refers to a population of cells that is at least about 75%, preferably at least about 85%, more preferably at least about 90%, and most preferably at least about 95% pure, with respect to the cells making up a total cell population. Recast, the terms "substantially pure" or "essentially purified", with regard to a population of Procr$^+$ pro-endocrine progenitor cells, refers to a population of cells that contain fewer than about 20%, more preferably fewer than about 15%, 10%, 8%, 7%, most preferably fewer than about 5%, 4%, 3%, 2%, 1%, or less than 1%, of cells that are not Procr$^+$ pro-endocrine progenitor cells as defined by the terms herein. In some embodiments, the present

disclosre encompasses methods to expand a population of $Procr^+$ pro-endocrine progenitor cells, wherein the expanded population of $Procr^+$ pro-endocrine progenitor cells is a substantially pure population of $Procr^+$ pro-endocrine progenitor cells.

The terms "enriching" or "enriched" are used interchangeably herein and mean that the yield (fraction) of cells of one type is increased by at least 10% over the fraction of cells of that type in the starting culture or preparation.

The terms "renewal" or "self-renewal" or "proliferation" are used interchangeably herein, are used to refer to the ability of stem cells or progenitor cells to renew themselves by dividing into the same non-specialized cell type over long periods, and/or many months to years. In some instances, proliferation refers to the expansion of cells by the repeated division of single cells into two identical daughter cells.

The terms "diabetes" and "diabetes mellitus" are used interchangeably herein. The World Health Organization defines the diagnostic value of fasting plasma glucose concentration to 7.0 mmol/l (126 mg/dl) and above for Diabetes Mellitus (whole blood 6.1 mmol/l or 110 mg/dl), or 2-hour glucose level 11.1 mmol/L or higher (200 mg/dL or higher). Other values suggestive of or indicating high risk for Diabetes Mellitus include elevated arterial pressure 140/90 mm Hg or higher; elevated plasma triglycerides (1.7 mmol/L; 150 mg/dL) and/or low HDL-cholesterol (less than 0.9 mmol/L, 35 mg/dl for men; less than 1.0 mmol/L, 39 mg/dL women); central obesity (males: waist to hip ratio higher than 0.90; females: waist to hip ratio higher than 0.85) and/or body mass index exceeding 30 kg/m^2; microalbuminuria, where the urinary albumin excretion rate 20 µg/min or higher, or albumin:creatinine ratio 30 mg/g or higher). The term diabetes encompases all forms of diabetes, e.g. Type I, Type II and Type 1.5.

The terms "subject" and "individual" are used interchangeably herein, and refer to an animal, for example, a human from whom cells can be obtained and/or to whom treatment, including prophylactic treatment, with the cells as described herein, is provided. For treatment of those infections, conditions or disease states which are specific for a specific animal such as a human subject, the term subject refers to that specific animal. The "non-human animals" and "non-human mammals" as used interchangeably herein, includes mammals such as rats, mice, rabbits, sheep, cats, dogs, cows, pigs, and non-human primates. The term "subject" also encompasses any vertebrate including but not limited to mammals, reptiles, amphibians and fish. However, advantageously, the subject is a mammal such as a human, or other mammals such as a domesticated mammal, e.g. dog, cat, horse, and the like, or production mammal, e.g. cow, sheep, pig, and the like.

As used herein, the term "treating" and "treatment" refers to administering to a subject an effective amount of a composition so that the subject as a reduction in at least one symptom

of the disease or an improvement in the disease, for example, beneficial or desired clinical results. For purposes of this invention, beneficial or desired clinical results include, but are not limited to, alleviation of one or more symptoms, diminishment of extent of disease, stabilized (i.e., not worsening) state of disease, delay or slowing of disease progression, amelioration or palliation of the disease state, and remission (whether partial or total), whether detectable or undetectable. Treating can refer to prolonging survival as compared to expected survival if not receiving treatment. Thus, one of skill in the art realizes that a treatment may improve the disease condition, but may not be a complete cure for the disease. As used herein, the term "treatment" includes prophylaxis. Alternatively, treatment is "effective" if the progression of a disease is reduced or halted. "Treatment" can also mean prolonging survival as compared to expected survival if not receiving treatment. Those in need of treatment include those already diagnosed with a cardiac condition, as well as those likely to develop a cardiac condition due to genetic susceptibility or other factors such as weight, diet and health.

As used herein, the terms "administering," "introducing" and "transplanting" are used interchangeably in the context of the placement of cells, e.g., pancreatic organoids) of the present disclosure into a subject, by a method or route which results in at least partial localization of the introduced cells at a desired site. The cells (e.g., pancreatic organoids, pancreatic β cells or pancreatic β-like cells) can be implanted directly to the pancreas, or alternatively be administered by any appropriate route which results in delivery to a desired location in the subject where at least a portion of the implanted cells or components of the cells remain viable. The period of viability of the cells after administration to a subject can be as short as a few hours, e.g. twenty-four hours, to a few days, to as long as several years. In some instances, the cells can also be administered at a non-pancreatic location, such as in the liver or subcutaneously, for example, in a capsule (e.g., microcapsule) to maintain the implanted cells at the implant location and avoid migration of the implanted cells.

By "effective amount" is meant the amount of a required to ameliorate the symptoms of a disease relative to an untreated patient. The effective amount of active compound(s) used to practice the present invention for therapeutic treatment of a disease varies depending upon the manner of administration, the age, body weight, and general health of the subject. Ultimately, the attending physician or veterinarian will decide the appropriate amount and dosage regimen. Such amount is referred to as an "effective" amount.

Ranges provided herein are understood to be shorthand for all of the values within the range. For example, a range of 1 to 50 is understood to include any number, combination of numbers, or sub-range from the group consisting 1, 2, 3, 4, 5, 6, 7, 8, 9, 10, 11, 12, 13, 14, 15, 16, 17, 18, 19, 20, 21, 22, 23, 24, 25, 26, 27, 28, 29, 30, 31, 32, 33, 34, 35, 36, 37, 38, 39, 40, 41, 42,

43, 44, 45, 46, 47, 48, 49, or 50.

As used herein the term "comprising" or "comprises" is used in reference to compositions, methods, and respective component(s) thereof, that are present in a given embodiment, yet open to the inclusion of unspecified elements.

As used herein the term "consisting essentially of" refers to those elements required for a given embodiment. The term permits the presence of additional elements that do not materially affect the basic and novel or functional characteristic(s) of that embodiment of the disclosure.

The term "consisting of" refers to compositions, methods, and respective components thereof as described herein, which are exclusive of any element not recited in that description of the embodiment.

As used in this specification and the appended claims, the singular forms "a," "an," and "the" include plural references unless the context clearly dictates otherwise. Thus, for example, references to "the method" includes one or more methods, and/or steps of the type described herein and/or which will become apparent to those persons skilled in the art upon reading this disclosure and so forth.

Various aspects and embodiments are described in further detail in the following subsections. Any compositions or methods provided herein can be combined with one or more of any of the other compositions and methods provided herein.

Procr$^+$ Pro-Endocrine Progenitor Cells

It has been surprisingly discovered that Procr$^+$ pro-endocrine progenitor cells reside in the adult pancreas as a small subset (about 1-3%) of cells present in islets. Procr is a Wnt target gene that encodes a protein residing on the surface of the pro-endocrine progenitor cells. The human PROCR is a highly glycosylated type I transmembrane protein of 238 amino-acids (UniProtKB ID No. Q9UNN8). These amino acids comprise a signal peptide (amino acids 1017), an extracellular domain (amino acids 18-210), a 21-aa transmembrane domain (amino acids 211-231), and a 7-aa intracytoplasmic sequence (amino acids 232-238) together coding for an ~46 kDa protein. Deglycosylation will reduce the protein mass to 25 kDa.

PROCR is the receptor for protein C, a key player in the anticoagulation pathway. The protein C anticoagulant pathway serves as a major system for controlling thrombosis, limiting inflammatory responses, and potentially decreasing endothelial cell apoptosis in response to inflammatory cytokines and ischemia. The essential components of the pathway include thrombin, thrombomodulin, PROCR, protein C and protein S. The pathway is initiated when thrombin binds to thrombomodulin on the surface of endothelium. PROCR augments protein C activation by binding protein C and presenting it to the thrombin-thrombomodulin activation

complex. Activated protein C (aPC) retains its ability to bind PROCR, and this complex appears to be involved in some of the cellular signaling mechanisms that down-regulate inflammatory cytokine formation (TNF, IL-6). PROCR is shed from the vasculature by inflammatory mediators and thrombin. PROCR binds to activated neutrophils in a process that involves proteinase 3 and Mac-1.

PROCR can be cleaved to release a soluble form (sPROCR) in the circulation. This sPROCR is detected as a single species of 43 kDa, resulting from shedding of membrane PROCR by the action of a metalloprotease, which is stimulated by thrombin and by some inflammatory mediators. Soluble PROCR binds PC and aPC with similar affinity, but its binding to aPC inhibits the anticoagulant activity of aPC by blocking its binding to phospholipids and by abrogating its ability to inactivate factor Va. sPROCR can be detected in plasma. In normal persons, sPROCR is present in levels of 83.6 +/- 17.2 ng/ml. Elevated levels of sPROCR are positively correlated to a higher risk for thrombosis. Furthermore, a haplotype (A3 allele) has been linked to elevated levels of sPROCR (264 +/-174 ng/ml).

The full gene sequence of human Procr is 44819 bp (GenBank ID No. NC_000020.11). The human cDNA sequence is 717 bp in length (GenBank ID No. NM_006404.4). The full gene sequence of mouse Procr gene is 4354 bp (GenBank ID No. NC_000068.7).

In some embodiments, $Procr^+$ cells isolated from mouse pancreas can express *Rspo1*, *Fgf1*, *Upk3b* and *Hoxa5* (as well as other genes shown in FIG. 2F), and the expression of these genes constitutes a unique, and previously unreported, expression signature for these progenitor cells. These $Procr^+$ progenitor cells can exhibit EMT characteristics. In some embodiments, the EMT characteristics include co-expression of epithelial markers EpCam, Krt8, and Cldn10 and mesenchymal markers Mmp2, Colla1, and Vim. EMT plays a pivotal role during pancreatic islet formation. Committed endocrine precursor cells detach from the trunk epithelium, presumably via EMT, before the formation of the endocrine islets. It has also been proposed that at later stages ductal cells can serve as facultative endocrine progenitors, which is thought to happen through reawakening of the embryonic EMT process. Under specific culture conditions, β-cells can undergo EMT and dedifferentiate, thereby losing their mature characteristics. The resultant fibroblast-like cells can be extensively expanded and re-differentiated into endocrine cell types.

$Procr^+$ cells descend from $Ngn3^+$ cells, which appear to be in a partial EMT state, co-expressing epithelial markers and mesenchymal markers. $Ngn3^+$ cells exist within the embryonic endocrine precursor cell population, with similar EMT characteristic and shared signature genes such as *Procr*, *Rspo1*, *Hoxa*5, and *Dcn*. The $Ngn3^+$ endocrine precursor

represents a transient cell type in the embryonic pancreas. While the majority of $Ngn3^+$ endocrine precursors lose their precursor state after maturation into endocrine cells, it appears likely that a subpopulation is retained in a pro-endocrine progenitor state post organogenesis. This reserve population does not express Ngn3, but it retains EMT features and the gene expression signature.

These $Procr^+$ cells can be isolated from the adult pancreas using the methods described herein. In various aspects of the present disclosure, $Procr^+$ pro-endocrine progenitor cells are isolated and then cultured under conditions suitable for generating pancreatic organoids. In some embodiments, mouse $Procr^+$ pro-endocrine progenitor cells also express one or more of *Procr*, *Rspo1*, *Hoxa*5 and *Dcn*. In some embodiments, a $Procr^+$ progenitor cell can be isolated from an islet by contacting the cell with an antibody that specifically binds Procr. In some embodiments, $Procr^+$ progenitor cells are isolated by fluorescence activated cell sorting (FACS). Other methods known in the art for isolating cells based on marker expression are contemplated herein.

Organoid Production

Identifying a reservoir of pro-endocrine progenitor cells (e.g., $Procr^+$ pro-endocrine cells) in the pancreas itself allows for either *in situ* or *ex vivo* expansion approach to increase β-cell mass. The expansion and differentiation capacities of the pro-endocrine progenitors can be exploited to establish a culture system for the expansion and induction of islet-like organoids. The resulting organoids are dominated by β-cells surrounded by a mantle of α-, δ- and PP-cells, which is important for organoid function as proper glucose regulation requires coordination between the various islet cell types.

Isolated $Procr^+$ cells can be used to generate organoids that exhibit pancreatic functions (e.g., glucose sending and insulin production and secretion). In some embodiments, $Procr^+$ pro-endocrine progenitor cells can be isolated from adult islet cells and cultured to produce the organoids of the present disclosure are derived can be obtained from any pancreatic source. For example, islet cells may be obtained from a commercial source or from a human source. In some embodiments, the source of the islet cells is a human cadaver. In some embodiments, the source of the islet cells is a human patient with abnormal pancreatic function (e.g., Type 1 or Type 2 diabetes patient, or MODY (maturity onset diabetes of the young) patient). $Procr^+$ pro-endocrine progenitor cells present in islets obtained from a human patient can be cultured to produce organoids that comprise insulin-producing glucose sensitive islet cells (i.e., β-like cells).

In general, to form an organoid, isolated cells are first expanded. To expand cells (i.e., to form colonies of the isolated cells), the cells are cultured in an organoid medium under

conditions suitable for cellular growth and reproduction. An organoid medium can be a serum-free medium supplemented with growth factors to facilitate cell growth and reproduction. In some embodiments, the organoid medium does not contain sufficient differentiation factors to cause the cells to differentiate. In some embodiments, the organoid medium contains no differentiation factors. Growth factors that can be used in an organoid medium include, but are not limited to Wnt agonists CHIR99021 or NGS, TGF-beta pathway inhibitors SB431542 or A83-01, Rho-ROCK pathway inhibitor Y27632, Bmp inhibitor Noggin, EGF (epidermal growth factor), ITS, FGF2 (fibroblast growth factor 2), Heparin, activating antibodies of Integrin beta 1, and B27. Additionally, growth-promoting conditions can include any condition (e.g., culture media, incubation time, frequency of media changes, and the like) that activates the Wnt, FGF, integrin and/or BMP signaling pathways. Growth promoting conditions can require inhibition of other cellular signaling pathways. For example, in some embodiments, growth promoting conditions can include inhibiting the TGFβ and/or Rho-ROCK pathways.

One exemplary organoid medium for culturing mouse cells is DMEM/F12 (with Penicillin-Streptomycin) plus 1-5% (e.g., 2%) B27, 0.1-5% (e.g., 1%) ITS, 10-200 (e.g., 50) ng ml^{-1} EGF, 0.1-5 (e.g., 2) μg ml^{-1} heparin, 1-50 (e.g., 10) ng ml^{-1} FGF2 and 1-20 (e.g., 5) ng ml^{-1} VEGFa. Another exemplary organoid medium for culturing human cells is DMEM/F12 (with Penicillin-Streptomycin) plus 1-5% (e.g., 2%) B27, 0.1-5% (e.g., 1%) ITS, 10-200 (e.g., 50) ng ml^{-1} EGF, 0.1-5 (e.g., 2) μg ml^{-1} heparin, 1-50 (e.g., 10) ng ml^{-1} FGF2, 1-10 (e.g., 3) μM CHIR99021, 1-10 (e.g., 2) μM A83-01, 10-500 (e.g., 100) ng ml^{-1} Noggin, 1-50 (e.g., 10) μM Y27632.

Isolated progenitor cells can be cultured in a microenvironment that mimics at least, in part, a cellular niche in which the cells naturally reside. The cellular niche can be mimicked by culturing the stem cells in the presence of biomaterials, such as matrices, scaffolds, and culture substrates that represent key regulatory signals controlling cell fate. The biomaterials can be natural, semi-synthetic and synthetic biomaterials, and/or mixtures thereof. A scaffold provides a two-dimensional or three-dimensional network. Suitable synthetic materials for the scaffold include polymers selected from porous solids, nanofibers, and hydrogels, such as peptides including self-assembling peptides, hydrogels composed of polyethylene glycol phosphate, polyethylene glycol fumarate, polyacrylamide, polyhydroxyethyl methacrylate, polycellulose acetate, and/or co-polymers thereof (see, for example, Saha et al., 2007, *Curr. Opin. Chem. Biol.* 11(4): 381-387; Saha et al., 2008, *Biophysical Journal* 95: 4426-4438; Little et al., 2008, *Chem. Rev.* 108, 1787-1796). As is known to a skilled person, the mechanical properties such as the elasticity of the scaffold influences proliferation, differentiation and migration of stem cells. A preferred scaffold comprises biodegradable (co)polymers that are replaced by natural occurring

components after transplantation in a subject, for example to promote tissue regeneration and/or wound healing. It is furthermore preferred that the scaffold does not substantially induce an immunogenic response after transplantation is a subject. the scaffold can be supplemented with natural, semi-synthetic or synthetic ligands, which provide the signals that are required for proliferation and/or differentiation, and/or migration of stem cells. In a preferred embodiment, the ligands comprise defined amino acid fragments. Examples of the synthetic polymers comprise Pluronic® F127 block copolymer surfactant (BASF), and Ethisorb® (Johnson and Johnson).

A cellular niche is in part determined by the progenitor cells and surrounding cells, and the extracellular matrix (ECM) that is produced by the cells in the niche. In some embodiments, isolated cells are attached to an ECM. ECM is composed of a variety of polysaccharides, water, elastin, and glycoproteins, wherein the glycoproteins comprise collagen, entactin (nidogen), fibronectin, and laminin. ECM is secreted by connective tissue cells. Different types of ECM are known, comprising different compositions including different types of glycoproteins and/or different combination of glycoproteins. The ECM can be provided by culturing ECM-producing cells, such as fibroblast cells, in a receptacle, prior to the removal of these cells and the addition of isolated progenitor cells. Examples of extracellular matrix-producing cells are chondrocytes, producing mainly collagen and proteoglycans, fibroblast cells, producing mainly type IV collagen, laminin, interstitial procollagens, and fibronectin, and colonic myofibroblasts producing mainly collagens (type I, III, and V), chondroitin sulfate proteoglycan, hyaluronic acid, fibronectin, and tenascin-C. Alternatively, the ECM can be commercially provided. Examples of commercially available extracellular matrices are extracellular matrix proteins (Invitrogen) and Matrigel™ (BD Biosciences). The use of an ECM for culturing progenitor cells enhanced long-term survival of the cells and the continued presence of undifferentiated cells. In addition, the presence of an ECM allows culturing of three-dimensional tissue organoids.

A suitable ECM for use can include, in some embodiments, at least two distinct glycoproteins, such as two different types of collagen or a collagen and laminin. The ECM can be a synthetic hydrogel extracellular matrix or a naturally occurring ECM. An exemplary ECM is provided by Matrigel™ (BD Biosciences), which comprises laminin, entactin, and collagen IV.

In some embodiments, isolated $Procr^+$ cells can be co-cultured with endothelial cells at a ratio of about 1:10 to about 10:1, e.g., about 1:5, about 1:3, or about 1:1. Endothelial cells provide a critical niche component, and in some embodiments, the co-culture medium is supplemented with VEGFa.

Organoids can be passaged every 5–30 days to expand. For passage, organoids can be

released from the Matrigel using dispase and dissociated into single cells (e.g., with trypsin-EDTA). The single cell suspension can then be mixed with freshly isolated CD31+ ECs in a ratio of 1:1, followed by replating in a split ratio of about 1:2-1:10, or about 1:3-1:8, or about 1:4-1:6. Organoids can be passaged at least 20 times (about 6 months), at least 30 times, or indefinitely, with no deceleration of expansion rate.

This duration of expansion provides time for organoids to mature such that β-like cells are capable of producing and secreting insulin in response to a glucose stimulus. Then these passaged organoids can be taken out of expansion cycle and allowed to mature for an additional period of time (e.g., about 1-4 weeks or about 2-3 weeks or about 3 weeks (28-30 days upon being replated as single cells), mature organoids can appear that resemble the primary organoids. In some embodiments, organoids are tested to determine their capacity to produce and secrete insulin. In some embodiments, the testing is performed *in vitro*. In some embodiments, the testing is performed *in vivo*, for example, after an organoid is transplanted into a recipient (e.g., a mouse or human). Insulin production and/or secretion in or by an organoid can be assessed by any technique known in the art. For example, the expression of insulin can be assessed by enzyme-linked immunosorbent assay (ELISA) or other immunoassay that utilizes an antibody that specifically binds insulin (or another molecule of interest expressed in the organoid, including but not limited to glucagon, somatostatin, and pancreatic polypeptide. In some embodiments, detection of insulin production in an organoid can be assessed *in vitro* by obtaining at least one organoid in a culture and testing it directly. Insulin secretion by an organoid can be detected *in vitro* in the culture medium by any means known in the art. For example, a culture may be spun down and the organoid-free (or substantially free) supernatant tested for insulin. In some embodiments, *in vivo* insulin production by transplanted organoids can be assessed via analysis of a blood draw from a subject having received treatment with organoids of the present disclosure and compared to insulin levels in the subject prior to treatment. Such measurements are routine in the art.

Use of Insulin Producing Organoids

Organoids derived from $Procr^+$ pro-endocrine progenitor cells, such as those organoids described herein or organoids produced using the methods described herein are useful as therapeutics and prophylactics for the treatment and prevention of diabetes mellitus (DM), or any disease or condition that is responsive to the presently described insulin producing organoids.

The number of the organoids described herein in the pharmaceutical composition necessary to achieve an optimal or satisfactory result may vary between subjects being treated.

For example, the number of organoids necessary for a person with a complete loss of endogenous insulin production will likely be less than the amount of organoids necessary for a patient who has retained at least some endogenous insulin production. In some embodiments, the number of organoids present in the pharmaceutical composition can be between about 100 to about 10,000,000 organoids, about 1,000-1,000,000 organoids, or about 10,000-100,000 organoids, or any number smaller, larger or therebetween. Determining the precise effective dose may be based on factors for each individual subject, including their size, age, sex, weight, and condition. Dosages can be readily ascertained by those skilled in the art from this disclosure and the knowledge in the art. The skilled artisan can also readily determine the number of organoids and the amount of optional additives, vehicles, and/or carriers in compositions and to be administered in methods of the invention.

The present disclosure features compositions and methods that are useful for therapeutic approaches for treating diabetes. More specifically, the organoids described above are administered to those in need (e.g., a human diabetic), which can ameliorate, reduce, or otherwise treat or prevent a patient's abnormal pancreatic function. In some embodiments, the organoids are derived from pro-endocrine progenitor cells obtained from the patient, optionally followed by correcting mutations (if any) by gene editing such as CRISPR. Obtaining autologous islet cells from the patient lessens the risk of rejection of the organoids when administered to the patient. In some embodiments, the organoids are derived from pro-endocrine progenitor cells obtained from a heterologous human subject (such as a bank or library of organoids).

The administration of the organoids of the present disclosure for the treatment of diabetes (or any other disease or condition that may be responsive to the organoids) may be by any suitable means that results in a concentration of the therapeutic organoid that is effective in ameliorating, treating, or preventing diabetes.

In some embodiments, the organoids are transplanted directly into the patient's pancreas or another locus in the body, such as liver, spleen, renal capsule, omental pouch, skin, muscle, bone marrow (see, e.g., doi: 10.3389/fmed.2018.00202, incorporated herein by reference). The subject may also be administered anti-rejection medication to less the probability that the transplanted organoids are rejected by the patient's immune system.

In one aspect, the invention provides a method of monitoring treatment progress. The method includes the step of determining a level of insulin (or other marker (e.g., glucagon, somatostatin, or pancreatic polypeptide) or diagnostic measurement (e.g., screen, assay) in a subject suffering from or susceptible to diabetes or other disorder or symptoms thereof associated with impaired pancreatic islet function, in which the subject has been administered a

therapeutic amount of Procr$^+$ organoids disclosed herein sufficient to treat the disease or symptoms thereof. The level of insulin (or other marker) determined in the method can be compared to known levels of insulin in either healthy normal controls or in other afflicted patients to establish the subject's disease status. In another embodiment, a second level of insulin in the subject is determined at a time point later than the determination of the first level, and the two levels are compared to monitor the course of disease or the efficacy of the therapy. In certain preferred embodiments, a pre-treatment level of insulin (or other marker) in the subject is determined prior to beginning treatment according to this invention; this pre-treatment level of insulin (or other marker) can then be compared to the level of insulin (or other marker) in the subject after the treatment commences, to determine the efficacy of the treatment.

Screening Assays

Some aspects of the present disclosure provide screening assays in which Procr$^+$ pro-endocrine progenitor cells or organoids of the present disclosure are used in an *in vitro* setting to test the efficacy of insulin production agonists or antagonists, or other compounds, compositions, or agents for inducing or otherwise affecting the differentiation of pancreatic pro-endocrine progenitor cells. The organoids, in some embodiments, are derived from Procr$^+$ pro-endocrine progenitor cells obtained for a healthy subject. In other embodiments, the organoids are derived from a subject having diabetes or another disease or condition characterized by impaired pancreatic islet function. If the insulin production agonist or other compound or composition is effective in promoting increased insulin, then insulin will accumulate in the culture medium and can be quantified. In some instances, the compound or composition administered to the organoid may be detrimental to the health of the organoid. For example, the organoid may cease growing and/or reproducing, may display an altered morphology, or may die. Such results would suggest that the compound or composition has a toxic profile.

In some embodiments, an *in vitro* screen comprising an organoid of the present disclosure can be used to better understand β-cell or islet function or other endocrine cell function. In some embodiments, organoids generated from Procr$^+$ pro-endocrine progenitor cells derived from a subject having a disease or disorder (e.g., diabetes) can be studied to better understand the molecular and cellular contributors to the subject's disease or condition, including gene mutation and microenvironment factors.

The following examples are put forth so as to provide those of ordinary skill in the art with a complete disclosure and description of how to make and use the assay, screening, and therapeutic methods of the invention, and are not intended to limit the scope of what the

inventors regard as their invention.

EXAMPLES

Example 1: Long-term expansion of pancreatic islet organoids from resident Procr+ progenitors

A Procr$^+$ progenitor population in adult islets

As Procr is a surface protein which has been reported to mark stem cells in several adult tissues, including the mammary gland (Wang et al., 2015), endothelium (Yu et al., 2016) and hematopoietic systems (Balazs et al., 2006; Fares et al., 2017; Iwasaki et al., 2010; Zhou et al., 2016), we searched for Procr-positive cells in murine islets using Single Cell (sc) RNAseq. Pancreases from 8-week old adult mice were dissociated and endocrine cells were enriched (see Methods section below). 7,160 cells were profiled using sc RNAseq approaches (**FIGs. 1A-1D**). Each cluster was mapped to known abundant endocrine (α-, β-, δ- and PP-cells), abundant exocrine (acinar and duct cells), or rare (mesenchymal, endothelial, immune cells, and stellate) cell types (**FIGs. 1D-1G**). A single cluster contained cells distinct from any known cell population (**FIGs. 1F-1H**). This novel population displayed unique signature genes, including *Rspo1*, *Fgf1*, *Upk3b*, *Hoxa5*, and *Procr* (**FIGs. 1H-1K**), but did not express known endocrine or exocrine differentiation markers as shown by t-distributed stochastic neighborhood embedding (*t*-SNE) analysis (**FIG. 1D, 1E, 1G, 1K**). Gene ontology (GO) analysis identified enrichment of cell migration-, epithelial-to-mesenchymal transition (EMT)- and Wnt signaling pathway-GO terms (**FIG. 1L**). The signature expression of Wnt agonist gene *Rspo1* and Wnt target gene *Procr* indicated enhanced Wnt signaling pathway activity. The co-expression of epithelial markers (*EpCAM*, *Krt8*, and *Cldn10*) and mesenchymal markers (*Mmp2, Col1a1* and *Vim*) in the new population shown by *t*-SNE analysis supported its EMT characteristics (**FIG. 1M**).

EMT is implicated in the formation of the endocrine islets by committed endocrine precursor cells (Rukstalis and Habener, 2007). The lack of differentiation marker expression in the new population also suggested a potential precursor state. To gain insight into the nature of the new population, expression data was merged with previously reported datasets of embryonic endocrine progenitors (Byrnes et al., 2018; Scavuzzo et al., 2018). The new population seen in adult pancreas aligned with a cluster of Neurog3 (Ngn3)$^+$ cells at embryonic day 14.5 (E14.5) (**FIGs. 2A-2B**). Interestingly, this population at E14.5 also displays EMT features, i.e., the combined expression of epithelial and mesenchymal markers (**FIG. 2C**). This E14.5 population was Ngn3$^+$, whereas the adult counterpart was Ngn3$^-$ (**FIG. 2D**). Importantly, the E14.5 population shared a gene signature, including *Rspo1*, *Fgf1*, *Dcn, Upk3b*, *Hoxa5*, and *Procr* (**FIG. 2E-2G**). The resemblance of the E14.5 population to the embryonic endocrine precursor

suggested that the Procr$^+$ population represented a progenitor state. Thus, precursor-progeny relationships between the identified endocrine populations were examined by pseudo temporal analysis using monocle 2 (Qiu et al., 2017). This predicted two developmental trajectories: one toward the β-cell and one toward the α-cell (**FIGs. 2H-2I**).

Sorting Procr$^+$ cells from islets

Islets and non-islet tissues were separated by hand-pick. Islet cell preparations underwent negative selection of blood lineage, positive selection of epithelial cells, followed by further separation into Procr$^+$ (Lin$^-$, EpCAM$^+$, Procr$^+$) and Procr$^-$ (Lin-, EpCAM$^+$, Procr$^-$) populations (**FIGs. 3A-3B**). The anti-Procr antibody used was PE or APC anti mouse Procr (clone 1560) from eBioscience. A small population (1.0±0.14%) of islet cells were Procr+ (**FIG. 3B-3C**). Considering that rare mesenchymal, stellate, and endothelial cells can express Procr as shown by sc RNAseq (**FIG. 1H**), Procr$^+$ and Procr$^-$ cells were isolated from the non-islet tissue also. qPCR analysis indicated that signature genes of the new population, e.g., Rspo*1*, *Fgf1*, *Upk3b*, and *Hoxa5* are exclusively expressed in Procr$^+$ islet cells (**FIG. 3D**).

Ngn3-Cre; *R26-tdTomato* mice were next analyzed in which all endocrine lineages were marked in tdTomato, as they all are derived from embryonic Ngn3$^+$ pancreatic endocrine precursors (Gu et al., 2002). FACS analysis confirmed that Procr$^+$ islet cells were all tdTomato$^+$ (**FIG. 3E**), identifying the cells as progeny of Ngn3$^+$ endocrine precursors. Notably, they appeared to represent a new type of progeny lacking α-, β-, δ-, and PP-cell differentiation marker expression.

To visualize this population, a double-reporter allele with a membrane GFP (mGFP)-2A-LacZ cassette inserted at the ATG of *Procr* (**FIGs. 3F-3I**) was generated. As shown by whole-mount X-gal staining, Procr expression occurred in a small number of cells in a dispersed pattern in the islets (**FIG. 3J**). mGFP$^+$ cells were further validated by Procr antibody using FACS (**FIG. 3K**). Whole-mount islet staining confirmed that mGFP$^+$ (Procr$^+$) cells do not express endocrine differentiation markers (**FIG. 3L**), yet co-express the epithelial marker EpCAM and the mesenchymal marker Col1a1 (**FIG. 3M**), which was consistent with sc RNAseq analysis.

Single Procr$^+$ islet cells form islet-like organoids in culture

It was hypothesized that Procr$^+$ islet cells can serve as a cellular source for new β-cells *in vitro*. Procr$^+$ islet cells were FACS-isolated and plated at clonal density in 3D culture with serum-free media, supplemented with growth factors, including B27, ITS, EGF, heparin, and FGF2. While unsorted islet cells had a very low colony-forming efficiency (i.e., 1 colony

formed out of 2,000 plated total cells), $Procr^+$ islet cells exhibited a 130-fold increased clonogenicity (i.e., 1 out of 15 plated cells formed a colony) (**FIG. 4A**). In contrast, $Procr^-$ islet cells were not able to form colonies (**FIG. 4B**). However, colonies derived from either unsorted islet cells or $Procr^+$ islet cells could not sustain for more than 7 days.

Endothelial cell (ECs), proposed as a critical niche component proposed as a critical niche component, were then added in co-culture (supplemented with VEGFa, see Methods section below). $Procr^+$ islet cells exhibited robust colony formation ability (i.e., 1 colony formed out of 4 plated $Procr^+$ cells) when co-cultured with ECs. Colonies were readily observed from day 5. By day 8, colonies were observed with an average diameter of 145 μm (**FIG. 5A**). In contrast, $Procr^-$ islet cells remained as single cells (**FIG. 5A**). $Procr^+$ cell-derived colonies were continuously cultured in the same conditions for a total of 28 days. The formation of more elaborated structures was observed, with large epithelial organoids in the center, surrounded and infiltrated by endothelial networks (**FIG. 5B**). The average organoid diameter reached 210 μm (**FIGs. 5B-5C**), similar to the size of mouse islets *in vivo*.

Insulin (Ins) expression was examined as an indication of functional β-cell formation. Ins staining was absent at day 7 and appeared at low levels at day 28 (**FIG. 5D**). After glucose stimulation (12 hrs incubation with low glucose followed by 12 hrs treatment with high glucose for a total of 3 rounds, see Methods section below), Ins expression in day 28 organoids reached a level comparable to that of freshly isolated islets (**FIGs. 5D-5E**). However, the same glucose stimulation treatment had only modest effects on Ins expression in day 7 organoids, suggesting that prolonged culture is critical for β-cell formation. β-cell key regulatory factors, *MafA*, *Ucn3*, and *Pdx1*, rose to similar levels in day 28 high-glucose treated organoids as compared to freshly isolated islets, as measured by qPCR analysis (**FIG. 5F**). The day 28 organoids rapidly increased cytosolic Ca^{2+} concentrations in response to glucose and subsequently returned to baseline (**FIG. 5G**), indicating their capability of responding acutely to glucose (Mohammed et al., 2009). Analysis of ultrastructure by transmission electron microscopy (TEM) revealed that day 28 organoids contain abundant endocrine granules (**FIGs. 5H-5I**). ELISAs confirmed secretion of insulin in the media upon glucose stimulation of day 28 organoids (**FIG. 5J**). In addition to the abundant Ins^+ β-like cells, the organoids contained smaller numbers of glucagon $(Gcg)^+$ α-like cells, somatostatin $(Sst)^+$ δ-like cells, and pancreatic polypeptide $(Ppy)^+$ PP-like cells reminiscent of the composition of fresh islets (**FIGs. 5K-5N**). Thus, a culture system was established that harnessed the pro-endocrine progenitor-like capacity of $Procr^+$ cells, which allowed generation of islet-like organoids *in vitro*. Cells within these organoids were capable of producing packaged insulin granules, of glucose sensing, and of insulin secretion.

Islet-like organoids can be expanded in vitro long-term

The organoids described above were expanded through passaging. Dissociated single cells were replated every 7-8 days at a ratio of 1:4-6 (i.e., cells from 1 well were replated to 4-6 wells) in the same culture condition and supplemented with fresh ECs (see Methods section below). In this culture system, the average organoid size remained stable during passaging (**FIGs. 6A, 6B**). However, the number of organoids grew 3- to 7-fold with each passage (**FIG. 6C**). Organoids could be passaged at least 20 times, or 6 months, with no deceleration of expansion rate (**FIG. 6C**).

When passaged organoids were taken out of expansion cycle and allowed to mature for an additional 3 weeks (i.e., 28-30 days upon being replated as single cells; see **FIG. 6D**), and mature organoids appeared that resembled the primary organoids described above. 7th and 15th passage organoids are given as examples, showing similar percentages of α-, β-, δ-, and PP- cells (**FIG. 6E-6H**), glucose sensing and insulin secretion abilities, insulin granule numbers, and Ca^{2+} response when compared to the primary passage organoids (**Fig. 5G-5H, FIGs. 6I-6N**). These results suggest that the expansion and differentiation capacities of the cells were maintained long-term.

Long-term cultured organoids reverse diabetes in vivo

Long-term cultured organoids were transplanted into the kidney capsule of streptozotocin (STZ)-induced diabetic mice to test the full potential of the organoids. The mice were monitored for glycemic improvement. 1000 organoids (from 7th or 15th passage, taken at day 7 of culture) or 300 freshly isolated islets, which contained similar cell numbers (~300,000 cells), were transplanted per recipient mouse. At 1-week post-transplantation, blood glucose levels were clearly reduced (**FIG. 7A**), and body weight loss was stopped (**FIG. 7B**). The glycemic improvement was maintained throughout the analysis period (**FIG. 7A**). Notably, the organoid-transplanted groups exhibited similar rescue effects as the fresh islet-transplanted group (**FIGs. 7A and 7C**). At 1-month post-transplantation, mice transplanted with organoids exhibited glucose clearance ability and serum insulin levels almost identical to the mice receiving fresh islets (**FIGs. 7C-7D**). Thus, the transplanted organoids were capable of secreting insulin and ameliorating progressive hyperglycemia in a diabetic mouse model.

The grafted organoid cells were removed and analyzed 1 month after transplantation. All four endocrine cells types were detected with the vast majority being Ins^+ β-cells (**FIGs. 7E-7F**). The grafted cells also contained a high density of endocrine granules as shown by TEM (**FIG. 7G**). The identities of these cells were further analyzed by sc RNAseq. The grafted cells, after maturation *in vivo*, clustered with primary endocrine cells (**FIG. 7H-7K**). In particular, the

genes that encode islet cell markers, hormones, and transcriptional regulators were expressed at comparable levels between the primary mouse endocrine cells and the grafted organoid cells (**FIG. 7L-7N**).

Discussion

In the current study, we identify a population of pro-endocrine progenitor cells in adult mouse pancreas. These cells do not express known mature endocrine cell markers, feature EMT characteristic, and express Procr on their surface. Isolated Procr+ islet cells can grow in clonal density into islet-like organoids, which comprise all endocrine cell types and are capable of glucose-sensing and insulin secretion. These organoids can be exponentially expanded in vitro by serial passage over long periods. The long-term cultured islet-like organoids can reverse diabetes in vivo.

EMT plays a pivotal role during pancreatic islet formation. Committed endocrine precursor cells detach from the trunk epithelium, presumably via EMT, before the formation of the endocrine islets (Rukstalis and Habener, 2007). It has also been proposed that -at later stages- ductal cells can serve as facultative endocrine progenitors, which is thought to happen through reawakening of the embryonic EMT process (Al-Hasani et al., 2013). Under specific culture conditions, β-cells can undergo EMT, and dedifferentiate to lose their mature characteristics. The resultant fibroblast-like cells can be extensively expanded, and re-differentiation into endocrine cell types (Gershengorn et al., 2004; Ouziel-Yahalom et al., 2006; Russ et al., 2008). In the current study, we identify a population of cells in healthy adult islets, that appear to be in a partial EMT state, co-expressing epithelial markers and mesenchymal markers. Intriguingly, a counterpart cell population also appears to exist within the embryonic endocrine precursor cell population, with similar EMT characteristic and shared signature genes such as *Procr*, *Rspo1*, *Hoxa5* and *Dcn* etc. The $Ngn3^+$ endocrine precursor represents a transient cell type in the embryonic pancreas. While the majority of $Ngn3^+$ endocrine precursors lose their precursor state after maturation into endocrine cells, it appears likely that a subpopulation is retained in a pro-endocrine progenitor state post organogenesis. This reserve population no longer expresses Ngn3, but it retains EMT features and the indicated signature genes. Using Ngn3-Cre mediated lineage tracing, we confirm that $Procr^+$ cells (pro-endocrine progenitors) descend from $Ngn3^+$ endocrine precursors.

As an alternative source of these cells, we cannot formally rule out the ductal tree. There is growing body of evidence for the existence of a pancreas progenitor pool within the ductal tree of the adult pancreas. Severe damage to the pancreas can stimulate non-endocrine precursors, such as duct cells, to proliferate and differentiate towards acinar (Criscimanna et al.,

2011; Furuyama et al., 2011), duct (Criscimanna et al., 2011; Furuyama et al., 2011; Kopp et al., 2011), and also endocrine lineages (including -cells) (Criscimanna et al., 2011; Inada et al., 2008; Pan et al., 2013; Van de Casteele et al., 2013; Xu et al., 2008). In the current study, we analyze Procr^{+} pro-endocrine progenitors at the state when they already physically reside in islets. We visualize these cells by LacZ and mGFP knock-in reporter, we FACS-isolate these cells by EpCAM+ and Procr+ surface marker in hand-picked islets. We further interrogate their clonogenicity, expansion and multipotent endocrine lineage differentiation capacities in culture.

Identifying a reservoir of pro-endocrine progenitor cells in the pancreas itself allows for either in situ or ex vivo expansion approach to increase β-cell mass. The current study explores the latter possibility. We harness the expansion and differentiation capacities of the pro-endocrine progenitors, by establishing a culture system for the expansion and induction of the islet-like organoids. The resulting organoids are dominated by β-cells surrounded by a mantle of α-, δ- and PP-cells. We demonstrate these organoids to be a useful cell source for ameliorating diabetes in mouse model. Increasing evidence indicates that proper glucose regulation requires coordination between the various islet cell types (Johnston et al., 2016; van der Meulen et al., 2015). It may therefore be advantageous to produce whole islets in vitro rather than to differentiate cells into a specific cell type.

In summary, this study identifies a novel pro-endocrine progenitor in adult mouse pancreas, and establishes an in vitro method for long-term expansion and induction of islet-like organoids. Eventually, this progenitor population may be exploited for their existence in human and treatment of diabetes.

Methods

Key Resources Table

REAGENTS or RESOURCE	SOURCE	IDENTIFIER
Antibodies		
FITC anti mouse CD31 (clone MEC 13.3)	BD	cat#553372; RRID: AB_394818
FITC anti mouse CD45 (clone 30-F11)	BD	cat#553079; RRID: AB_394609
FITC anti mouse Ter119 (clone TER-119)	BD	cat#557915; RRID: AB_396936
Biotin anti mouse CD31 (clone MEC 13.3)	BD	cat#553371; RRID: AB_394817
Biotin anti mouse CD45 (clone 30-F11)	BD	cat#553080; RRID: AB_394610
Biotin anti mouse Ter119 (clone TER-119)	BD	cat#553672; RRID: AB_394985
PE anti mouse Procr (clone 1560)	eBioscience	cat#12-2012-82; RRID: AB_914317
APC anti mouse Procr (clone 1560)	eBioscience	cat#17-2012-82; RRID: AB_11041975
PE-Cy7 anti mouse EpCAM (clone G8.8)	Biolegend	cat#118216; RRID: AB_1236471
Rabbit anti-mouse Insulin (polyclonal)	Proteintech	cat#15848-1-AP; RRID: AB_10597100
Mouse anti-mouse Gcg (clone K79bB10)	Sigma	cat#G2654; RRID: AB_259852
Mouse anti-mouse Insulin (clone K36AC10)	Sigma	cat#I2018; RRID: AB_260137
Rabbit anti-mouse Sst (polyclonal)	Sigma	cat#HPA019472; RRID: AB_1857360

Mouse anti-mouse Sst (clone ICDCLS)	eBioscience	cat#13-9751-82; RRID: AB_2572823
Goat anti-mouse Ppy (polyclonal)	Sigma	cat#SAB2500747; RRID: AB_10611538
Rat anti-mouse EpCAM (clone G8.8)	eBioscience	cat#17-5791-82; RRID: AB_2716944
Rabbit anti-mouse Col1a1 (polyclonal)	Abcam	cat#ab34710; RRID: AB_731684
Chicken anti-GFP (polyclonal)	Thermo	cat#A10262; RRID: AB_2534023
Chemicals, Peptide and Recombinant Proteins		
RNAiso plus	Takara	cat#9109
HEPES	Sigma	cat#H4034
Type IV collagenase	Worthington	cat#LS004189
HBSS	Thermo	cat#C14175500CP
DMEM/F12	Hyclone	cat#SH30023.01B
DMEM 1640	Gibco	cat#C11875500
Histopaque-1077	Sigma	cat#10771
0.05% trypsin-EDTA	Gibco	cat#25300
DNase I	Sigma	cat#D4263
TSQ	Invitrogen	cat#M668
Matrigel	BD	cat#354230
Penicillin-Streptomycin	Thermo	cat#15140-122
B27	Thermo	cat#0080085-SA
ITS	Thermo	cat#41440
EGF	BD	cat#354001
Heparin	Sigma	cat#H4784
FGF2	Sigma	cat#SRP2092
VEGFa	R&D	cat#494-VE-005
Dispase	BD	cat#354235
Formaldehyde	Sigma	cat#F8775
Glutaraldehyde	Sigma	cat#G6257
NP-40	Sigma	cat#NP40S
$K_3[Fe(CN)_6]$	Sigma	cat#455946
$K_4[Fe(CN)_6]$	Sigma	cat#455989
$MgCl_2$	Sigma	cat#449172
X-gal	Takara	cat#9031
PFA	Sigma	cat#P6148
Triton-X 100	Sigma	cat#T9284
DAPI	Thermo	cat#D1306
OCT	Thermo	cat#D6506
Streptozotocin	Sigma	cat#V900890
Aqueous osmium tetraoxide	Sigma	cat#75632
Epon812	Sigma	cat#45347
Fluo4-AM	Thermo	cat#F14201
Fetal bovine serum	PAN	cat#P30-3302
Glucose	Sigma	cat#47829
Uranyl acetate	Sigma	cat#73943
Lead citrate	Sigma	cat#15326
DMSO	Sigma	cat#D2650
Critical Commercial Assays		
SYBR green Mix	Roche	cat#04913914001
PrimeScript RT master Mix	Takara	cat#RR036A
Ultra-sensitive insulin ELISA Kit	APLCO	cat#80-INSMSU-E01
Chromium Single cell 3' library kit v2	10X genomics	cat#PN-120233
OneTouch glucometer	Roche	cat#06988547022
Deposited Data		
Single-cell RNA-seq datasets	this paper	OEP000249, OEP000250
Experimental Models: Organisms/Strains		
Ngn3-Cre	Jackson lab	#006333
Rosa26-tdTomato	Jackson lab	#007909
FVB/NJ	Jackson lab	#001800

C57BL/6	Jackson lab	#000664
Nude	Jackson lab	#002019
Actin-DsRed	Jackson lab	#006051
ICR	SLAC	N/A
Procr$^{mGFP\text{-}2A\text{-}LacZ}$	this paper	N/A
Software and Algorithms		
Graphpad Prism 6	Graphpad software	www.graphpad.com
Adobe Photoshop CC2017	Adobe	www.adobe.com/product/photoshop.html
Adobe illustrator CC2017	Adobe	www.adobe.com/product/photoshop.html
Imaris v8.2	Imaris	imaris.oxinst.com
Rstudio	Rstudio	www.rstudio.com
Flow Jo vX	Flow Jo	www.flowjo.com
Cell Ranger v2	10X genomics	support.10xgenomics.com
Loupe Cell Browser	10X genomics	support.10xgenomics.com
Seurat R package v3	Butler et al., 2018	satijalab.org/seurat/get_started_v1_2.html
Monocle R package v2	Qiu et al., 2017	cole-trapnell-lab.github.io/monocle-release/
DAVID 6.8	LHRI	david.ncifcrf.gov/home.jsp
Oligonucleotides		
mouse Hprt qPCR forward primer: TCAGTCAACGGGGGACATAAA	this paper	N/A (SEQ ID NO: 1)
mouse Hprt qPCR reverse primer: GGGGCTGTACTGCTTAACCAG	this paper	N/A (SEQ ID NO: 2)
mouse Procr qPCR forward primer: CTCTCTGGGAAAACTCCTGACA	this paper	N/A (SEQ ID NO: 3)
mouse Procr qPCR reverse primer: CAGGGAGCAGCTAACAGTGA	this paper	N/A (SEQ ID NO: 4)
mouse Rspo1 qPCR forward primer: GCAACCCCGACATGAACAAAT	this paper	N/A (SEQ ID NO: 5)
mouse Rspo1 qPCR reverse primer: GGTGCTGTTAGCGGCTGTAG	this paper	N/A (SEQ ID NO: 6)
mouse Fgf1 qPCR forward primer: CAGCTCAGTGCGGAAAGTG	this paper	N/A (SEQ ID NO: 7)
mouse Fgf1 qPCR reverse primer: TGTCTGCGAGCCGTATAAAAG	this paper	N/A (SEQ ID NO: 8)
mouse Upk3b qPCR forward primer: AGACCTGATTGCCTACGTGC	this paper	N/A (SEQ ID NO: 9)
mouse Upk3b qPCR reverse primer: GGTGTCCTTAGTTGAGACATGCT	this paper	N/A (SEQ ID NO: 10)
mouse Hoxa5 qPCR forward primer: CTCATTTTGCGGTCGCTATCC	this paper	N/A (SEQ ID NO: 11)
mouse Hoxa5 qPCR reverse primer: ATCCATGCCATTGTAGCCGTA	this paper	N/A (SEQ ID NO: 12)
mouse Ins1 qPCR forward primer: TGGCTTCTTCTACACACCCAAG	this paper	N/A (SEQ ID NO: 13)
mouse Ins1 qPCR reverse primer: ACAATGCCACGCTTCTGCC	this paper	N/A (SEQ ID NO: 14)
mouse Mafa qPCR forward primer: GTCATCCGACTGAAACAGAA	this paper	N/A (SEQ ID NO: 15)
mouse Mafa qPCR reverse primer: GCCAACTTCTCGTATTTCTC	this paper	N/A (SEQ ID NO: 16)
mouse Ucn3 qPCR forward primer: AAGCCTCTCCCACAAGTTCTA	this paper	N/A (SEQ ID NO: 17)
mouse Ucn3 qPCR reverse primer: GAGGTGCGTTTGGTTGTCATC	this paper	N/A (SEQ ID NO: 18)
mouse Pdx1 qPCR forward primer:	this paper	N/A (SEQ ID NO: 19)

CCCCAGTTTACAAGCTCGCT mouse Pdx1 qPCR reverse primer: CTCGGTTCCATTCGGGAAAGG	this paper	N/A (SEQ ID NO: 20)

Experimental animals

Rosa26-tdTomato, *Ngn3-Cre*, *Actin-DsRed*, *Procr*$^{mGFP\text{-}2A\text{-}LacZ}$, wild-type CD1, C57BL/6, FVB/NJ, and Nude mice were used in this study. The *Procr*$^{mGFP\text{-}2A\text{-}Lacz}$ mouse strain was generated by knocking in a cassette of *mGFP-2A-LacZ* behind start codon of the *Procr* gene. The targeting construct, southern blot validation, and genotyping methods are shown in **FIGS. 3G-3I**. All the animal experimental procedures were approved by the Animal Care and Use Committee of Shanghai Institute of Biochemistry and Cell Biology, Chinese Academy of Sciences, with a project license number of IBCB0065.

Islets enrichment and purification

Mouse pancreas was perfused by injection of 2-4 ml digestion buffer (DMEM 1640 medium containing type IV collagenase (1000-1500 U/ml), 10% FBS (fetal bovine serum), and 25 mM HEPES) from the common duct. The pancreas was then dissected carefully to keep the integrity of the perfused tissue and then incubated at 37°C for 5-6 min followed by gently shaking for 3-6 min. The proper perfusion and digestion time are critical for islet yield and structure integrity. After digestion, the tissue was suspended in 20 ml HBSS with 10% FBS and rigorously shaken up and down 40 times within 20 seconds and followed by two HBSS washes. The digested tissue was then filtered with 500 μm cell strainers. To enrich islets, the filtered sample underwent density gradient centrifugation or was transferred under the microscope for hand-picking of islets. To prepare the density gradient centrifugation, the tissue was first re-suspended in 10 ml histopaque-1077 and slowly covered by 10 ml HBSS without breaking the interface. The re-suspended tissue was centrifuged at 2,400 rpm for 22 min with the slowest acceleration and braking to obtain the enriched islets compartment at the HBSS/histopaque-1077 interface. The purity of islets ranged from about 20% to 70% after the density gradient centrifugation step, depending on the quality of earlier perfusion and digestion process. To ensure high purity of islets, the samples were re-suspended in HBSS with 10% FBS for hand-pick. Islets with high purity were hand-picked under dissecting microscope for at least 3 rounds.

Islets X-gal staining

X-gal staining of purified islets was performed following the standard protocol with minor changes. In brief, islets were fixed in Fix A solution (1% Formaldehyde, 0.2% Glutaraldehyde, 0.02% NP-40 in PBS) at 4°C for 30 min, washed 3 times with PBS, then stained

in X-gal staining solution (1 mg/ml X-gal, 5 mM $K_3[Fe(CN)_6]$, 5 mM $K_4[Fe(CN)_6]$, 2 mM $MgCl_2$ in PBS) at room temperature for 5 h. After staining, islets were washed with PBS and the whole mount images were captured by Zeiss inverted microscope.

Immunofluorescence, whole mount staining and microscopy

To prepare samples for frozen sections, the dissected pancreas was fixed in 4% PFA at 4°C for 4 h, washed 3 times with PBS and then embedded with Optimum Cutting Temperature (OCT). Tissue sections were incubated with primary antibodies at 4 °C overnight, followed by washing in PBST (PBS + 0.1% Triton-X 100) and incubation with secondary antibodies and DAPI for 2 h at room temperature. The sections were then washed and mounted for confocal imaging.

To perform whole mount staining, islets or cultured organoids were fixed in 4% PFA at 4°C for 1 h followed by 3 PBS washes. The islets or cultured organoids were then blocked with the whole mount blocking buffer at room temperature for 1h. The blocking buffer contained 10% FBS in PBST. Primary antibodies were diluted in blocking buffer and incubated at 4°C overnight after washing 3 times with PBST. The secondary antibodies and DAPI were incubated at 4°C overnight. Islets or organoids were then washed and mounted with mounting medium for confocal imaging.

All confocal images were captured by Leica SP8 confocal detection system fitted on a Leica DMI6000 microscope.

Preparation of islets single cell suspension and FACS analysis

Purified islet samples were treated with 2 ml 0.05% trypsin-EDTA at 37°C for 4 min, followed by digestion with 0.1 mg/ml DNase I for 4 min and gently pipetting the sample about 20 times. The digested cells were filtered through a 70 μm cell strainer.

For FACS analysis and cell sorting, antibody incubation was performed on ice for 25 min in HBSS with 5% FBS at a dilution of 1:200. All analyses and sorting experiments were performed using FACS Jazz (Becton Dickinson). The purity of the sorted population was routinely checked and ensured to be more than 95%.

Co-culture and passage of mouse pancreatic islet organoids

200 μl Matrigel was coated in one well of a 48-well plate and transferred into 37°C ESCO incubator to gel. Mouse islet $EpCAM^+$, $Procr^{+/-}$ cells were FACS-sorted from hand-picked islets of wild-type CD1, C57BL/6, or FVB mice. $CD31^+$ endothelial cells (ECs) were FACS-isolated from inguinal fat pad or skin of *Actin-DsRed* mice. Islet cells and ECs were

mixed in a ratio of 1:3 and plated within 500 μl mouse organoid medium comprising DMEM/F12 (with penicillin-streptomycin) plus 2% B27, 1% ITS, 50 ng/ml EGF, 2 μg/ml heparin, 10 ng/ml FGF2, and 5 ng/ml VEGFa. The medium was refreshed every 2-3 days. To induce β-cell maturation, glucose challenges were performed. 20 mM glucose in HBSS was mixed with the organoid medium in a 1:1 ratio to prepare high glucose medium with a final concentration of 11 mM glucose. Organoids were first cultured for 12 h in low glucose (2 mM) followed by 12 h treatment in high glucose (11 mM) for 3 rounds.

Organoids were passaged every 6–14 days. For passage, organoids were released from the Matrigel using dispase (37°C for 40 min) and dissociated into single cells with 1 ml 0.05% trypsin-EDTA (37°C for 6-9 min). The single cell suspension was mixed with freshly isolated $CD31^+$ ECs in a 1:1 ratio followed by replating in a 1:4-6 split ratio.

Glucose-stimulated insulin secretion

About 100 mouse organoids at day 28 culture were used. The organoids were first washed 3 times with Krebs buffer, then pre-incubated in low glucose (2 mM) for 2 h to remove residual insulin. The organoids were then washed 2 times in Krebs buffer followed by incubation in low-glucose for 30 min. The supernatant samples were collected, and organoids were washed 2 times in Krebs buffer followed by incubation in high glucose (20 mM) for 30 min, and the supernatant samples were collected. This process was repeated twice. Insulin levels contained in the supernatant samples were analyzed using mouse Ultrasensitive Insulin ELISA kit following standard protocols.

Transmission electron microscope (TEM)

To prepare samples for TEM, organoids or islets were fixed in 1% glutaraldehyde in 0.1 M sodium cacodylate buffer (pH 7.4) at 4°C overnight and post-fixed in 2% aqueous osmium tetraoxide at 4°C for 1.5 h. The samples were then dehydrated in gradual ethanol (30% to 100%) and propylene oxide, embedded in Epon812, and cured for 48 h at 60 °C. 50 nm ultrathin sections were collected on 200 mesh copper grids and stained with uranyl acetate (10 min) and lead citrate (5 min) before examination by transmission electron microscopy. Images were captured with FEI Tecnai G2 Spirit Transmission electron microscope.

Ca^{2+} imaging

Organoids were harvested after dispase dissociation and plated on 35 mm glass bottom dishes without Matrigel for 24 h. The cell clusters were washed twice with Krebs buffer and incubated with Fluo4-AM for 30 min. The Fluo4-AM was washed out with Krebs buffer, and

the cell clusters were incubated in 37 °C for an additional 15 min without the dye. The cell clusters were then staged on a *Nikon AI* inverted confocal microscope for the acquisition of high-resolution time series images. Time series images were acquired every 10 s. Conditions for the progression of glucose challenges and time of stimulation during imaging were as follows: 5 min in low glucose (2 mM), Krebs wash, 5 min in high glucose (20 mM), Krebs wash. This sequential treatment was performed three times, and then a final incubation for 5 min with 2 mM glucose containing 30 mM KCl was performed. For the measurement of the average fluorescence intensity, images were quantified by Imaris software (v8.2.0).

Transplantation in diabetic mice

Nude recipients were induced diabetes with a single intraperitoneal injection of streptozotocin (STZ, 160 mg per kg in pH 4.5 citrate buffer) 7 days prior to engraft. Nonfasted blood glucose was measured from tail vein samples with a OneTouch glucometer to select the diabetic recipients with blood glucose level increased to about 20 mM. 300 mouse islets or 1,000 organoids (7th or 15th passage, at day 7 culture) were engrafted underneath the kidney capsule of recipient mice. Nonfasted blood glucose and body weight were routinely measured after engrafting for 1 month. Glucose tolerance tests (GTTs) were performed following standard protocol 1 month after engrafting. In brief, mice were fasted overnight and received an intraperitoneal injection of 2 g per kg body weight glucose. Blood glucose levels were measured at 0, 15, 30, 60, 90, and 120 min after glucose challenges. Serum samples before and after glucose injection were also collected and measured by ELISA. Recipients were sacrificed 1 month after engrafting, and the regenerated tissues were harvested for section and endocrine markers staining or digested into single cells for transmission electron microscope analysis and 10X sc RNA-sequencing.

RNA isolation and qPCR

RNA isolation of primary cells or organoids were performed following manufacturer instructions. Samples were lysed in RNAiso plus. Extracted RNA was reverse transcribed into cDNA using the Primerscript RT master kit. qPCR samples were prepared with SYBR Green Mixture and detected using Applied Biosystems Stepone Plus machine. All qPCR primers were listed in Key Resource Table above.

Single cell RNA sequencing with 10X genomics chromium platform

For the primary pancreatic single cell RNAseq, 3 biological replicates were performed with ICR mice used in replicate-1 and replicate-2 and C57BL/6 mice used in replicate-3. Islets

were enriched by density gradient centrifugation as described above. To minimize the damage of exocrine enzymes released during tissue dissociation, hand-picking of islets was not performed as a purification step (hand-picking islets required at least 1h at room temperature). Alternatively, TSQ (6 - methoxy - 8 - *p* - toluenesulfonamido - quilone) was used to enrich endocrine cells by FACS sorting (Huch et al., 2013). The cells were re-suspended in a solution containing TSQ (0.2 mg/ml). After FACS sorting, the endocrine (TSQ^+) and non-endocrine (TSQ^-) compartments were mixed together at a 1:1 ratio to form one sequencing sample. The cell quality was checked under the microscope before loading onto the 3′ library chip and cell viability was ensured to be higher than 75%, with over 90% of cells ensured as singlets. 13,000 single cells were loaded, with a recovery of 3,706; 2,349; and 1,111 cells. Respectively, for each biological replicate. The output ratio between endocrine and non-endocrine compartments was higher than 1:1. This may have been due to the relative larger size of acinar cells, leading to them being underrepresented when using the 10X Genomics method (see below).

To retrieve the grafted cells for sequencing, the transplant was carefully dissected from the kidney, followed by mincing and digestion of the transplant with trypsin-EDTA and DNase I. Dissociated single cells underwent FACS sort for TSQ^+ cells, which were sequenced and then compared to primary mouse islet cells. 13,000 engrafted cells pooled from 3 recipient mice (1 mouse transplanted with 7th organoid and 2 mice with 15th organoid) were loaded, with a recovery of 2,129 cells.

For the library preparation, single cells were loaded onto 3′ library chips for the Chromium Single Cell 3′ Library (V2) according to the manufacturer's recommendations (10X Genomics). In brief, single cells were partitioned into gel beads in emulsion in the GemCode instrument with cell lysis and barcoded reverse transcription of RNA, followed by amplification, shearing, and 5′ adaptor and sample index attachment. Libraries were sequenced on an Illumina Hiseq PE150.

Filtering (demultiplexing), alignment to the mm10 transcriptome, and unique molecular identifier (UMI)-collapsing were performed using the Cell Ranger (V2) pipeline (10X Genomics). The Seurat 3 R package was used for data integration, analysis, and visualization as described in Butler et al., Nat Biotechnol *36*, 411-420 (2018), the contents of which are hereby incorporated by reference in their entirety. For detail, Seurat object was created by selecting genes expressed in at least two cells and cells that had at least 300 detected **genes** and 3,000 detected UMIs. Only six cells were filtered from replicate-3 primary pancreatic sample (from 1,111 cells to 1,105 cells). In analyses involving the E14.5 $Ngn3^+$ single cell RNAseq data from Byrnes et al., Nat Commun *9*, 3922 (2018) and Scavuzzo et al. Nat Commun *9*, 3356 (2018) (the contents of each are hereby incorporated by reference in their entirety), same filtering standards

were used for Seurat objects creation and $Ngn3^+$ cells were filtered by Neurog3 UMI>0. Variable genes were found by "**vst**" method, and the top 2,000 genes were selected for principal component analysis (PCA). Dimensionality reduction was performed with the t-stochastic neighboring embedding method (tSNE). The top 20 principal components (PCs) were used. Cell clustering was based on shared-nearest neighbor (SNN) method, and the resolution value was set to 0.9 for primary cells or primary V.S. engrafted cells and 0.8 for primary V.S. E14.5 $Ngn3^+$ cells. Some clusters were put together as one cell type based on the similarity of the expression profiles and marker genes. For data display, violin plots, heat maps, dot plots, and individual tSNE plots for the given genes were generated by using the Seurat toolkit VlnPlot, DoHeatmap, DotPlot, and FeaturePlot functions, respectively.

Pseudo temporal analysis of primary pancreas cells was performed using the Monocle 2 R package as described in Qui et al., Nat Methods *14*, 979-982 (2017), the contents of which are incorporated by reference in their entirety. Alpha, beta, delta, PP and new population cells were directly transferred from Seurat to Monocle 2 for the creation of the monocle CellDataSet object, and 321 cells were further filtered. The top 2,000 variable genes identified by Seurat were used as ordering genes. The "DDRTree" method was used for dimensionality reduction, and the max_components was set to 2 to generate one branching point. The split heat map was generated from selected genes showing significant change through pseudotime (q-value<E-10).

Statistics

Unpaired, two-tailed Student's t-test was performed and the p-value was calculated using GraphPad PRISM 6 when two groups of samples were compared. For all experiments with error bars, the std. error of mean (S.E.M) was calculated to indicate the variation within each experiment.

Data availability

Sc RNAseq data is available at the website www.biosino.org/node/index, with access NO. OEP000249 and OEP000250.

Example 2: Long-term culture and expansion of human pancreatic islet organoids

Transplantations of islet and whole pancreas from cadaveric organ donation provided the proof-of-concept of glucose homeostasis restoration after replenishment of the deficiency of β cells responsible for the disease (Lysy et al., 2013). Scarcity of donors has led to the search for strategies of generating β-cells in vitro. It has proven challenging to make new β-cells in vitro. Cell therapy for diabetes requires identifying candidate cell sources and new culture strategies.

Our previous study (see Example 1) in murine pancreas identified a new population of pro-endocrine progenitor cells. The cells do not express pancreas differentiation markers and can be sorted from islets based on surface Protein C receptor (Procr) expression. These cells can form islet-like organoid in culture that are glucose-responsive, insulin-secreting and can be expanded for long-term. In the current study, we exploited the existence of such a pro-endocrine progenitor population in human and their implication in generating new human beta cells in vitro.

To probe the existence of $PROCR^+$ cells in human islet, immunostaining of PROCR in sections of human pancreas was performed. A small population of $PROCR^+$ islet cells were detected within islets (**FIG. 8A**). Interestingly, these $PROCR^+$ cells did not express endocrine differentiation markers (**FIG. 8A**), similar to its counterpart in mice. $PROCR^+$ cells were also found in the exocrine compartment of the human pancreas (**FIG. 8B**).

Next, these $PROCR^+$ islet cells were isolated and cultured. The human islets were obtained by collagenase perfusion and density gradient centrifugation, followed by hand-pick purification. Due to the cleavage or endocytosis of PROCR from the cell surface during collagenase perfusion, we were not able to isolate $PROCR^+$ cells from primary islets. However, by experimenting collagenase and other conditions, we believe that $PROCR^+$ cells can be isolated using an anti-PROCR antibody from human islets, similar to mouse experiments in Example 1. Nonetheless, total islet cells from human were cultured. To this end, dissociated single cells were stained with TSQ (6 - methoxy - 8 - *p* - toluenesulfonamido - quilone, a fluorescent zinc indicator, for enriching endocrine cells) and underwent positive selection for TSQ^+ cells by FACS sorting. Representative FACS profile showed three different levels of TSQ uptake in human islet samples, TSQ-high, TSQ-low, and TSQ-negative (**FIG. 9A**). These three populations were sorted, followed by cytospin and staining with endocrine (INS, GCG) and exocrine (AMY, KRT19) markers. It was found that the TSQ-high fraction also showed enriched exocrine markers expression (**FIG. 9B**), consistent with the findings in mouse.

Next, TSQ-high cells (endocrine/islet cells) in 3D culture from various donor tissues were sorted and cultured (**FIG. 9C**). To establish a culture medium for human islet cells, on the base of a basic medium used in mouse islet organoid culture (DMEM/F12 + EGF + ITS + FGF2 + Heparin + B27), small molecules and growth factors were screened, including Wnt agonists CHIR99021 or NGS (a Wnt pathway activation peptide), TGF-beta pathway inhibitors SB431542 or A83-01, Rho-ROCK pathway inhibitor Y27632, Bmp agonist Bmp2, or Bmp inhibitor Noggin for the ability to support growth (**FIG. 10A-10C**). Based on the colony formation rate and colony/organoid size, a growth-promoting condition (DMEM/F12 + EGF + ITS + FGF2 + Heparin + Y27632 + B27 + CHIR99021 + Noggin + A83-01) was established,

which required activation of Wnt, FGF, and BMP signaling and inhibition of the TGFβ and Rho-ROCK pathways (**FIG. 10C**). Activating Integrin beta 1 antibody (1nM) can also help growth. Organoids formed in this culture conditions contain majority of INS^+ β-like cells and few GCG^+ α-like cells (**FIG. 10D**), resemblance of the cellular composition of human islets.

Islet organoids were generated from three different donors. The organoid forming efficiency was consistently about 0.8% (**FIG. 11A**), suggesting that the organoids were unlikely formed from contaminated non-endocrine cells. Indeed, endocrine islet organoids and exocrine ductal organoid displayed distinct phenotypes. Islet organoids were more compact, with a "bunch-of-grapes" structure similar to islets (**FIG. 11B (day 12)**), whereas ductal organoids exhibited a typical "ring-like" structure (**FIG. 11B (day 14)**). At culture day 18, the organoid sizes ranged from 50-300 μm (**FIG. 11C**). When dissociated to single cells and replated in the same culture condition, the organoids expanded for 3-9 folds in number during each passage (**FIG. 11C**), with a slight decrease in average sizes in passaged organoid and maintained stable for many passages (**FIG. 11C-11D**).

Insulin (INS) expression was examined as an indication of functional β-cell formation. Whole mount immunostaining was performed in primary organoids. The majority of organoid cells exhibited high levels of insulin (**FIGs. 12A-12B**). These organoids also contained few GCG^+ alpha-like cells (**FIG. 12A-12B**), similar to the observation in mouse islet organoids. Unlike ductal organoids that exhibited ductal marker SOX9 expression (**FIG. 12C**), the islet organoids did not express SOX9 (**FIGs. 12A-12B**). In addition, these islet organoids could respond acutely to glucose. The organoid cells rapidly increased cytosolic Ca^{2+} concentrations in response to glucose and subsequently returned to baseline (**FIG. 12D**). The insulin expression was also confirmed in passaged organoids (**FIG. 12E**), suggesting that β-cell differentiation can be achieved after long-term culture and expansion.

EdU incorporation assay indicated the existence of population of proliferative cells within the organoids (**FIG. 13A**), suggesting the coexistence of proliferating/undifferentiated cells and differentiated hormone-expressing cells within the organoids. PROCR expression in these organoids was analyzed by FACS. About 2.5% of cells in human islet organoids were $Procr^+$ (**FIG. 13B**), similar to the Procr+ cell proportion found in mouse islet organoids. Furthermore, $Procr^+$ cells in the organoid exhibited about 10-fold higher EdU incorporation compared to $Procr^-$ cells (**FIG. 13C**), suggesting that these cells are more proliferative and could be the major contributor of organoid formation.

Together, this data shows that the methods and composition described herein can generate functional human β-like cells *in vitro*. Isolated human islet cells can grow in clonal density into islet-like organoids, which comprise various endocrine cell types and are capable of

glucose-sensing and insulin secretion. These organoids can be exponentially expanded *in vitro* by serial passage for long-term.

Methods

Patients and clinical specimens

All human islets or specimens were obtained from Changzheng Hospital. The use of samples for research was approved by ethical committees and informed consent were obtained from donors.

Statistics

Unpaired, two-tailed Student's t-test was performed, and the p-value was calculated using GraphPad PRISM 6 when two groups of samples were compared. For all experiments with error bars, the standard error of mean (S.E.M) was calculated to indicate the variation within each experiment.

Islets enrichment and purification

Human islets enrichment was performed by Changzheng Hospital with standard protocol (perfusion followed by density gradient centrifugation). Islets with high purity were used for clinical transplantation. Islets with lower purity (~5%-20%) were further enriched by hand pick and used in this study. The purity of islets ranged from ~ 20%-70% based on TSQ staining and FACS analysis.

Preparation of islets single cell suspension and FACS analysis

The single cell suspension was obtained by treating purified islets with 2 ml 0.05% trypsin-EDTA at 37°C for 5 min and 0.1 mg ml^{-1} DNase I for further 5 min, gently pipetting for about 20 times. Then cells were filtered through 70 μm cell strainer.

For FACS analysis of PROCR, antibody incubation was performed on ice for 25 min in HBSS with 5% FBS at a dilution of 1:200. To gate out the exocrine and other cell lineages, dissociated single cells were re-suspended in a solution containing TSQ (0.2 mg ml^{-1}). The TSQ-high cells were sorted for culture to ensure the generated organoids were endocrine-derived. All analysis and sorting experiments were performed using FACS Jazz machine (Becton Dickinson). The purity of the sorted population was routinely checked and ensured to be more than 95%.

Establishment of culture system for human islet organoid generation and passage

200 μl Matrigel was coated in one well of 48-well plate and transferred into 37°C ESCO

incubator for solidification. TSQ-high human pancreas cells were FACS sorted and plated within 500 μl human organoid medium consists of DMEM/F12 (with Penicillin-Streptomycin) plus 2% B27, 1% ITS, 50 ng ml^{-1} EGF, 2 μg ml^{-1} heparin, 10 ng ml^{-1} FGF2, 3 μM CHIR99021, 2 μM A83-01, 100 ng ml^{-1} Noggin, 10 μM Y27632. The medium was refreshed every 2-3 days.

Organoids were passaged every 7–21 days. For passage, organoids were released from the Matrigel using dispase (37°C for 30 min) and dissociated into single cells with 1 ml 0.05% trypsin-EDTA (37°C for 3-6 min). Then single cells were re-suspended in medium and plated in a split ratio of 1:3-1:8.

Immunofluorescence, whole mount staining and microscopy

To prepare samples for frozen sections, the dissected pancreas was fixed in 4% PFA at 4°C for 4 h, washed with PBS for 3 times and then embedded with Optimum Cutting Temperature (OCT). Tissue sections were incubated with primary antibodies at 4 °C overnight, followed by washing in PBST (PBS+0.1% Triton-X 100), incubation with secondary antibodies and DAPI for 2 h at room temperature, then sections were washed and mounted for confocal imaging.

To perform whole-mount staining, human islets or cultured organoids were fixed in 4% PFA at 4°C for 1 h, followed by 3 times of PBS washing, then blocked with the whole mount blocking buffer at room temperature for 1h. The blocking buffer contained 10% FBS in PBST. Primary antibodies were diluted in blocking buffer and incubated at 4°C overnight, after washing with PBST for 3 times, the secondary antibodies and DAPI were incubated at 4°C overnight. Islets or organoids were then washed and mounted with mounting medium for confocal imaging.

All confocal images were captured by Leica SP8 confocal detection system fitted on a Leica DMI6000 microscope.

OTHER EMBODIMENTS

From the foregoing description, it will be apparent that variations and modifications may be made to the invention described herein to adopt it to various usages and conditions. Such embodiments are also within the scope of the following claims.

The recitation of a listing of elements in any definition of a variable herein includes definitions of that variable as any single element or combination (or subcombination) of listed elements. The recitation of an embodiment herein includes that embodiment as any single embodiment or in combination with any other embodiments or portions thereof.

All patents and publications mentioned in this specification are herein incorporated by

reference to the same extent as if each independent patent and publication was specifically and individually indicated to be incorporated by reference.

Reference

Al-Hasani, K., Pfeifer, A., Courtney, M., Ben-Othman, N., Gjernes, E., Vieira, A., Druelle, N., Avolio, F., Ravassard, P., Leuckx, G., *et al.* (2013). Adult duct-lining cells can reprogram into beta-like cells able to counter repeated cycles of toxin-induced diabetes. Dev Cell *26*, 86-100.

Balazs, A.B., Fabian, A.J., Esmon, C.T., and Mulligan, R.C. (2006). Endothelial protein C receptor (CD201) explicitly identifies hematopoietic stem cells in murine bone marrow. Blood *107*, 2317-2321.

Bonner-Weir, S., Taneja, M., Weir, G.C., Tatarkiewicz, K., Song, K.H., Sharma, A., and O'Neil, J.J. (2000). In vitro cultivation of human islets from expanded ductal tissue. Proc Natl Acad Sci U S A *97*, 7999-8004.

Butler, A., Hoffman, P., Smibert, P., Papalexi, E., and Satija, R. (2018). Integrating single-cell transcriptomic data across different conditions, technologies, and species. Nat Biotechnol *36*, 411-420.

Byrnes, L.E., Wong, D.M., Subramaniam, M., Meyer, N.P., Gilchrist, C.L., Knox, S.M., Tward, A.D., Ye, C.J., and Sneddon, J.B. (2018). Lineage dynamics of murine pancreatic development at single-cell resolution. Nat Commun *9*, 3922.

Cheng, X., Ying, L., Lu, L., Galvao, A.M., Mills, J.A., Lin, H.C., Kotton, D.N., Shen, S.S., Nostro, M.C., Choi, J.K., *et al.* (2012). Self-renewing endodermal progenitor lines generated from human pluripotent stem cells. Cell Stem Cell *10*, 371-384.

Criscimanna, A., Speicher, J.A., Houshmand, G., Shiota, C., Prasadan, K., Ji, B., Logsdon, C.D., Gittes, G.K., and Esni, F. (2011). Duct cells contribute to regeneration of endocrine and acinar cells following pancreatic damage in adult mice. Gastroenterology *141*, 1451-1462, 1462 e1451-1456.

Fares, I., Chagraoui, J., Lehnertz, B., MacRae, T., Mayotte, N., Tomellini, E., Aubert, L., Roux, P.P., and Sauvageau, G. (2017). EPCR expression marks UM171-expanded CD34+ cord blood stem cells. Blood *129*, 3344-3351.

Furuyama, K., Kawaguchi, Y., Akiyama, H., Horiguchi, M., Kodama, S., Kuhara, T., Hosokawa, S., Elbahrawy, A., Soeda, T., Koizumi, M., *et al.* (2011). Continuous cell supply from a Sox9-expressing progenitor zone in adult liver, exocrine pancreas and intestine. Nat Genet *43*, 34-41.

Gao, R., Ustinov, J., Korsgren, O., and Otonkoski, T. (2005). In vitro neogenesis of human islets reflects the plasticity of differentiated human pancreatic cells. Diabetologia *48*, 2296-2304.

Gehart, H., van Es, J.H., Hamer, K., Beumer, J., Kretzschmar, K., Dekkers, J.F., Rios, A., and Clevers, H. (2019). Identification of Enteroendocrine Regulators by Real-Time Single-Cell Differentiation Mapping. Cell *176*, 1158-1173 e1116.

Gershengorn, M.C., Hardikar, A.A., Wei, C., Geras-Raaka, E., Marcus-Samuels, B., and Raaka, B.M. (2004). Epithelial-to-mesenchymal transition generates proliferative human islet precursor cells. Science *306*, 2261-2264.

Greggio, C., De Franceschi, F., Figueiredo-Larsen, M., Gobaa, S., Ranga, A., Semb, H., Lutolf, M., and Grapin-Botton, A. (2013). Artificial three-dimensional niches deconstruct pancreas development in vitro. Development *140*, 4452-4462.

Gu, G., Dubauskaite, J., and Melton, D.A. (2002). Direct evidence for the pancreatic lineage: NGN3+ cells are islet progenitors and are distinct from duct progenitors. Development *129*, 2447-2457.

Hardikar, A.A. (2016). Pancreatic Islet Biology, 1 edn (Switzerland: Springer International Publishing).

Huch, M., Bonfanti, P., Boj, S.F., Sato, T., Loomans, C.J., van de Wetering, M., Sojoodi, M., Li, V.S., Schuijers, J., Gracanin, A., *et al.* (2013). Unlimited in vitro expansion of adult bi-potent pancreas progenitors through the Lgr5/R-spondin axis. EMBO J *32*, 2708-2721.

Inada, A., Nienaber, C., Katsuta, H., Fujitani, Y., Levine, J., Morita, R., Sharma, A., and Bonner-Weir, S. (2008). Carbonic anhydrase II-positive pancreatic cells are progenitors for both endocrine and exocrine pancreas after birth. Proc Natl Acad Sci U S A *105*, 19915-19919.

Iwasaki, H., Arai, F., Kubota, Y., Dahl, M., and Suda, T. (2010). Endothelial protein C receptor-expressing hematopoietic stem cells reside in the perisinusoidal niche in fetal liver. Blood *116*, 544-553.

Jin, L., Feng, T., Shih, H.P., Zerda, R., Luo, A., Hsu, J., Mahdavi, A., Sander, M., Tirrell, D.A., Riggs, A.D., *et al.* (2013). Colony-forming cells in the adult mouse pancreas are expandable in Matrigel and form endocrine/acinar colonies in laminin hydrogel. Proc Natl Acad Sci U S A *110*, 3907-3912.

Kopp, J.L., Dubois, C.L., Schaffer, A.E., Hao, E., Shih, H.P., Seymour, P.A., Ma, J., and Sander, M. (2011). Sox9+ ductal cells are multipotent progenitors throughout development but do not produce new endocrine cells in the normal or injured adult pancreas. Development *138*, 653-665.

Lammert, E., Cleaver, O., and Melton, D. (2001). Induction of pancreatic differentiation by signals from blood vessels. Science *294*, 564-567.

Lysy, P.A., Weir, G.C., and Bonner-Weir, S. (2013). Making beta cells from adult cells within the pancreas. Curr Diab Rep *13*, 695-703.

Minami, K., Okuno, M., Miyawaki, K., Okumachi, A., Ishizaki, K., Oyama, K., Kawaguchi, M., Ishizuka, N., Iwanaga, T., and Seino, S. (2005). Lineage tracing and characterization of insulin-secreting cells generated from adult pancreatic acinar cells. Proc Natl Acad Sci U S A *102*, 15116-15121.

Mohammed, J.S., Wang, Y., Harvat, T.A., Oberholzer, J., and Eddington, D.T. (2009). Microfluidic device for multimodal characterization of pancreatic islets. Lab Chip *9*, 97-106.

Ouziel-Yahalom, L., Zalzman, M., Anker-Kitai, L., Knoller, S., Bar, Y., Glandt, M., Herold, K., and Efrat, S. (2006). Expansion and redifferentiation of adult human pancreatic islet cells. Biochem Biophys Res Commun *341*, 291-298.

Pagliuca, F.W., Millman, J.R., Gurtler, M., Segel, M., Van Dervort, A., Ryu, J.H., Peterson, Q.P., Greiner, D., and Melton, D.A. (2014). Generation of functional human pancreatic beta cells in vitro. Cell *159*, 428-439.

Pan, F.C., Bankaitis, E.D., Boyer, D., Xu, X., Van de Casteele, M., Magnuson, M.A., Heimberg, H., and Wright, C.V. (2013). Spatiotemporal patterns of multipotentiality in Ptf1a-expressing cells during pancreas organogenesis and injury-induced facultative restoration. Development *140*, 751-764.

Pan, F.C., and Wright, C. (2011). Pancreas organogenesis: from bud to plexus to gland. Dev Dyn *240*, 530-565.

Qiu, X., Mao, Q., Tang, Y., Wang, L., Chawla, R., Pliner, H.A., and Trapnell, C. (2017). Reversed graph embedding resolves complex single-cell trajectories. Nat Methods *14*, 979-982.

Ramiya, V.K., Maraist, M., Arfors, K.E., Schatz, D.A., Peck, A.B., and Cornelius, J.G. (2000). Reversal of insulin-dependent diabetes using islets generated in vitro from pancreatic stem cells. Nat Med *6*, 278-282.

Rezania, A., Bruin, J.E., Arora, P., Rubin, A., Batushansky, I., Asadi, A., O'Dwyer, S., Quiskamp, N., Mojibian, M., Albrecht, T., *et al.* (2014). Reversal of diabetes with insulin-producing cells derived in vitro from human pluripotent stem cells. Nat Biotechnol *32*, 1121-1133.

Rovira, M., Scott, S.G., Liss, A.S., Jensen, J., Thayer, S.P., and Leach, S.D. (2010). Isolation and characterization of centroacinar/terminal ductal progenitor cells in adult mouse pancreas.

Proc Natl Acad Sci U S A *107*, 75-80.
Rukstalis, J.M., and Habener, J.F. (2007). Snail2, a mediator of epithelial-mesenchymal transitions, expressed in progenitor cells of the developing endocrine pancreas. Gene Expr Patterns *7*, 471-479.
Russ, H.A., Bar, Y., Ravassard, P., and Efrat, S. (2008). In vitro proliferation of cells derived from adult human beta-cells revealed by cell-lineage tracing. Diabetes *57*, 1575-1583.
Scavuzzo, M.A., Hill, M.C., Chmielowiec, J., Yang, D., Teaw, J., Sheng, K., Kong, Y., Bettini, M., Zong, C., Martin, J.F., *et al.* (2018). Endocrine lineage biases arise in temporally distinct endocrine progenitors during pancreatic morphogenesis. Nat Commun *9*, 3356.
Seaberg, R.M., Smukler, S.R., Kieffer, T.J., Enikolopov, G., Asghar, Z., Wheeler, M.B., Korbutt, G., and van der Kooy, D. (2004). Clonal identification of multipotent precursors from adult mouse pancreas that generate neural and pancreatic lineages. Nat Biotechnol *22*, 1115-1124.
Smukler, S.R., Arntfield, M.E., Razavi, R., Bikopoulos, G., Karpowicz, P., Seaberg, R., Dai, F., Lee, S., Ahrens, R., Fraser, P.E., *et al.* (2011). The adult mouse and human pancreas contain rare multipotent stem cells that express insulin. Cell Stem Cell *8*, 281-293.
Sneddon, J.B., Borowiak, M., and Melton, D.A. (2012). Self-renewal of embryonic-stem-cell-derived progenitors by organ-matched mesenchyme. Nature *491*, 765-768.
Sugiyama, T., Benitez, C.M., Ghodasara, A., Liu, L., McLean, G.W., Lee, J., Blauwkamp, T.A., Nusse, R., Wright, C.V., Gu, G., *et al.* (2013). Reconstituting pancreas development from purified progenitor cells reveals genes essential for islet differentiation. Proc Natl Acad Sci U S A *110*, 12691-12696.
Van de Casteele, M., Leuckx, G., Baeyens, L., Cai, Y., Yuchi, Y., Coppens, V., De Groef, S., Eriksson, M., Svensson, C., Ahlgren, U., *et al.* (2013). Neurogenin 3+ cells contribute to beta-cell neogenesis and proliferation in injured adult mouse pancreas. Cell Death Dis *4*, e523.
Wang, D., Cai, C., Dong, X., Yu, Q.C., Zhang, X.O., Yang, L., and Zeng, Y.A. (2015). Identification of multipotent mammary stem cells by protein C receptor expression. Nature *517*, 81-84.
Xu, X., D'Hoker, J., Stange, G., Bonne, S., De Leu, N., Xiao, X., Van de Casteele, M., Mellitzer, G., Ling, Z., Pipeleers, D., *et al.* (2008). Beta cells can be generated from endogenous progenitors in injured adult mouse pancreas. Cell *132*, 197-207.
Yatoh, S., Dodge, R., Akashi, T., Omer, A., Sharma, A., Weir, G.C., and Bonner-Weir, S. (2007). Differentiation of affinity-purified human pancreatic duct cells to beta-cells. Diabetes *56*, 1802-1809.
Yu, Q.C., Song, W., Wang, D., and Zeng, Y.A. (2016). Identification of blood vascular endothelial stem cells by the expression of protein C receptor. Cell Res *26*, 1079-1098.
Zhou, F., Li, X., Wang, W., Zhu, P., Zhou, J., He, W., Ding, M., Xiong, F., Zheng, X., Li, Z., *et al.* (2016). Tracing haematopoietic stem cell formation at single-cell resolution. Nature *533*, 487-492.

CLAIMS

1. A method of obtaining pro-endocrine progenitor cells, comprising:

contacting, *in vitro*, adult islet cells with an anti-Procr antibody or antigen-binding fragment thereof; and

isolating a $Procr^+$ pro-endocrine progenitor cell that binds to the anti-Procr antibody or fragment thereof, preferably using fluorescence assisted cell sorting (FACS).

2. A method of producing a pancreatic organoid *in vitro*, comprising:

providing a pro-endocrine progenitor cell isolated from adult islet cells; and

3D culturing *in vitro* the pro-endocrine progenitor cell in an organoid medium under conditions suitable to produce a pancreatic organoid comprising functional β-cells and/or β-like cells, wherein preferably the organoid medium further comprises a three-dimensional matrix such as Matrigel™.

3. The method of claim 1 or 2, wherein the adult islet cells are from human.

4. The method of claim 3, wherein the organoid medium comprises DMEM/F12 supplemented with one or more of: 1-5% (e.g., 2%) B27, 0.1-5% (e.g., 1%) ITS, 10-200 (e.g., 50) ng ml^{-1} EGF, 0.1-5 (e.g., 2) μg ml^{-1} heparin, 1-50 (e.g., 10) ng ml^{-1} FGF2, 1-10 (e.g., 3) μM Wnt agonist such as CHIR99021, 1-100 (e.g., 30) ng/ml Wnt surrogate such as NGS, 1-10 (e.g., 2) μM TGF-beta pathway inhibitors such as SB431542 or A83-01A83-01, 10-500 (e.g., 100) ng ml^{-1} Bmp inhibitor such as Noggin, 1-50 (e.g., 10) μM Rock inhibitor such as Y27632.

5. The method of claim 1 or 2, wherein the adult islet cells are from mouse, wherein the 3D culturing comprises co-culturing with a plurality of endothelial cells, and wherein the pro-endocrine progenitor cell expresses one or more of, preferably all of, Procr, Rspo1, Fgf1, Upk3B, and Hoxa5.

6. The method of claim 5, wherein the culture medium comprises DMEM/F12 supplemented with one or more of: 1-5% (e.g., 2%) B27, 0.1-5% (e.g., 1%) ITS, 10-200 (e.g., 50) ng ml^{-1} EGF, 0.1-5 (e.g., 2) μg ml^{-1} heparin, 1-50 (e.g., 10) ng ml^{-1} FGF2, and 1-20 (e.g., 5) ng ml^{-1} VEGFa.

7. The method of any one of claims 2-6, wherein the pro-endocrine progenitor cell expresses Procr.

8. The method of any one of claims 2-7, wherein the co-culturing step comprises culturing until the pro-endocrine progenitor cell forms a colony of about 100-200 μm in diameter, and continuously culturing the colony to form the mouse pancreatic organoid of about 150-500 μm in diameter.

9. A method of obtaining pancreatic organoids *in vitro*, comprising:

enriching endocrine cells from adult pancreas, preferably by one or more of the following methods: (1) staining dissociated adult pancreas cells with TSQ (6 - methoxy - 8 - *p* - toluenesulfonamido - quilone), followed by FACS; (2) contacting, *in vitro*, dissociated adult mouse islet cells with an anti-Procr antibody or antigen-binding fragment thereof, followed by FACS; and (3) hand-picking and dissociating islets from adult pancreas;

3D culturing the enriched endocrine cells in an organoid medium under conditions suitable to produce a pancreatic organoid comprising functional β-cells and/or β-like cells, wherein preferably the organoid medium further comprises a three-dimensional matrix.

10. The method of claim 9, wherein the organoid medium comprises Matrigel™ and DMEM/F12 supplemented with one or more of: 1-5% (e.g., 2%) B27, 0.1-5% (e.g., 1%) ITS, 10-200 (e.g., 50) ng ml^{-1} EGF, 0.1-5 (e.g., 2) μg ml^{-1} heparin, 1-50 (e.g., 10) ng ml^{-1} FGF2, 1-10 (e.g., 3) μM Wnt agonist such as CHIR99021, 1-100 (e.g., 30) ng/ml Wnt surrogate such as NGS, 1-10 (e.g., 2) μM TGF-beta pathway inhibitors such as SB431542 or A83-01A83-01, 10-500 (e.g., 100) ng ml^{-1} Bmp inhibitor such as Noggin, 1-50 (e.g., 10) μM Rock inhibitor such as Y27632.

11. The method of claim 9 or 10, wherein the pancreatic organoid is about 50-500 or about 100-300 μm in diameter.

12. The method of any one of claims 2-12, further comprising expanding the organoid through passaging for at least 10 times, at least 20 times, or at least 30 times.

13. The method of claim 12, further comprising culturing the expanded organoids for about 1-4 weeks to generate mature organoids.

14. The method of claim 13, wherein the mature organoid senses glucose and produces and secretes insulin in response to glucose.

15. A composition comprising a plurality of pro-endocrine progenitor cells isolated from adult islet cells, a culture medium and optionally a plurality of endothelial cells.

16. The composition of claim 15, wherein the pro-endocrine progenitor cells express Procr.

17. The composition of claim 16, wherein when the adult islet cells are derived from mouse, the pro-endocrine progenitor cells express one or more of Procr, Rspo1, Fgf1, Upk3B, and Hoxa5.

18. The composition of any one of claims 15-17, wherein the culture medium further comprises a three-dimensional matrix, preferably Matrigel™.

19. The composition of any one of claims 15-18, wherein the adult islet cells are from mouse

and wherein the culture medium comprises DMEM/F12 supplemented with one or more of: 1-5% (e.g., 2%) B27, 0.1-5% (e.g., 1%) ITS, 10-200 (e.g., 50) ng ml^{-1} EGF, 0.1-5 (e.g., 2) μg ml^{-1} heparin, 1-50 (e.g., 10) ng ml^{-1} FGF2, and 1-20 (e.g., 5) ng ml^{-1} VEGFa..

20. The composition of any one of claims 15-18, wherein the adult islet cells are from human and wherein the culture medium comprises DMEM/F12 supplemented with one or more of: 1-5% (e.g., 2%) B27, 0.1-5% (e.g., 1%) ITS, 10-200 (e.g., 50) ng ml^{-1} EGF, 0.1-5 (e.g., 2) μg ml^{-1} heparin, 1-50 (e.g., 10) ng ml^{-1} FGF2, 1-10 (e.g., 3) μM Wnt agonist such as CHIR99021, 1-100 (e.g., 30) ng/ml Wnt surrogate such as NGS, 1-10 (e.g., 2) μM TGF-beta pathway inhibitors such as SB431542 or A83-01A83-01, 10-500 (e.g., 100) ng ml^{-1} Bmp inhibitor such as Noggin, 1-50 (e.g., 10) μM Rock inhibitor such as Y27632.

21. A pancreatic organoid comprising functional β-cells and/or β-like cells differentiated in vitro from pro-endocrine progenitor cells, wherein the pro-endocrine progenitor cells are isolated from adult islet cells.

22. The organoid of claim 21, wherein the organoid senses glucose and produces and secretes insulin in response to glucose.

23. The organoid of claim 21 or 22, wherein the organoid is about 50-500 μm in diameter.

24. Use of the organoid of any one of claims 21-23, for treating or preventing diabetes, or for screening in vitro an agent for treating or preventing diabetes.

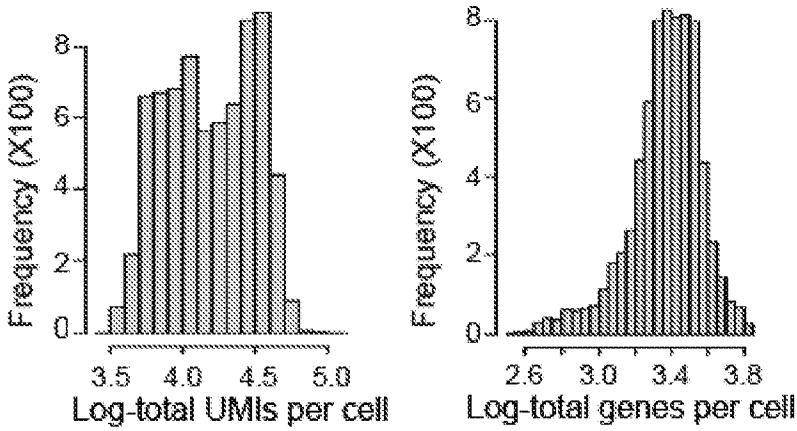


FIG. 1A

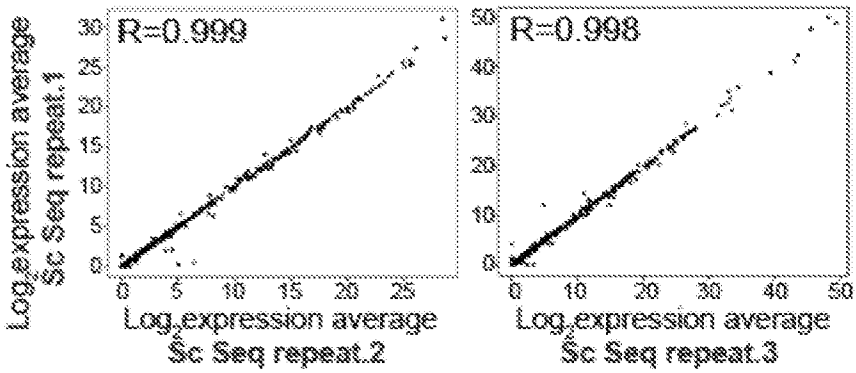


FIG. 1B

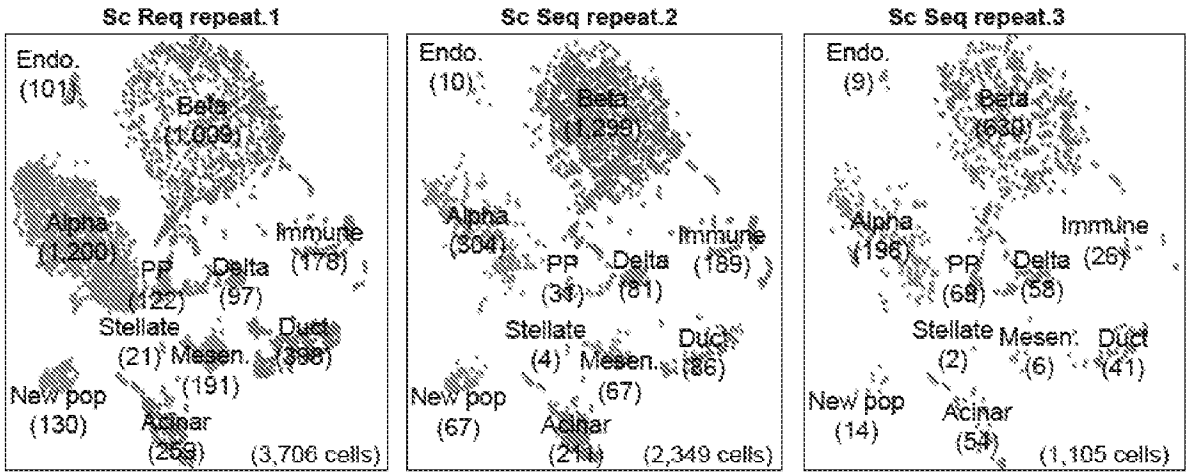


FIG. 1C

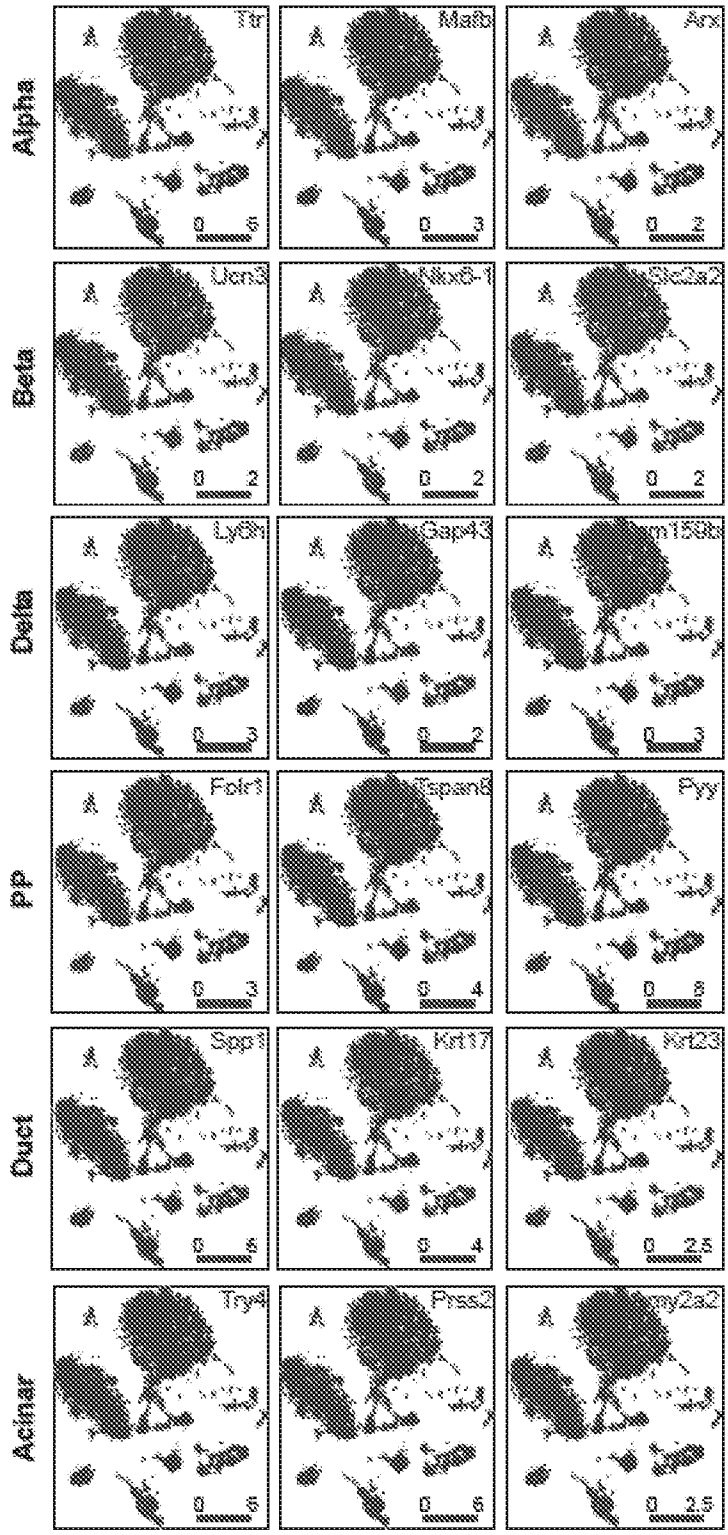

Alpha
Beta
Delta
PP
Duct
Acinar
Ttr
Mafb
Arx
Ucn3
Kcnb1
Slc2a2
Ly6h
Gap43
m153b
Fdrl1
Tspan8
Pyy
Spp1
Krt17
Krt23
Try4
Prss2
Cpa2a2

FIG. 1D

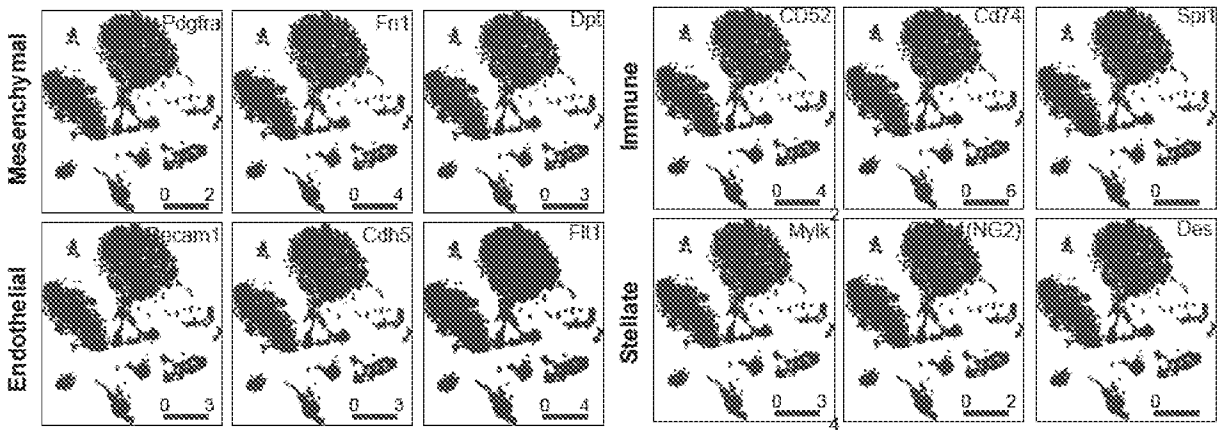

Mesenchymal
Pdgfra
Fn1
Dpt
Endothelial
Pecam1
Cdh5
Flt1
Immune
CD52
Cd74
Spi1
Stellate
Mylk
(NG2)
Des

FIG. 1E

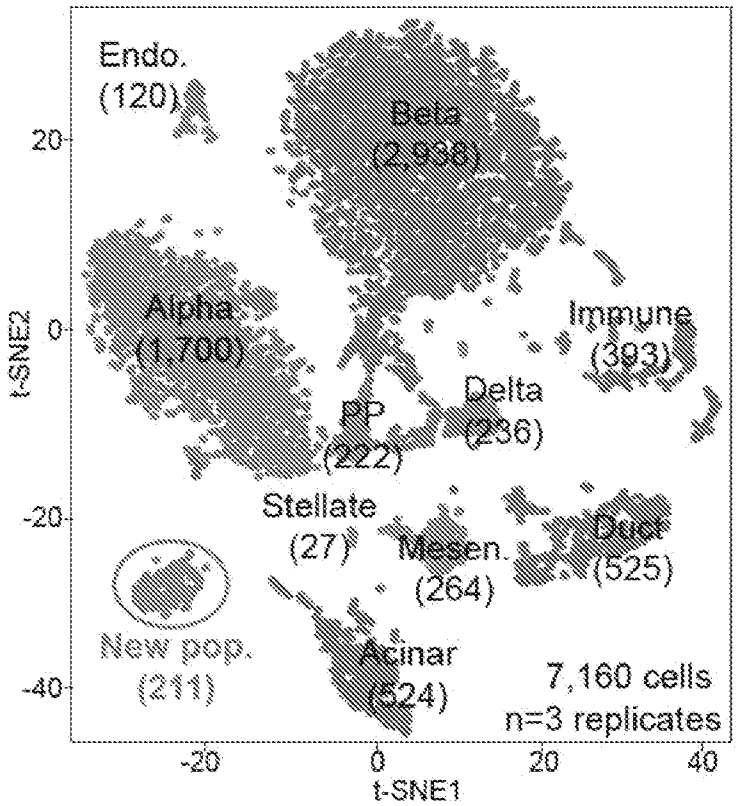

Endo.
(120)
Beta
(2,936)
Alpha
(1,700)
Immune
(393)
Delta
(236)
PP
(222)
Stellate
(27)
Mesen.
(264)
Duct
(525)
New pop.
(211)
Acinar
(524)
7,160 cells
n=3 replicates
t-SNE2
t-SNE1
20
0
-20
-40
-20
0
20
40

FIG. 1F

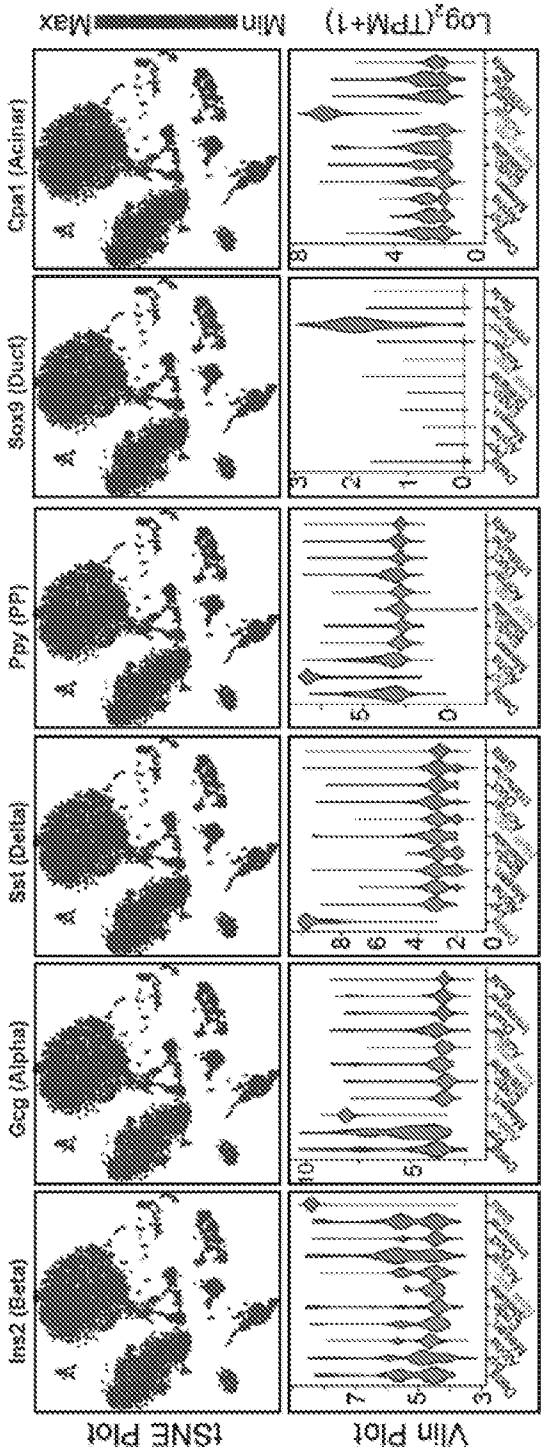

Ins2 (Beta)
Gcg (Alpha)
Sst (Delta)
Ppy (PP)
Sox9 (Duct)
Cpa1 (Acinar)
tSNE Plot
Vlln Plot
Log2(TPM+1)
Min
Max

FIG. 1G

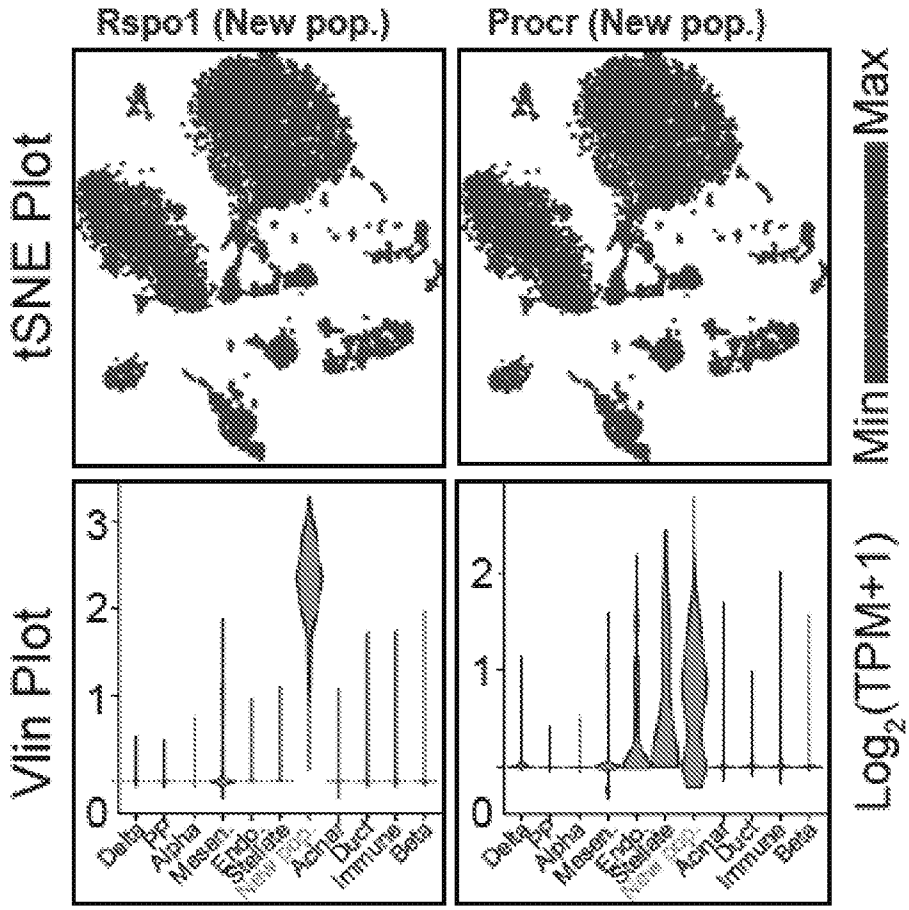

Rspo1 (New pop.)
Procr (New pop.)
tSNE Plot
Max
Min
Vlin Plot
Log2(TPM+1)
Delta
PP
Alpha
Mesen.
Endo.
Stellate
Acinar
Duct
Immune
Beta

FIG. 1H

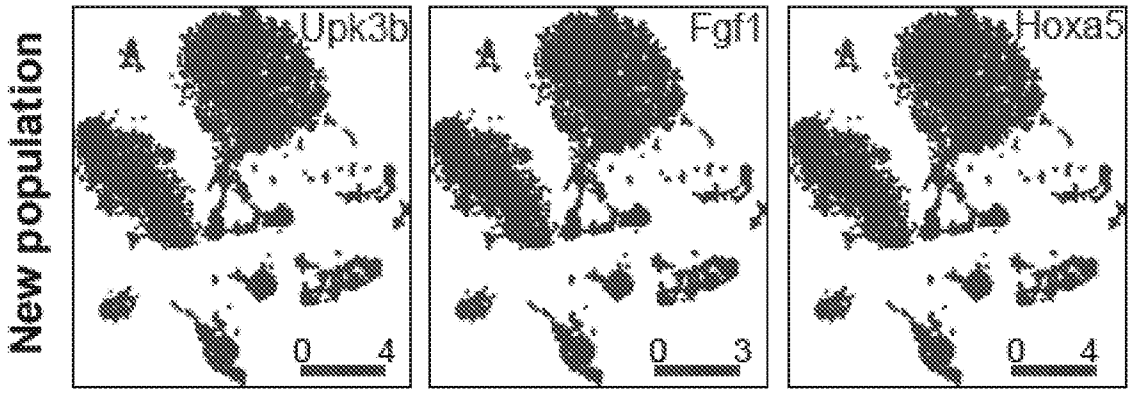

New population
Upk3b
Fgf1
Hoxa5
0 4
0 3
0 4

FIG. 1I

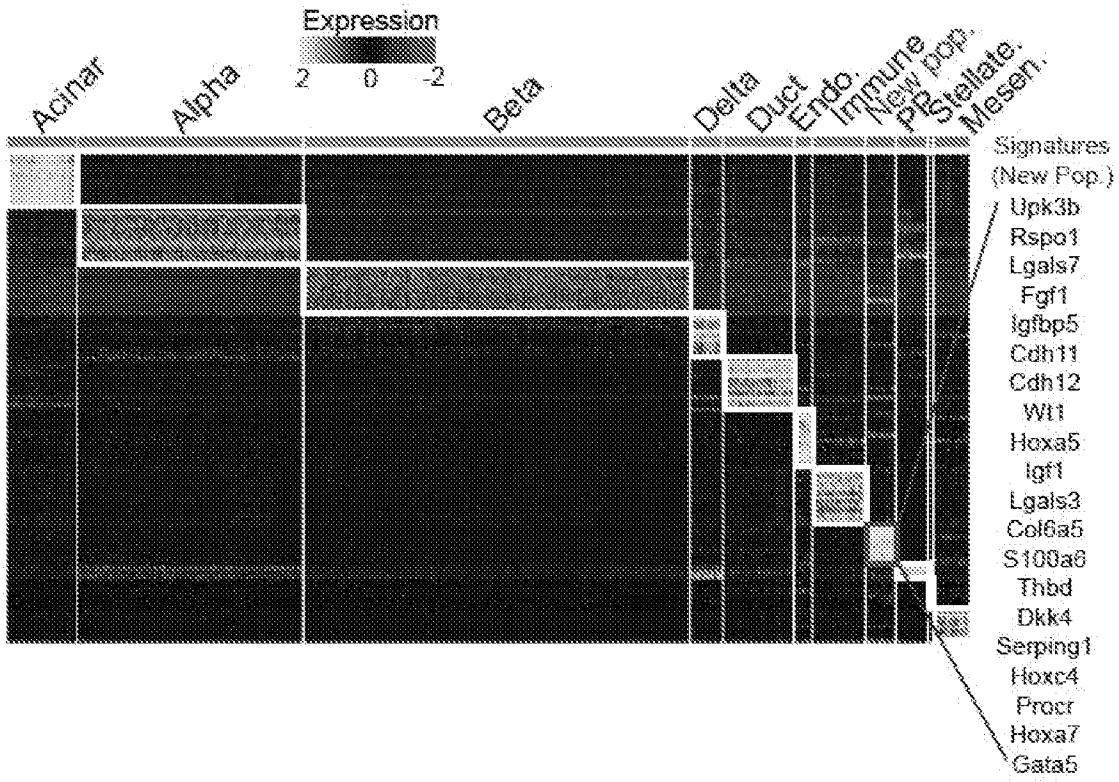

Expression
2
0
-2
Acinar
Alpha
Beta
Delta
Duct
Endo.
Immune
New pop.
PP
Stellate.
Mesen.
Signatures
(New Pop.)
Upk3b
Rspo1
Lgals7
Fgf1
Igfbp5
Cdh11
Cdh12
Wt1
Hoxa5
Igf1
Lgals3
Col6a5
S100a6
Thbd
Dkk4
Serping1
Hoxc4
Procr
Hoxa7
Gata5

FIG. 1J

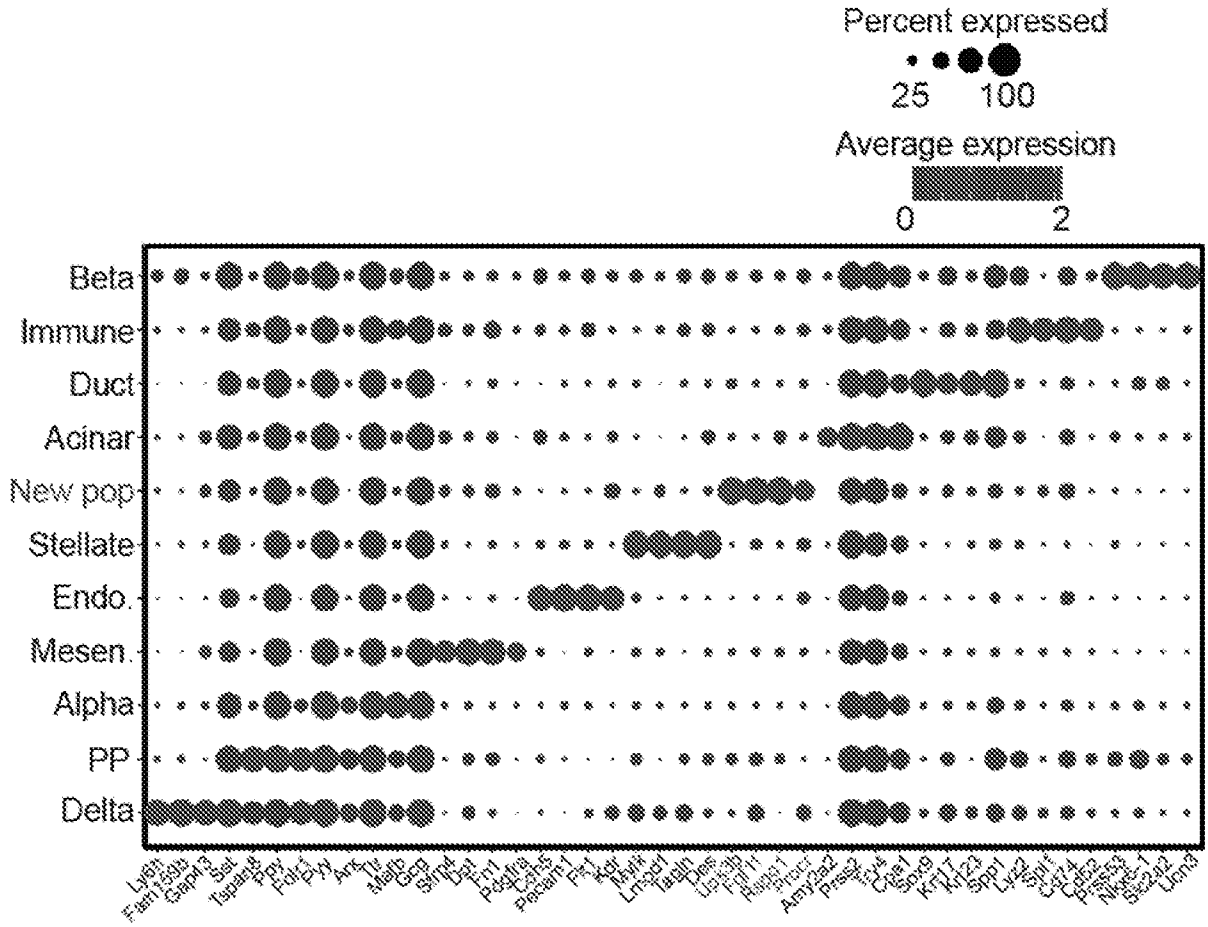

Percent expressed
25
100
Average expression
0
2
Beta
Immune
Duct
Acinar
New pop
Stellate
Endo.
Mesen.
Alpha
PP
Delta
Lyzs
Fam159b
Gapm3
Sst
Ispan8
Ppy
Folr1
Pyy
Ars
Tf
Mafb
Gcg
Slitrk4
Dpt
Ern1
Pdgfra
Cdh5
Pecam1
Fn1
Sdr
Rbp4
Lrrc4cl
Tagln
Des
Lrp1b
Fgfr1
Ramp1
Procr
Aqp3a2
Prss2
Cryl1
Cpa1
Sox9
Krt17
Krt23
Spp1
Lyz2
Spi1
C4f14
Cd52
Prss53
Nkrf
Slc2a2
Ucn3

FIG. 1K

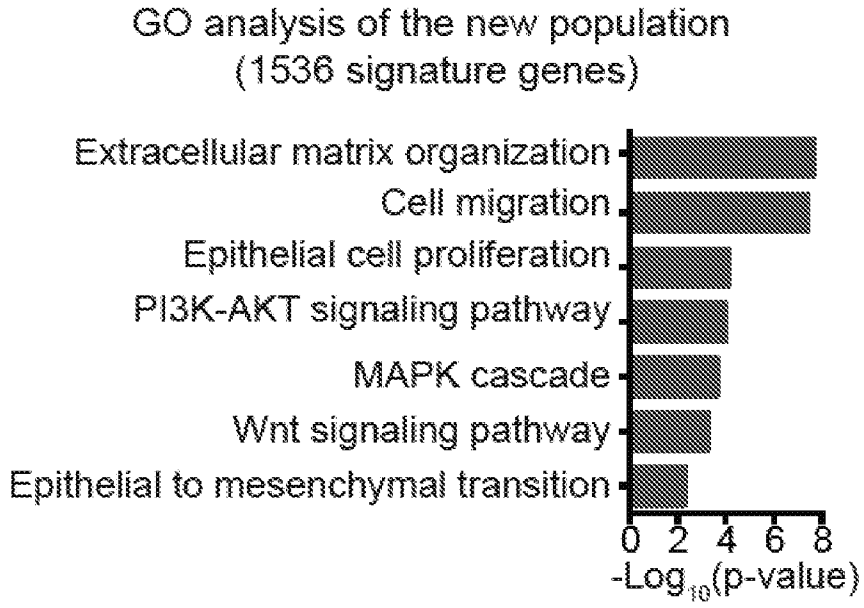

GO analysis of the new population
(1536 signature genes)
Extracellular matrix organization
Cell migration
Epithelial cell proliferation
PI3K-AKT signaling pathway
MAPK cascade
Wnt signaling pathway
Epithelial to mesenchymal transition
0
2
4
6
8
-Log10(p-value)

FIG. 1L

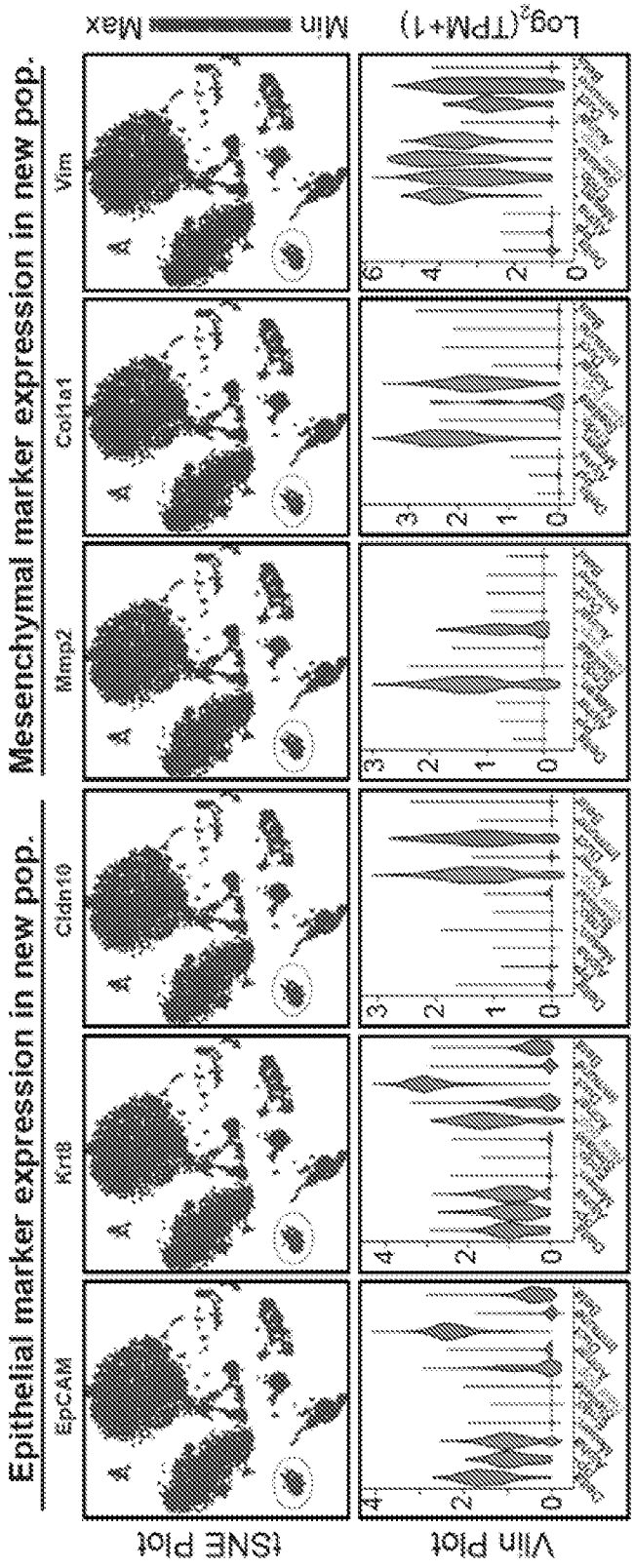

Epithelial marker expression in new pop.
Mesenchymal marker expression in new pop.
EpCAM
Krt8
Cldn10
Mmp2
Col1a1
Vim
tSNE plot
Vlln plot
Log2(TPM+1)
Min
Max

FIG. 1M

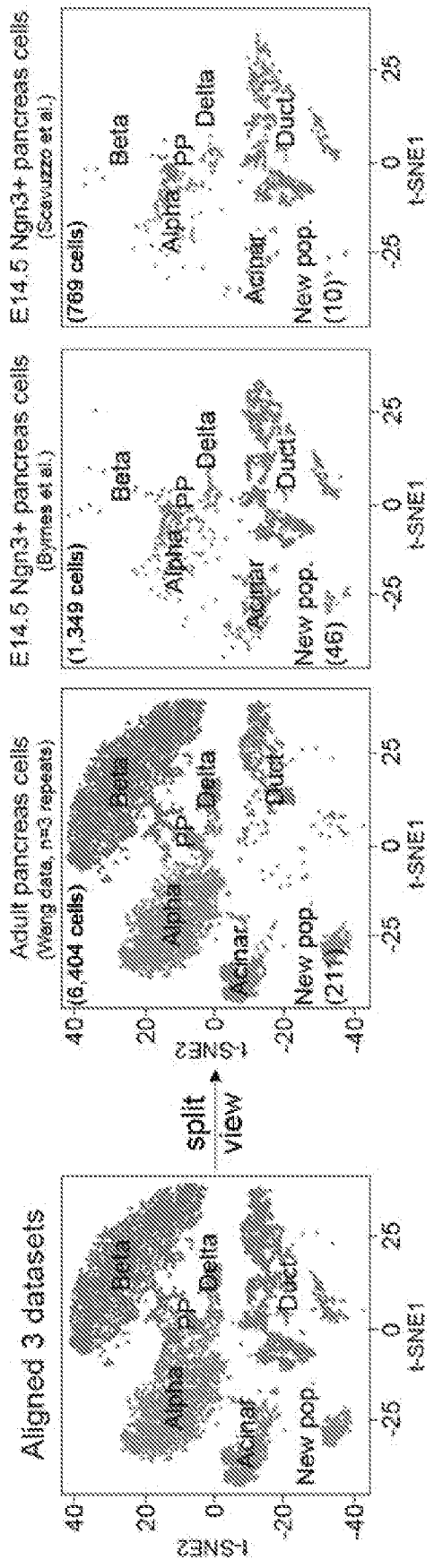

Aligned 3 datasets
Adult pancreas cells
(Wang data, n=3 repeats)
(6,404 cells)
E14.5 Ngn3+ pancreas cells
(Byrnes et al.)
(1,349 cells)
E14.5 Ngn3+ pancreas cells
(Scavuzzo et al.)
(769 cells)
Beta
Alpha
PP
Delta
Acinar
Duct
New pop.
(211)
(46)
(10)
split
view
t-SNE1
t-SNE2

FIG. 2A

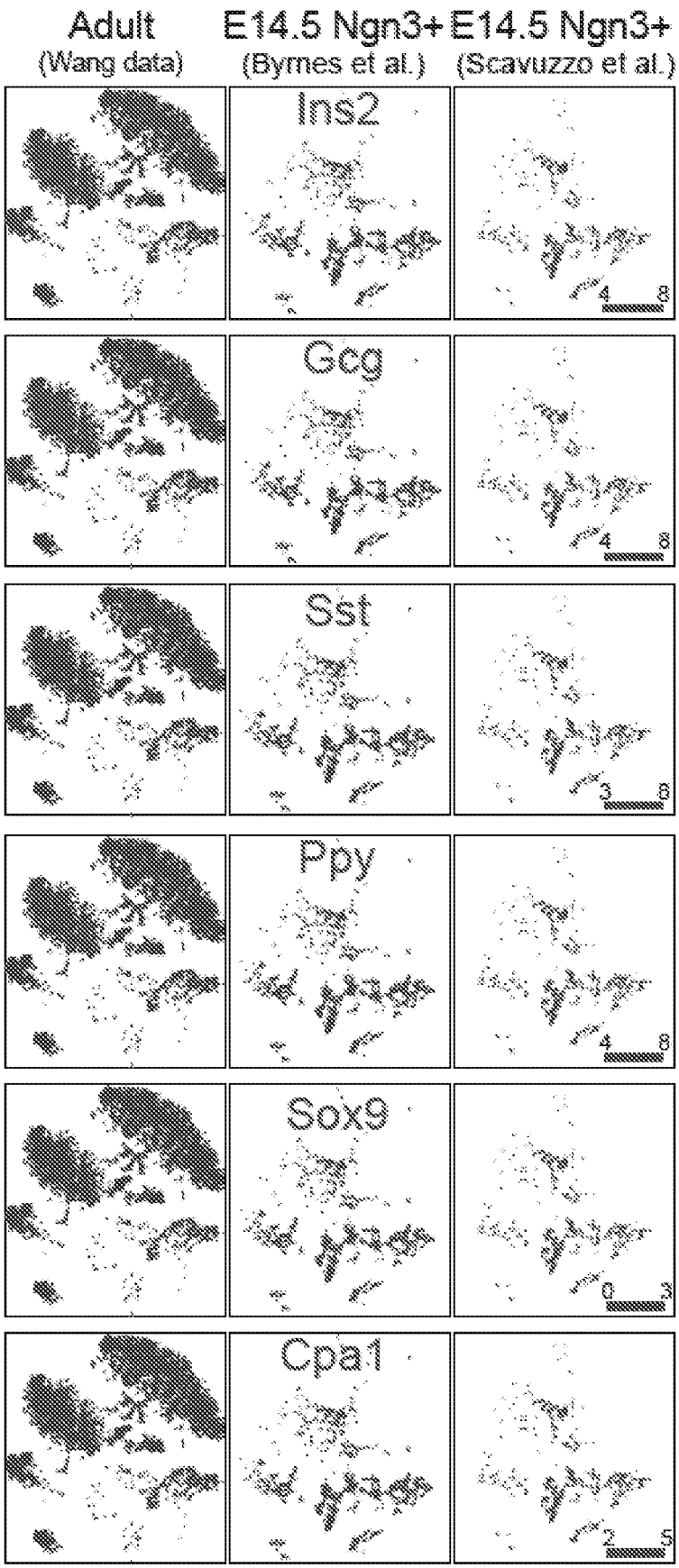

Adult
(Wang data)
E14.5 Ngn3+
(Byrnes et al.)
E14.5 Ngn3+
(Scavuzzo et al.)
Ins2
Gcg
Sst
Ppy
Sox9
Cpa1

FIG. 2B

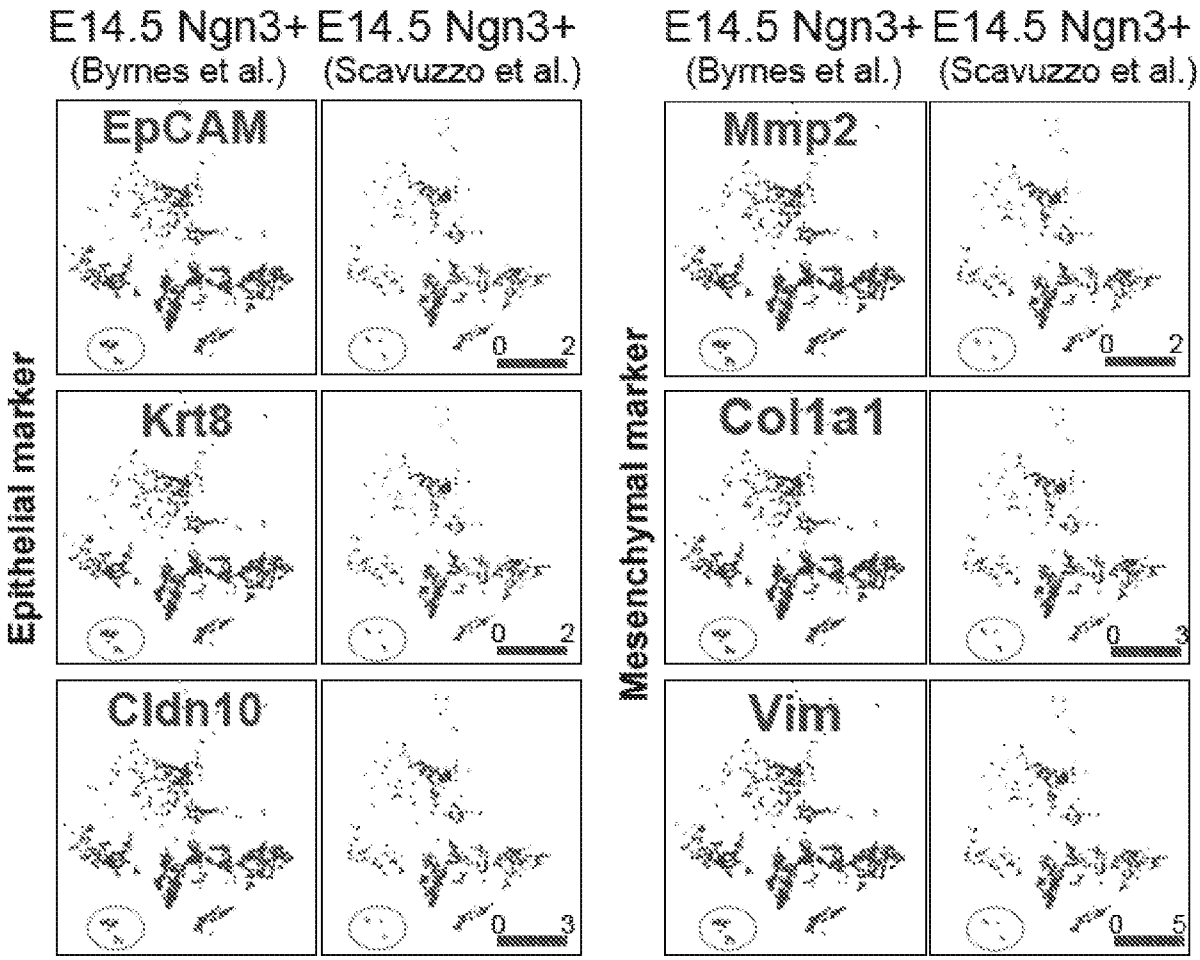

E14.5 Ngn3+ (Byrnes et al.)
E14.5 Ngn3+ (Scavuzzo et al.)
E14.5 Ngn3+ (Byrnes et al.)
E14.5 Ngn3+ (Scavuzzo et al.)
Epithelial marker
Mesenchymal marker
EpCAM
Krt8
Cldn10
Mmp2
Col1a1
Vim
0 2
0 2
0 3
0 2
0 3
0 5

FIG. 2C

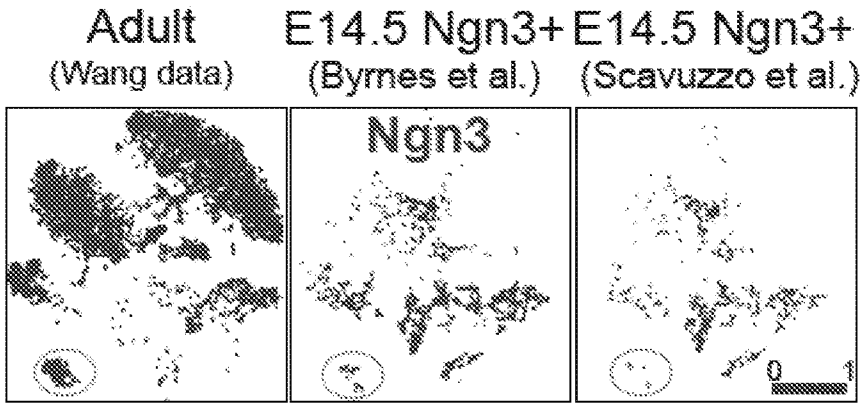

Adult
(Wang data)
E14.5 Ngn3+ (Byrnes et al.)
E14.5 Ngn3+ (Scavuzzo et al.)
Ngn3
0 1

FIG. 2D

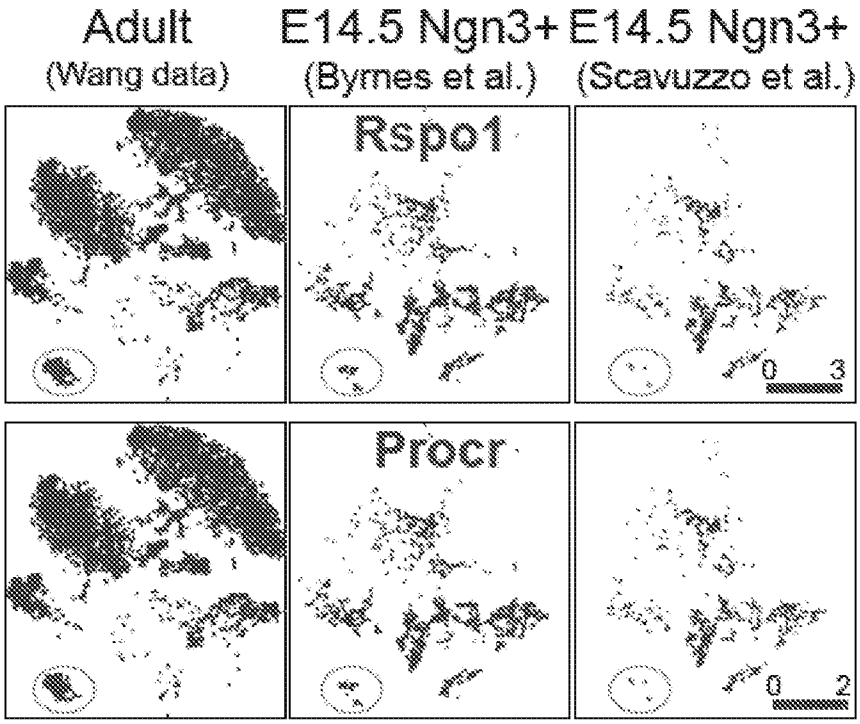

Adult
(Wang data)
E14.5 Ngn3+
(Bymes et al.)
E14.5 Ngn3+
(Scavuzzo et al.)
Rspo1
Procr
0 3
0 2

FIG. 2E

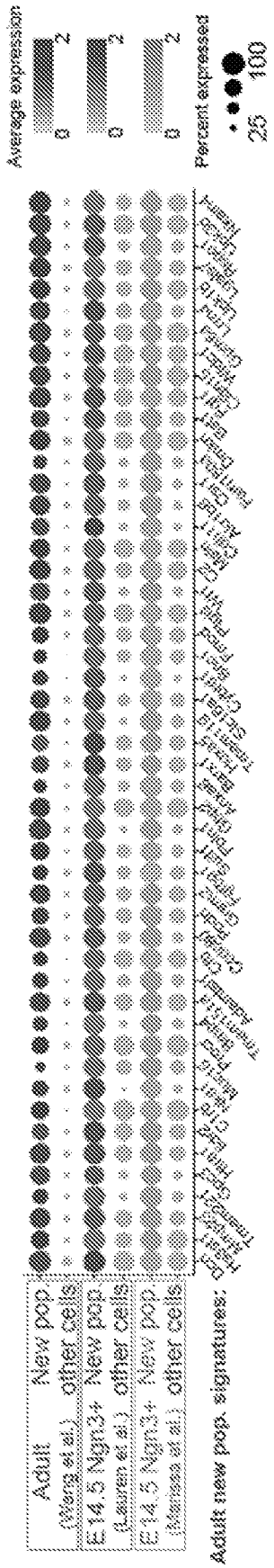

Average expression
Percent expressed
25
100
Adult (Wang et al.) New pop. other cells
E14.5 Ngn3+ (Lauren et al.) New pop. other cells
E14.5 Ngn3+ (Mansoa et al.) New pop. other cells
Adult new pop. signatures:

FIG. 2F

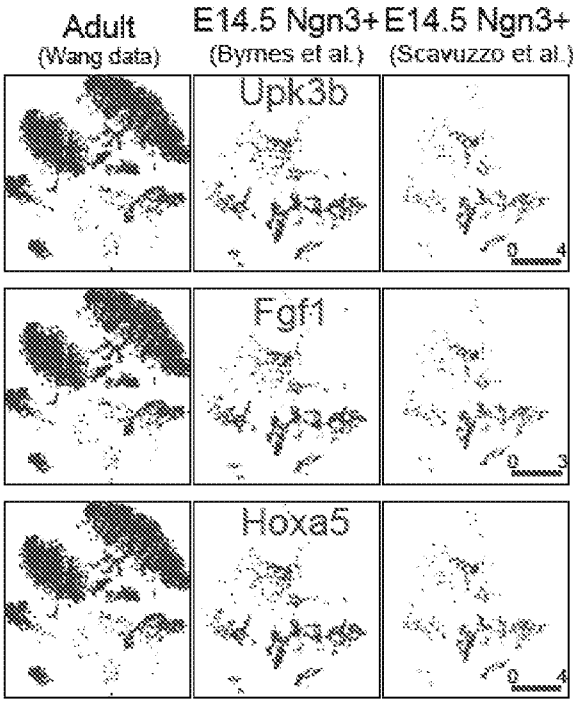

Adult
(Wang data)
E14.5 Ngn3+
(Byrnes et al.)
E14.5 Ngn3+
(Scavuzzo et al.)
Upk3b
Fgf1
Hoxa5

FIG. 2G

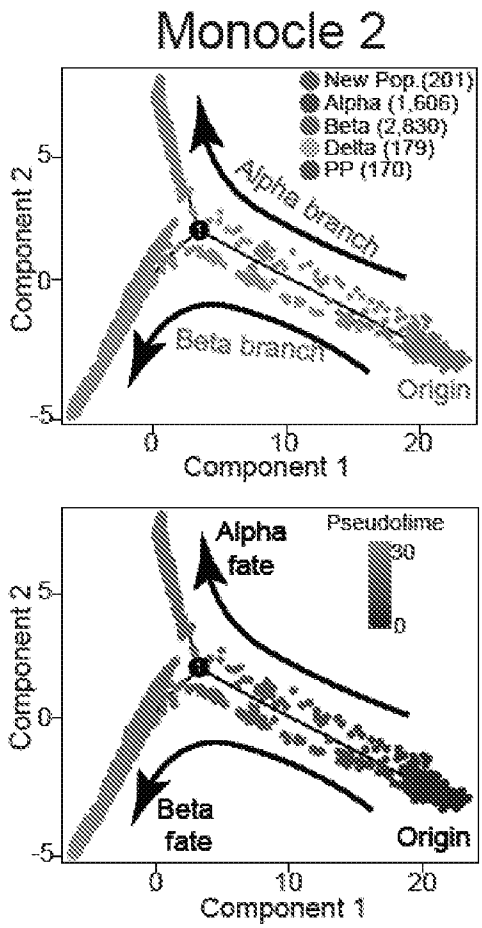

Monocle 2
New Pop.(281)
Alpha (1,606)
Beta (2,830)
Delta (179)
PP (170)
Alpha branch
Beta branch
Origin
Component 1
Component 2
Pseudotime
Alpha fate
Beta fate

FIG. 2H

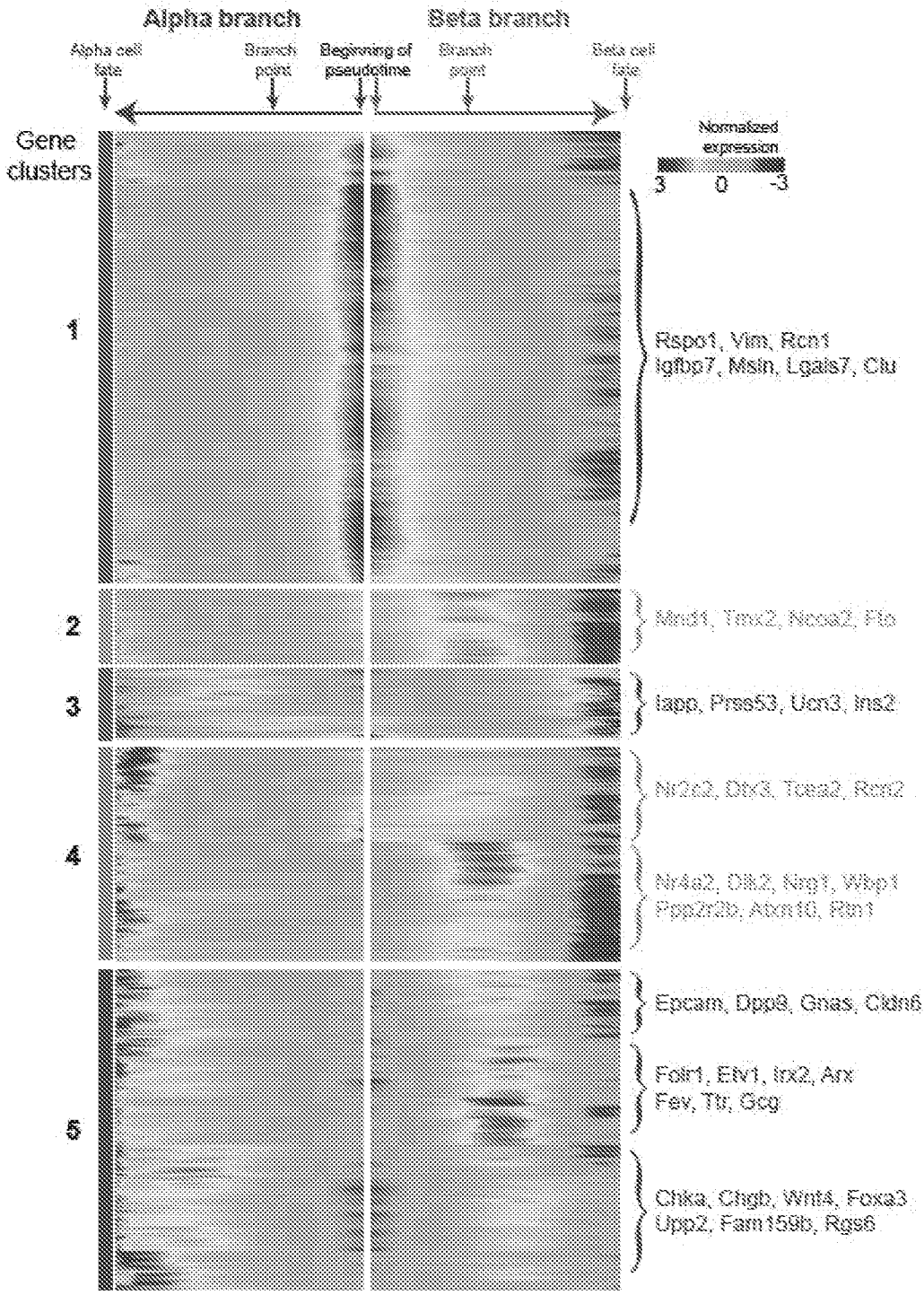

Alpha branch
Beta branch
Alpha cell fate
Branch point
Beginning of pseudotime
Branch point
Beta cell fate
Gene clusters
Normalized expression
3 0 -3
1
Rspo1, Vim, Rcn1
Igfbp7, Msln, Lgals7, Clu
2
Mnd1, Tmx2, Ncoa2, Flb
3
Iapp, Prss53, Ucn3, Ins2
4
Nr2c2, Dtx4, Tcea2, Rcn2
Nr4a2, Dlk2, Neg1, Wbp1
Ppp2r2b, Atxn10, Rtn1
5
Epcam, Dpp6, Gnas, Cldn6
Folr1, Etv1, Irx2, Arx
Fev, Ttr, Gcg
Chka, Chgb, Wnt4, Foxa3
Upp2, Fam159b, Rgs6

FIG. 2I

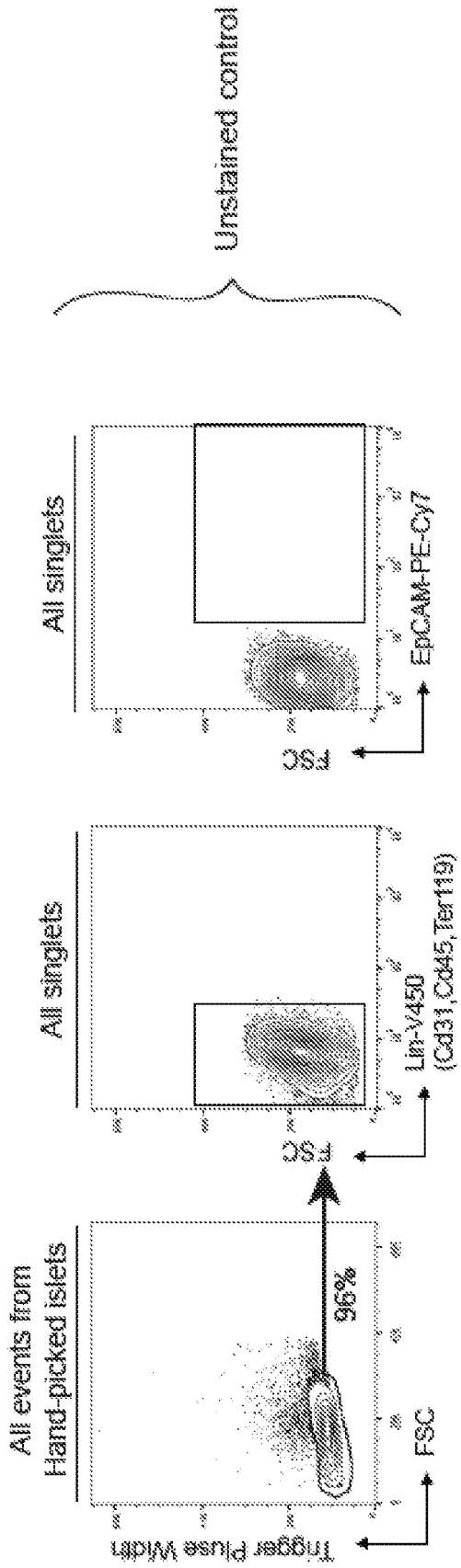

Unstained control
All singlets
FSC
EpCAM-PE-Cy7
All singlets
FSC
Lin-V450
(Cd31,Cd45,Ter119)
All events from
Hand-picked islets
96%
Trigger Pluse Width
FSC

FIG. 3A

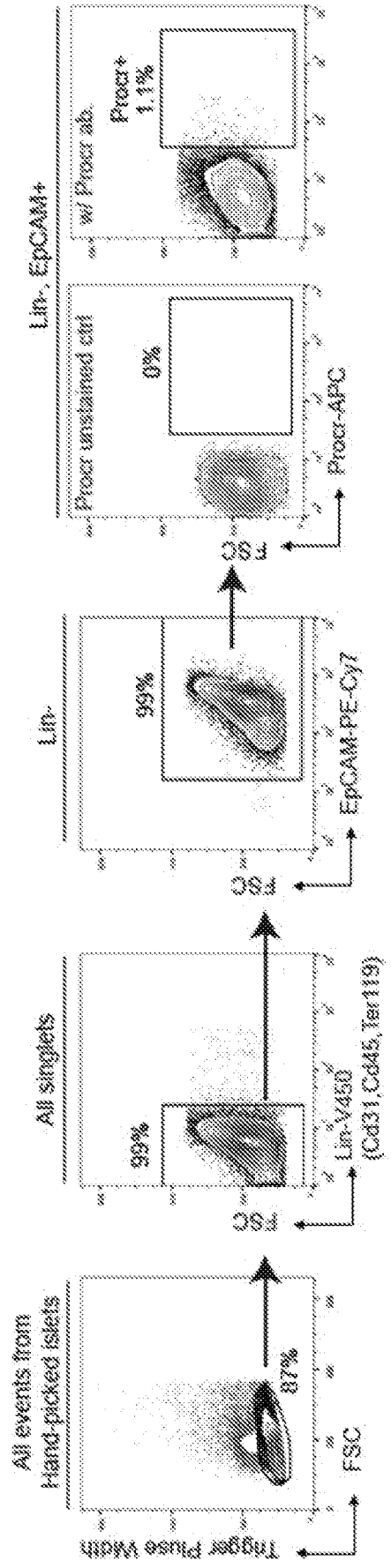

All events from Hand-picked islets
Trigger Pulse Width
FSC
87%
All singlets
FSC
99%
Lin-V450 (Cd31,Cd45,Ter119)
Lin-
FSC
99%
EpCAM-PE-Cy7
Lin-, EpCAM+
FSC
Procr unstained ctrl
0%
Procr-APC
w/ Procr ab.
Procr+ 1.1%

FIG. 3B

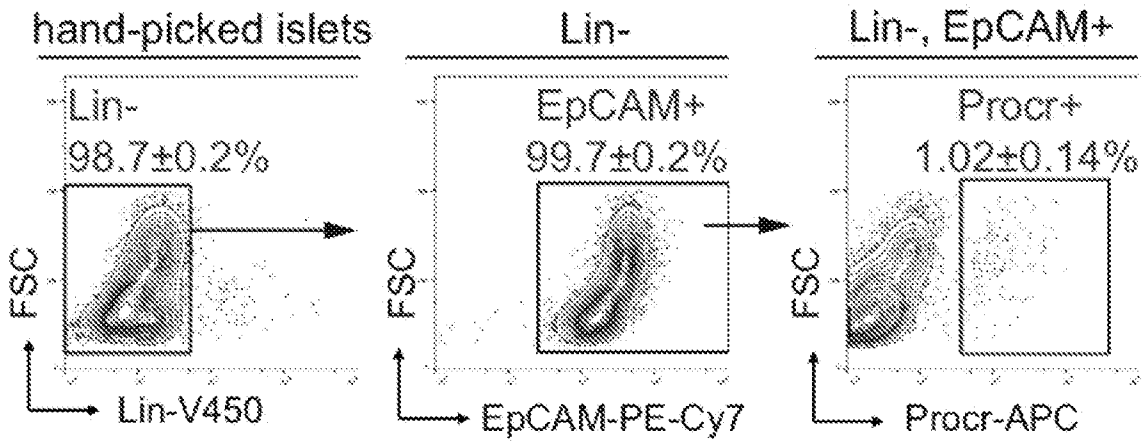


FIG. 3C

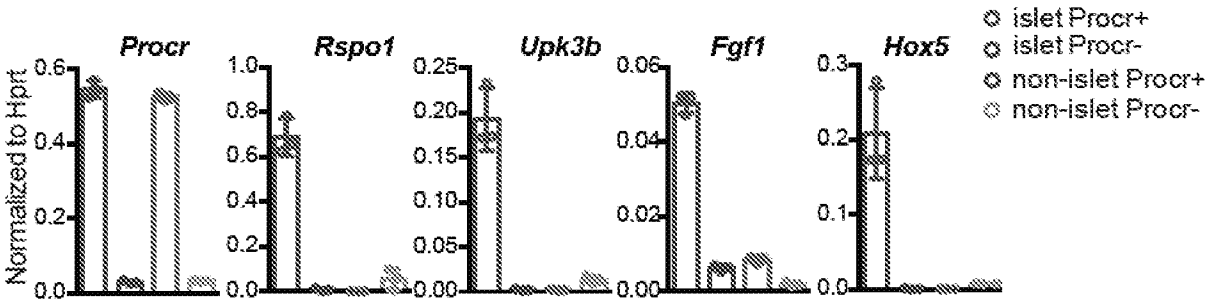


FIG. 3D

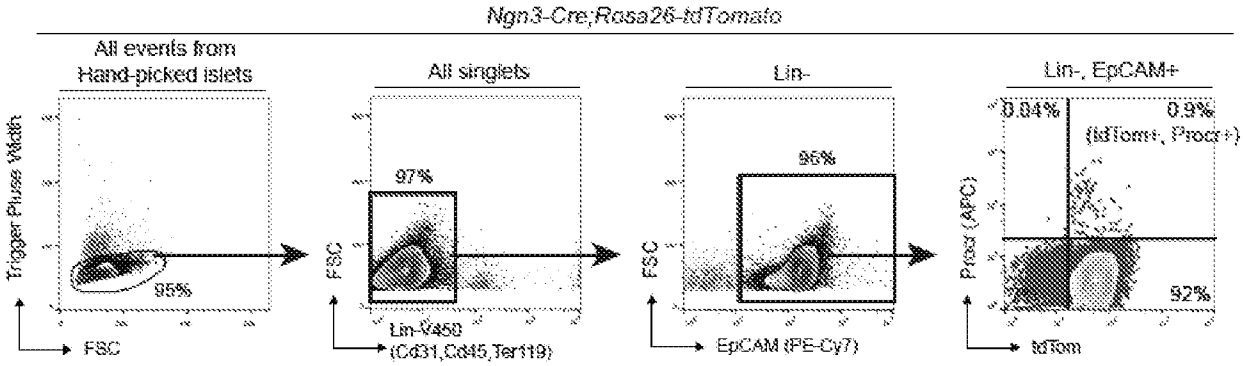


FIG. 3E

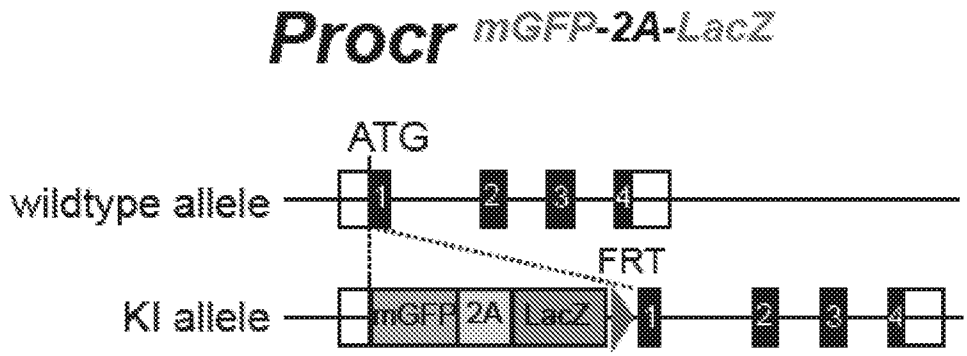


FIG. 3F

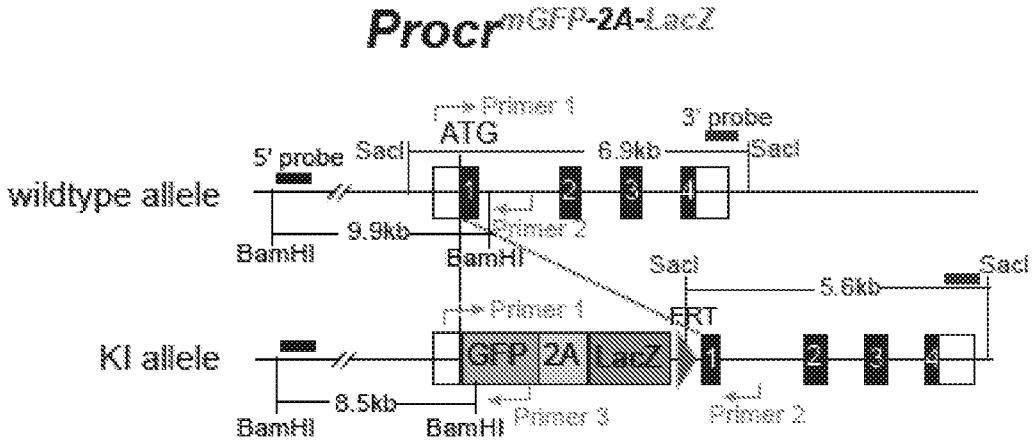


FIG. 3G

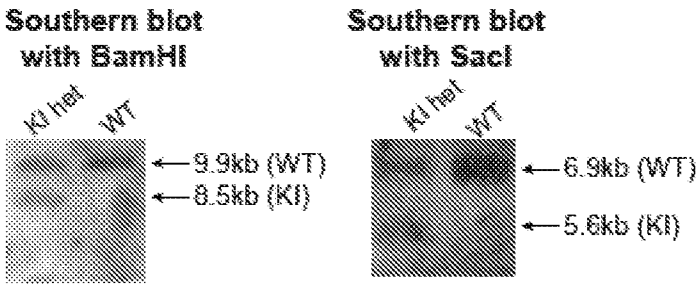


FIG. 3H

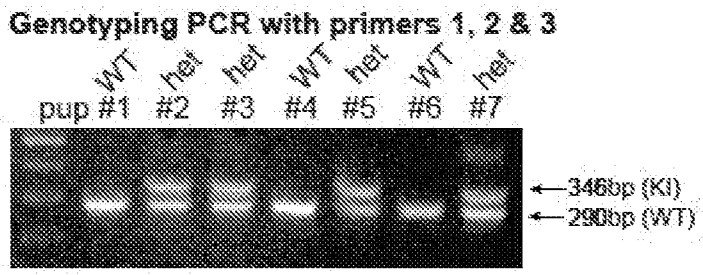


FIG. 3I

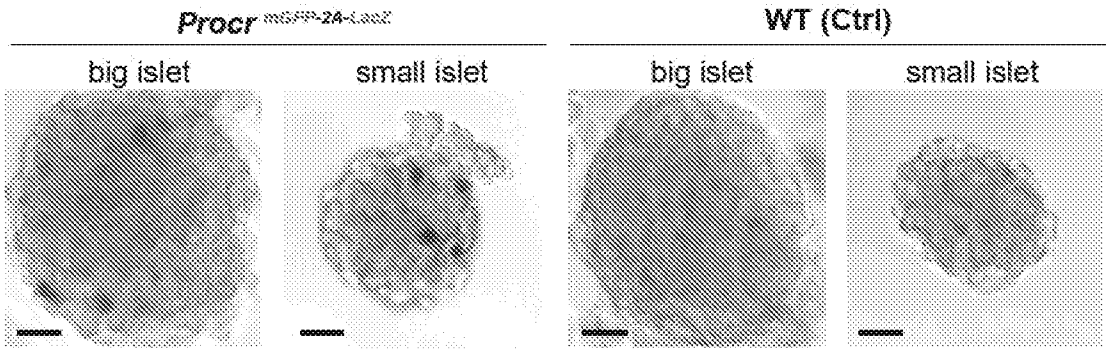


FIG. 3J

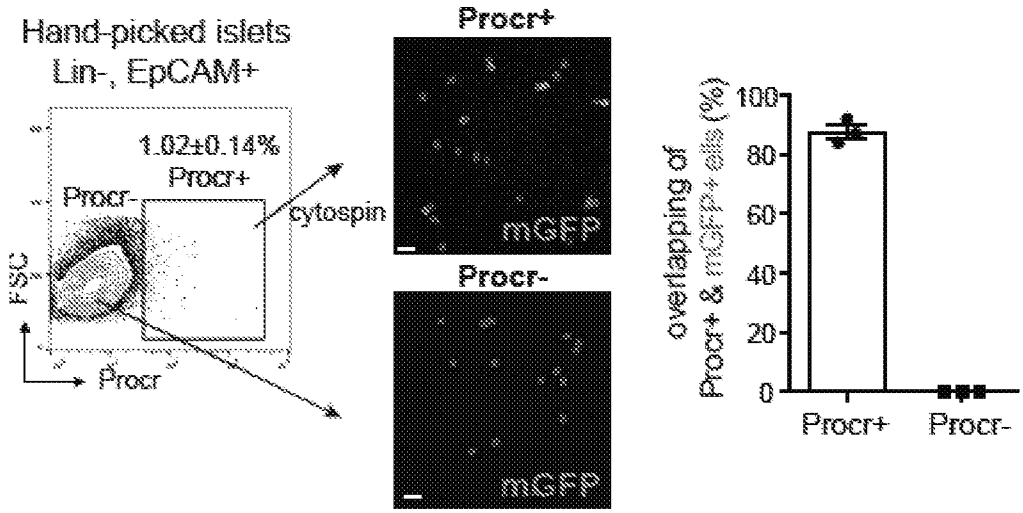


FIG. 3K

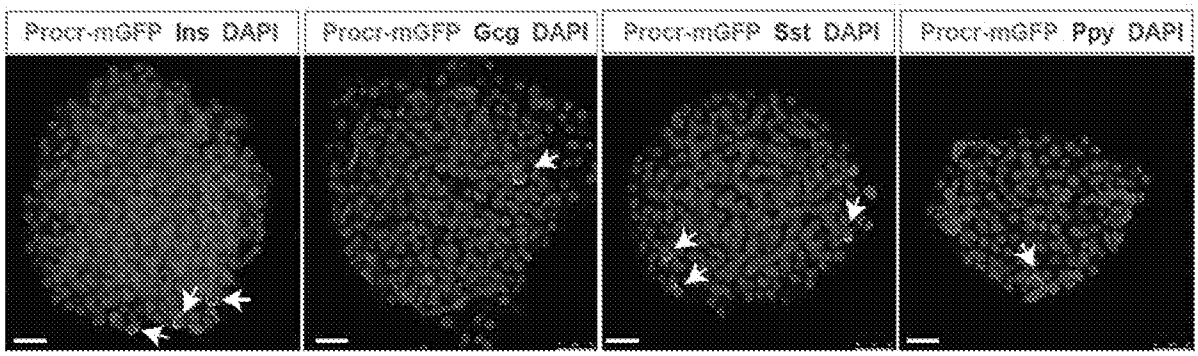


FIG. 3L

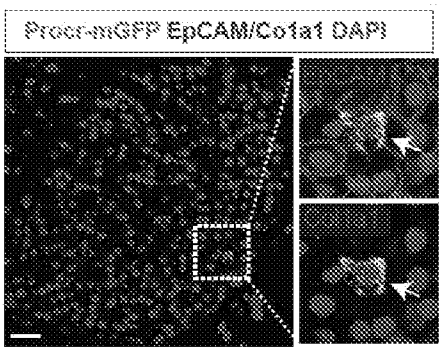


FIG. 3M

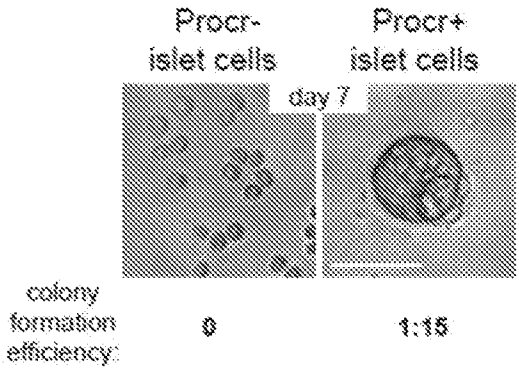


FIG. 4A

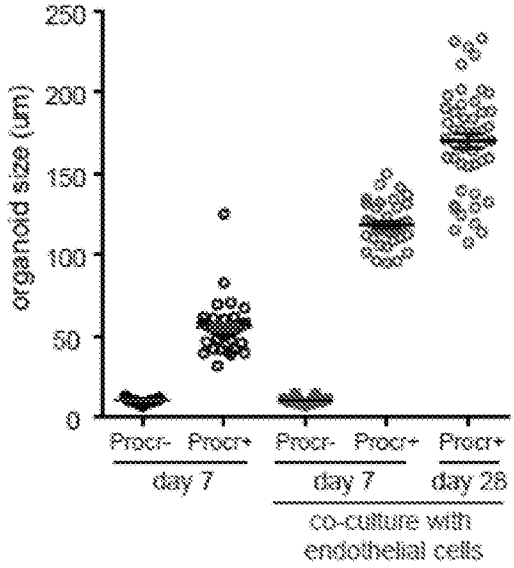


FIG. 4B

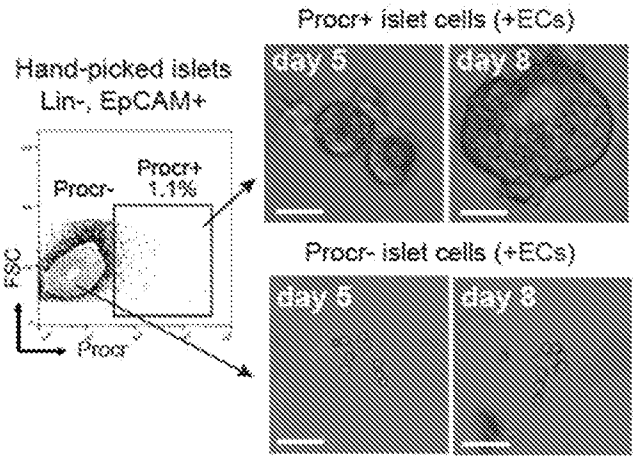


FIG. 5A

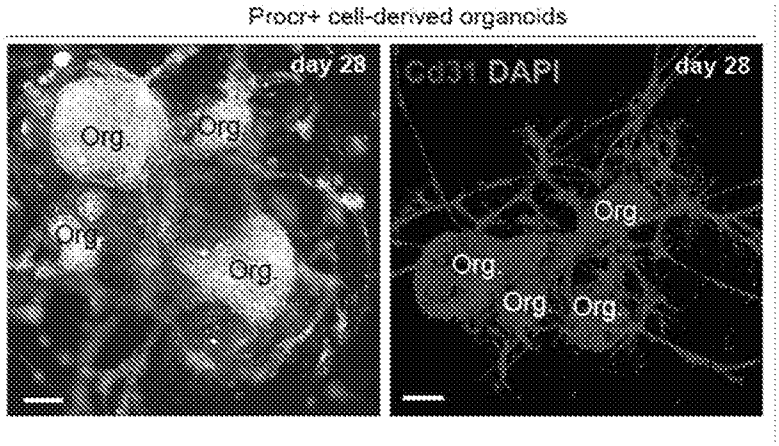


FIG. 5B

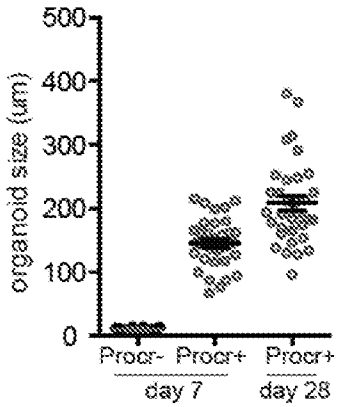


FIG. 5C

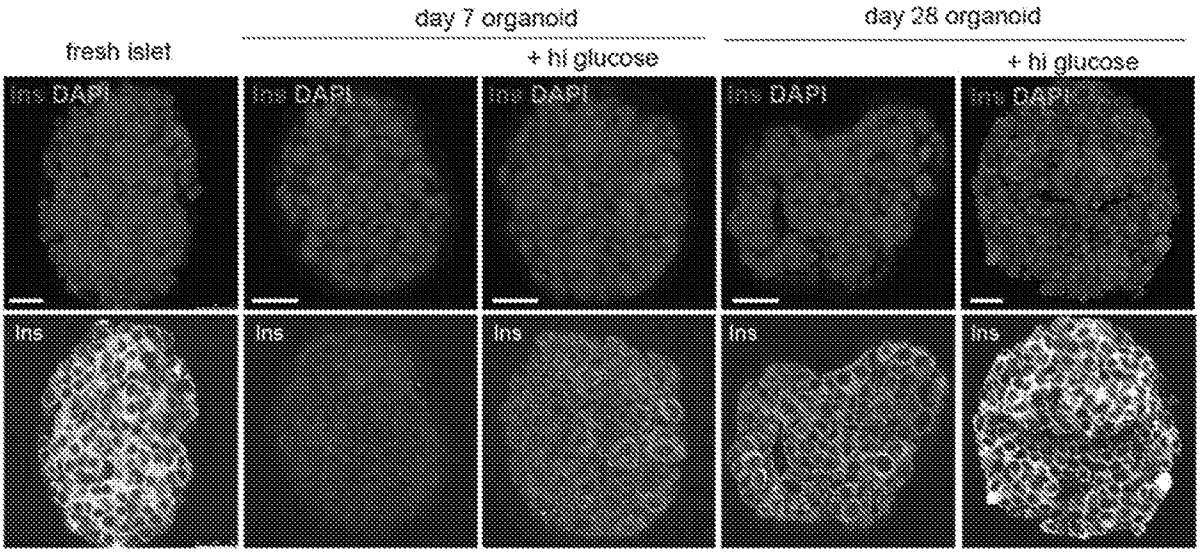


FIG. 5D

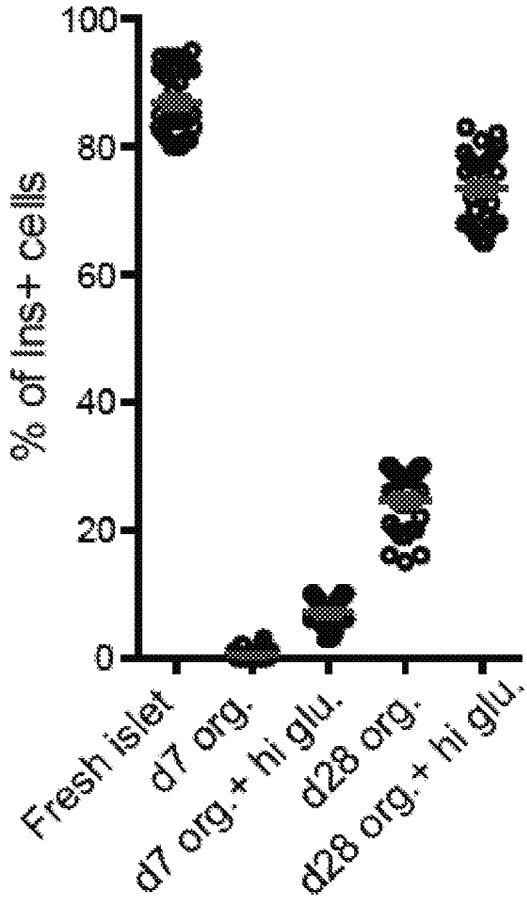

% of Ins+ cells
100
80
60
40
20
0
Fresh islet
d7 org.
d7 org.+ hi glu.
d28 org.
d28 org.+ hi glu.

FIG. 5E

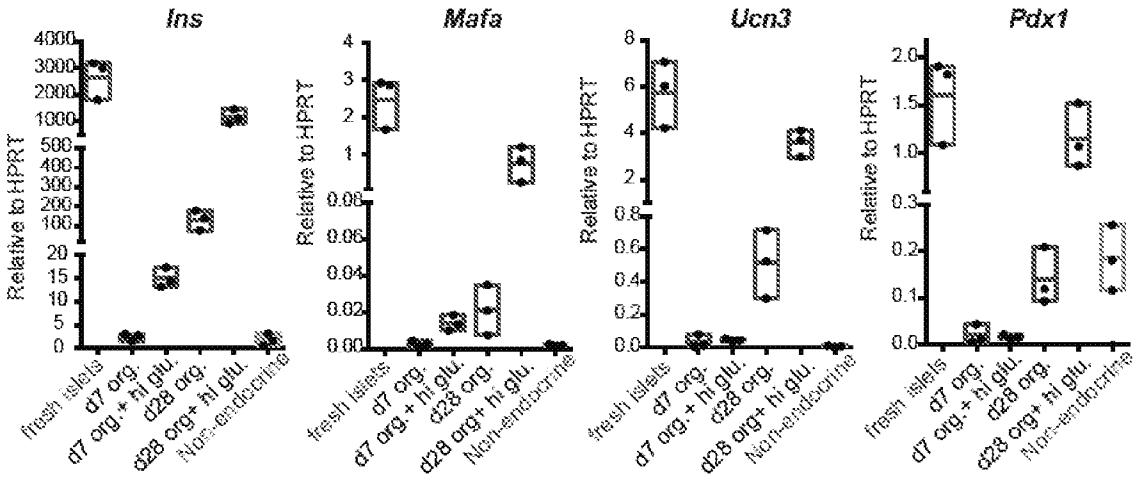

Ins
Mafa
Ucn3
Pdx1
Relative to HPRT
fresh islets
d7 org.
d7 org.+ hi glu.
d28 org.
d28 org+ hi glu.
Non-endocrine

FIG. 5F

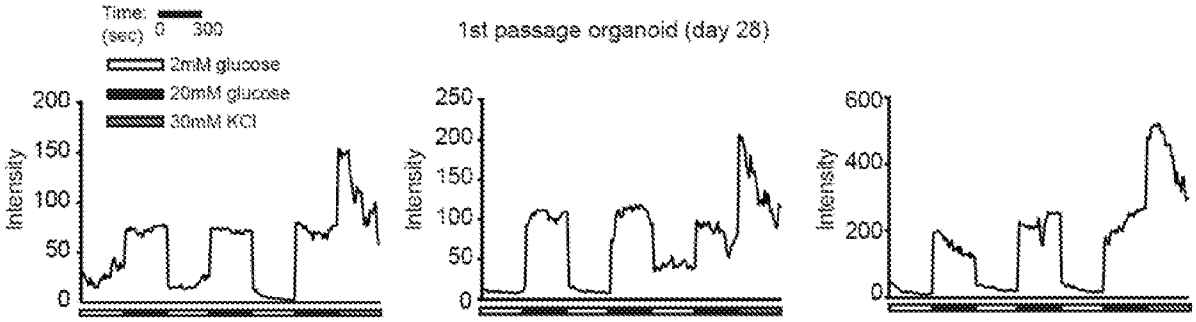


FIG. 5G

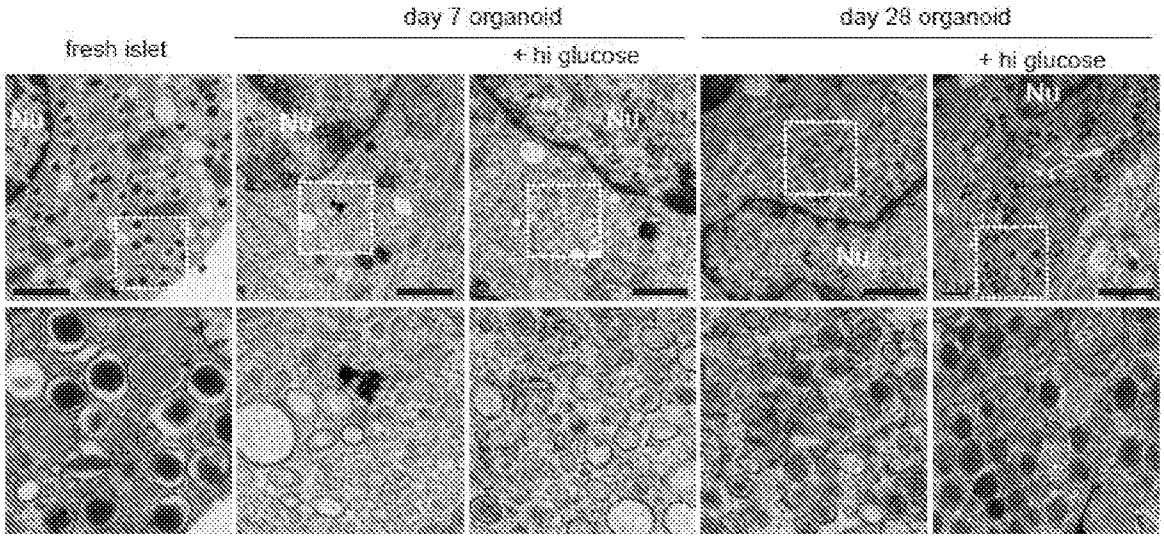


FIG. 5H

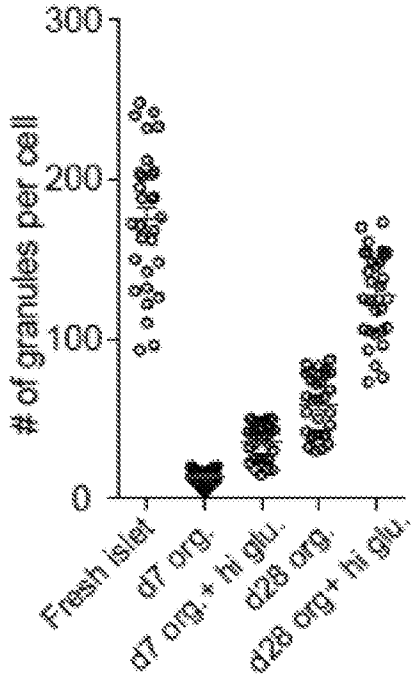


FIG. 5I

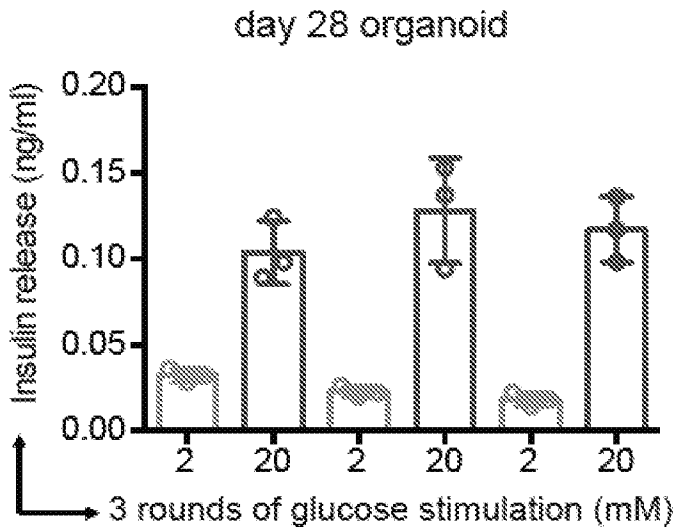


FIG. 5J

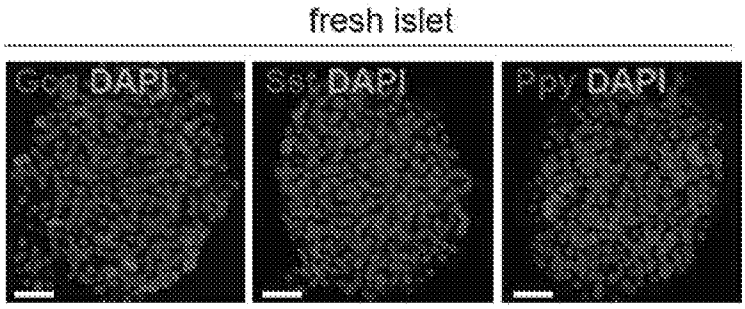


FIG. 5K

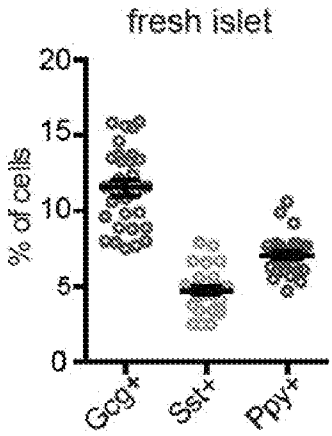


FIG. 5L

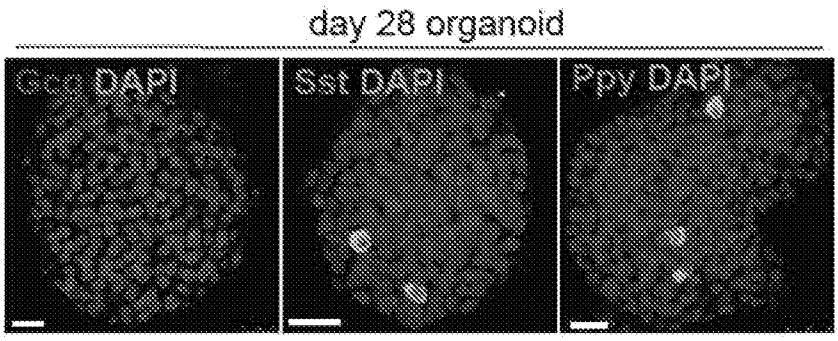


FIG. 5M

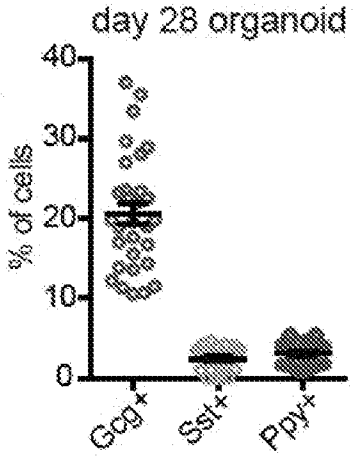


FIG. 5N

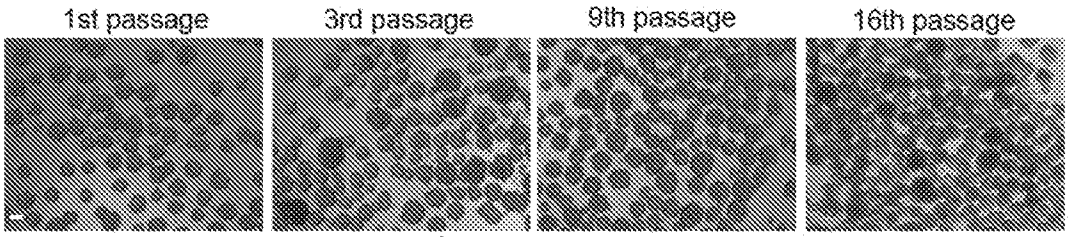


FIG. 6A

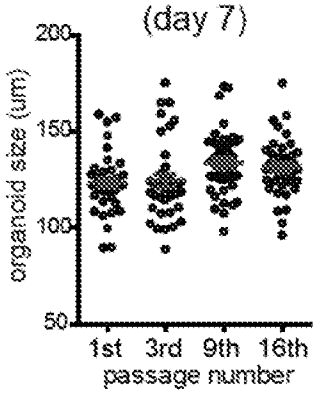


FIG. 6B

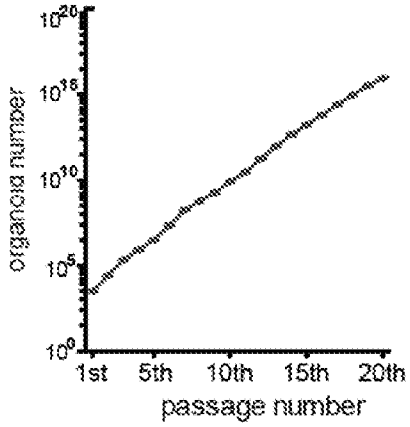


FIG. 6C

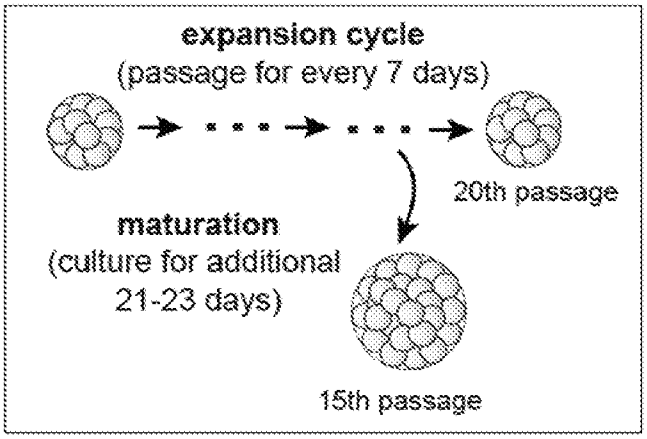


FIG. 6D

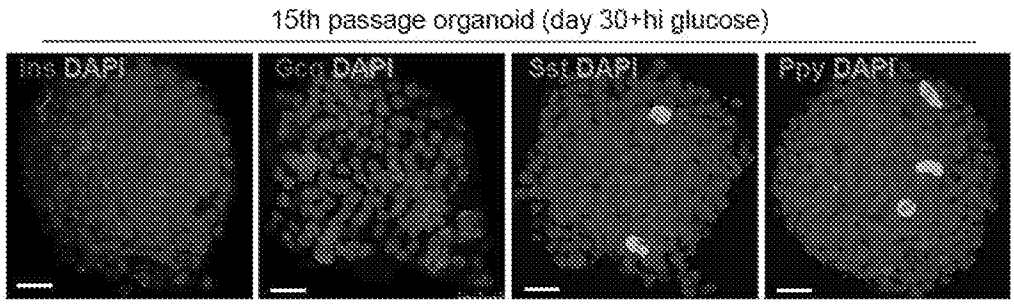


FIG. 6E

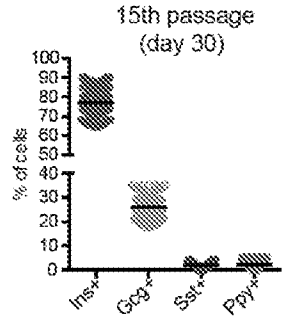


FIG. 6F

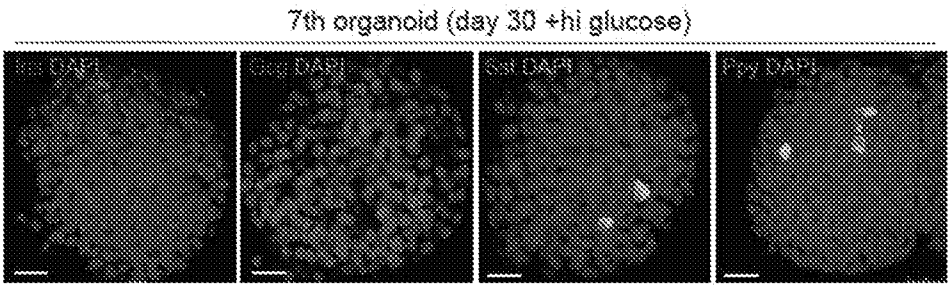


FIG. 6G

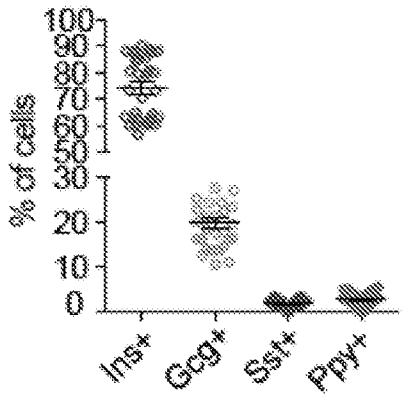


FIG. 6H

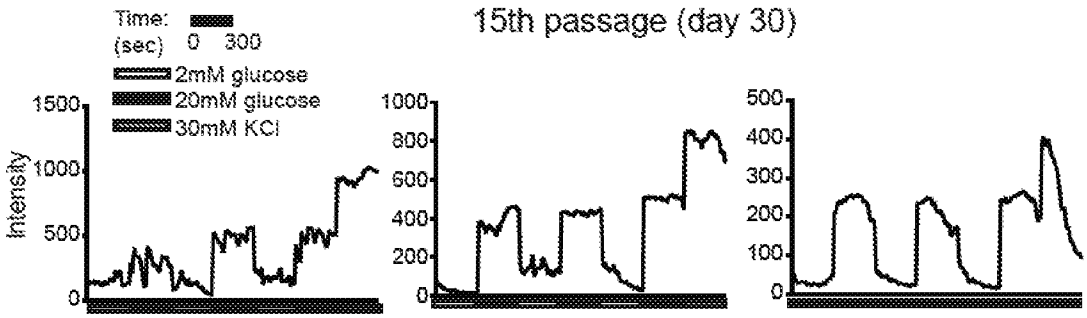


FIG. 6I

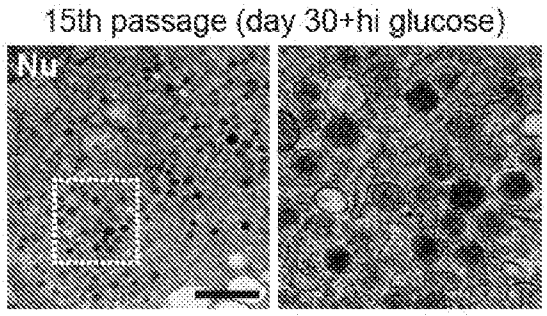


FIG. 6J

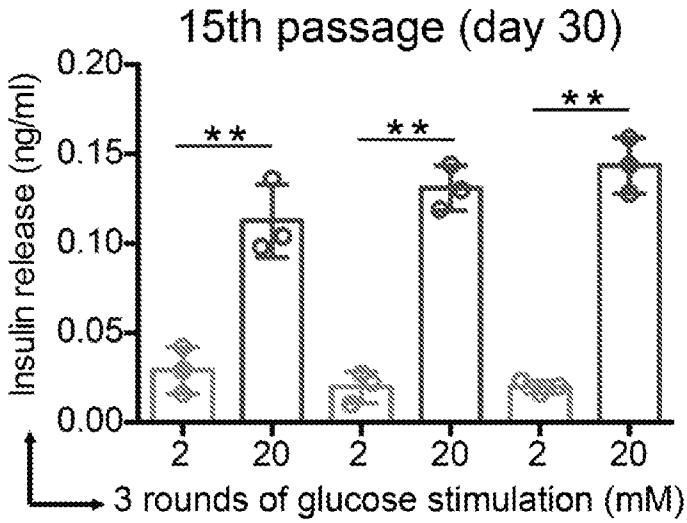


FIG. 6K

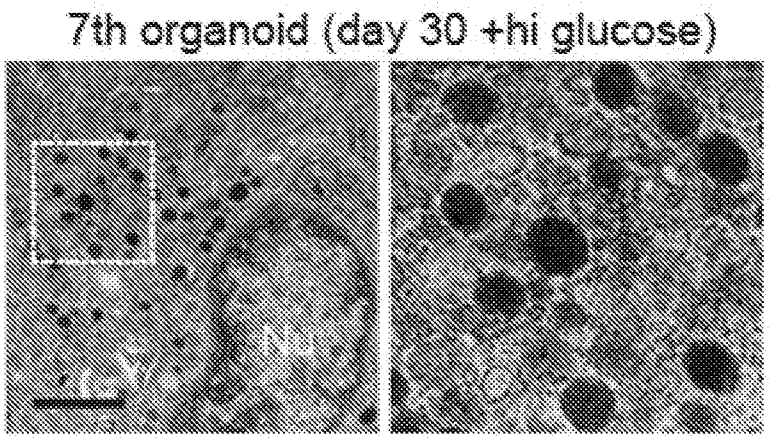


FIG. 6L

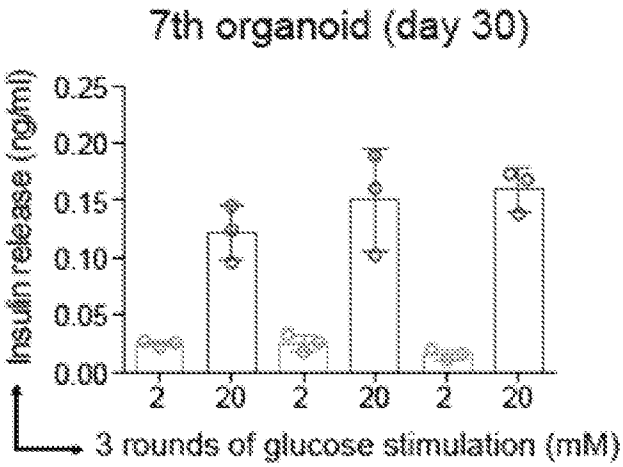


FIG. 6M

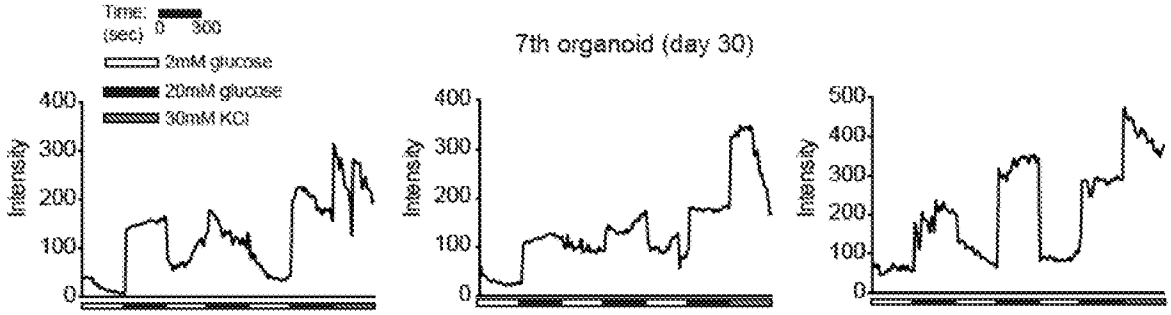


FIG. 6N

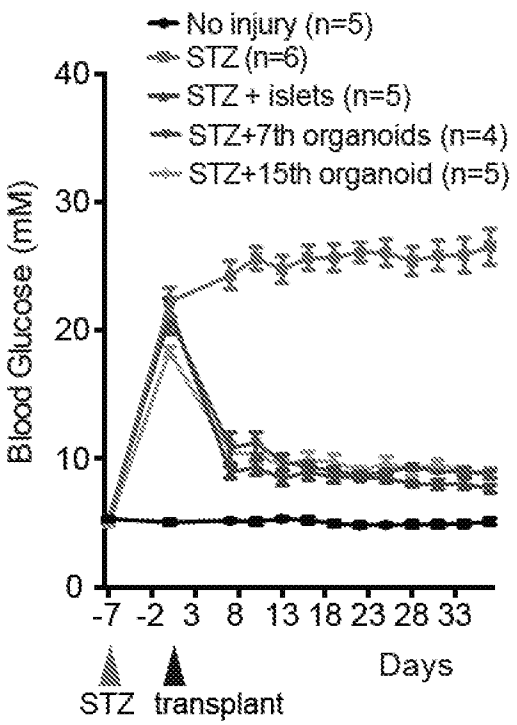


FIG. 7A

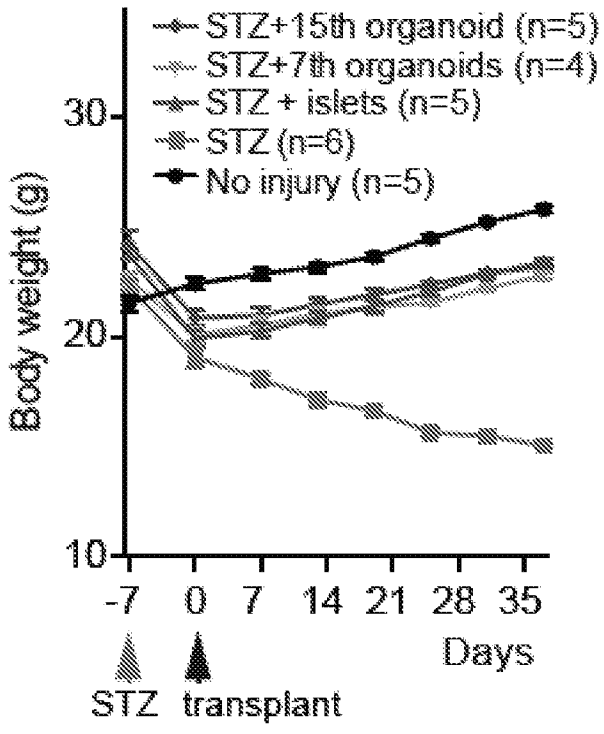


FIG. 7B

1 month after transplantaiton

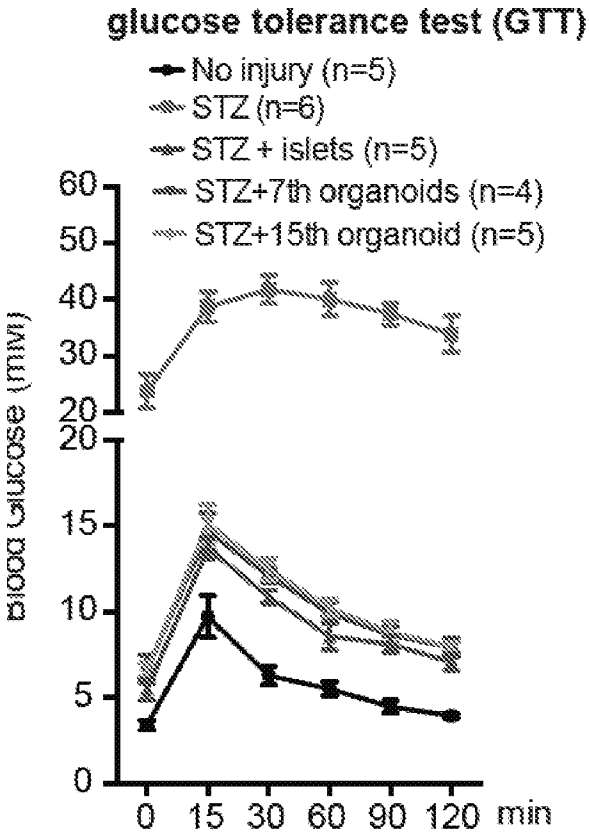


FIG. 7C

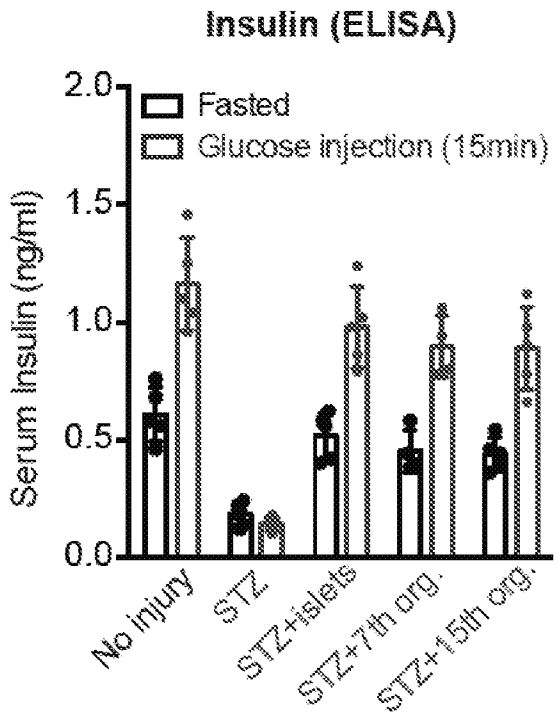


FIG. 7D

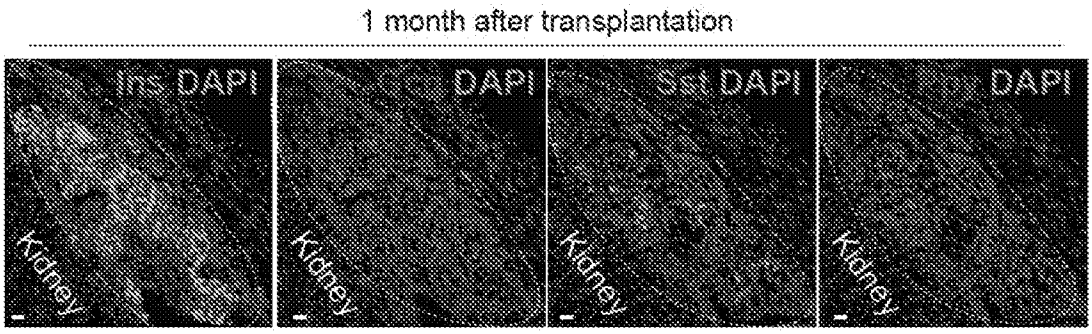


FIG. 7E

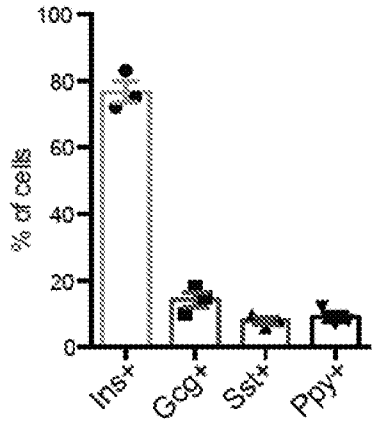


FIG. 7F

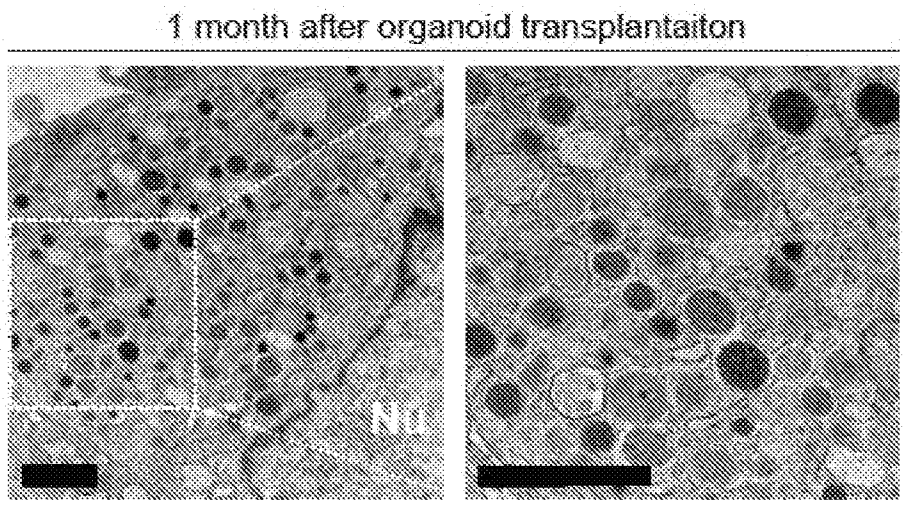


FIG. 7G

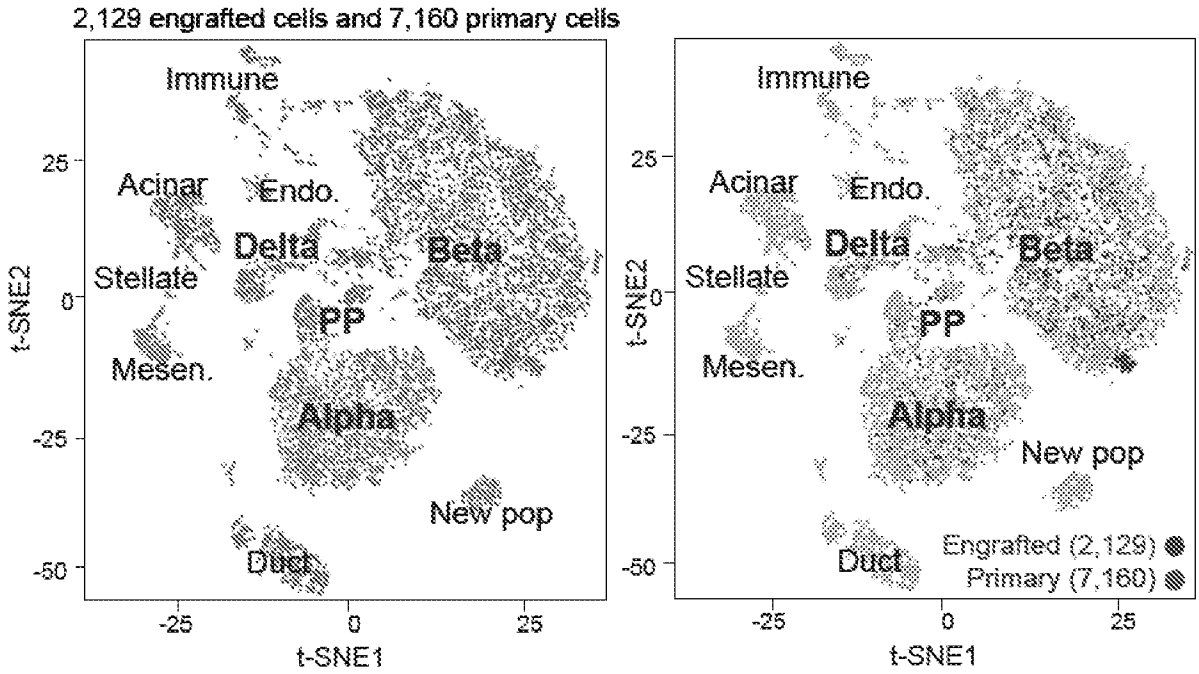

2,129 engrafted cells and 7,160 primary cells
Immune
Acinar
Endo.
Delta
Beta
Stellate
PP
Mesen.
Alpha
New pop
Duct
t-SNE2
t-SNE1
25
0
-25
-50
Engrafted (2,129)
Primary (7,160)

FIG. 7H

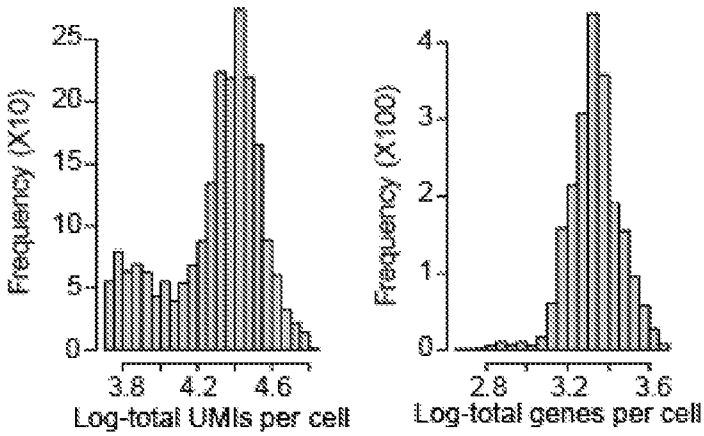

Frequency (X10)
Log-total UMIs per cell
3.8
4.2
4.6
Frequency (X100)
Log-total genes per cell
2.8
3.2
3.6

FIG. 7I

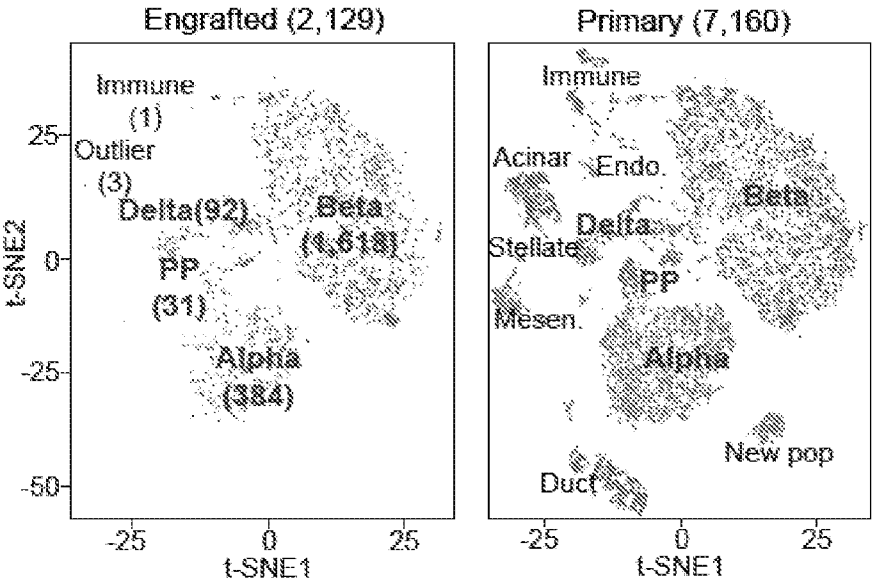

Engrafted (2,129)
Primary (7,160)
Immune
(1)
Outlier
(3)
Delta(92)
Beta
(1,618)
PP
(31)
Alpha
(384)
Immune
Acinar
Endo.
Beta
Delta
Stellate
PP
Mesen.
Alpha
New pop
Duct
t-SNE2
t-SNE1
t-SNE1
25
0
-25
-50
-25
0
25

FIG. 7J

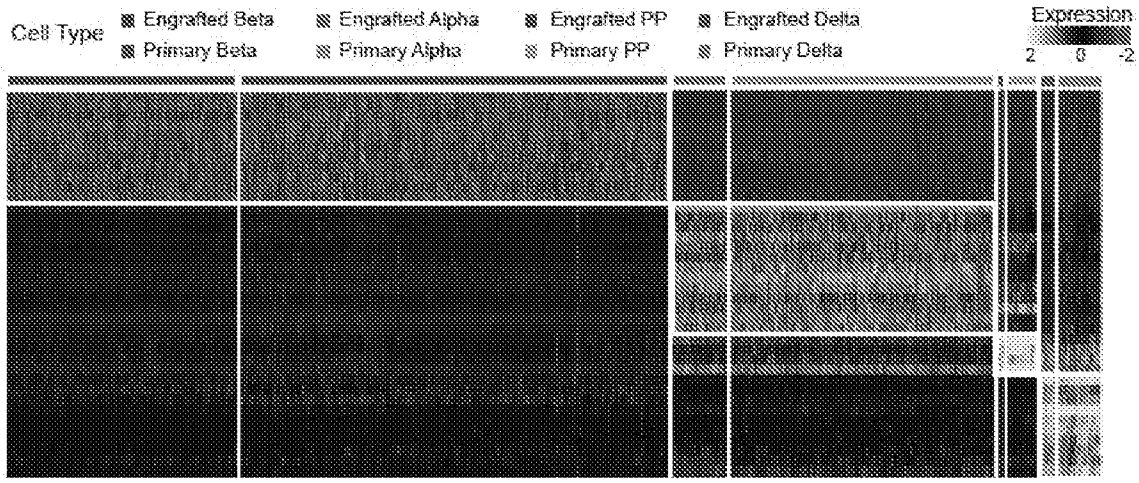

Cell Type
Engrafted Beta
Primary Beta
Engrafted Alpha
Primary Alpha
Engrafted PP
Primary PP
Engrafted Delta
Primary Delta
Expression
2
0
-2

FIG. 7K

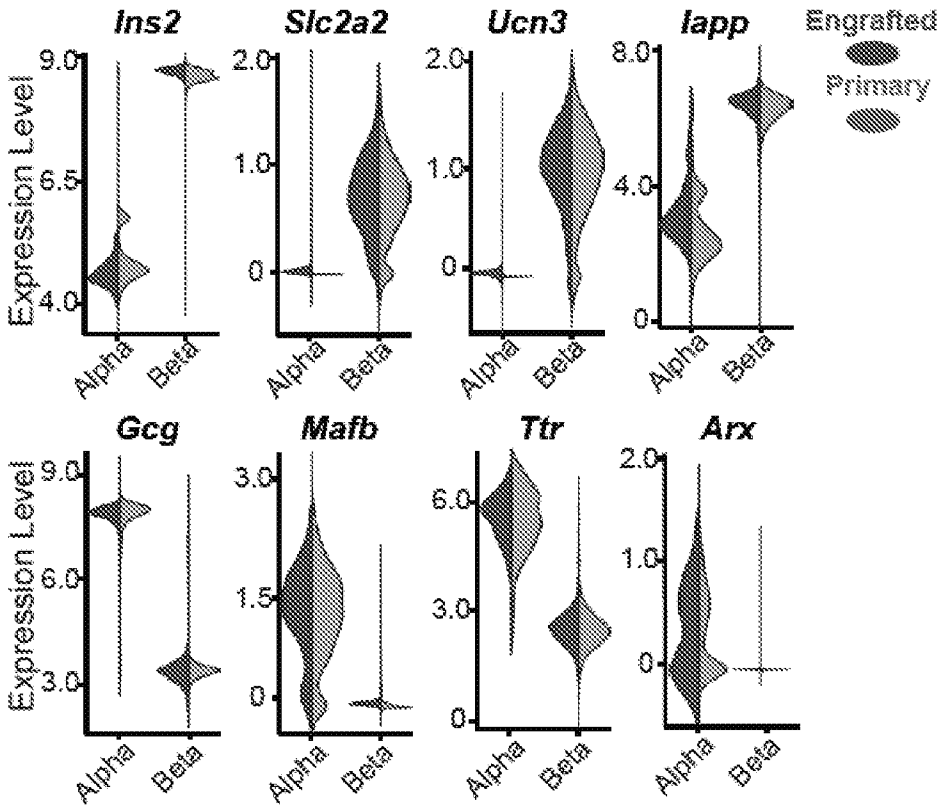

Ins2
Slc2a2
Ucn3
Iapp
Engrafted
Primary
Expression Level
Gcg
Mafb
Ttr
Arx
Alpha
Beta

FIG. 7L

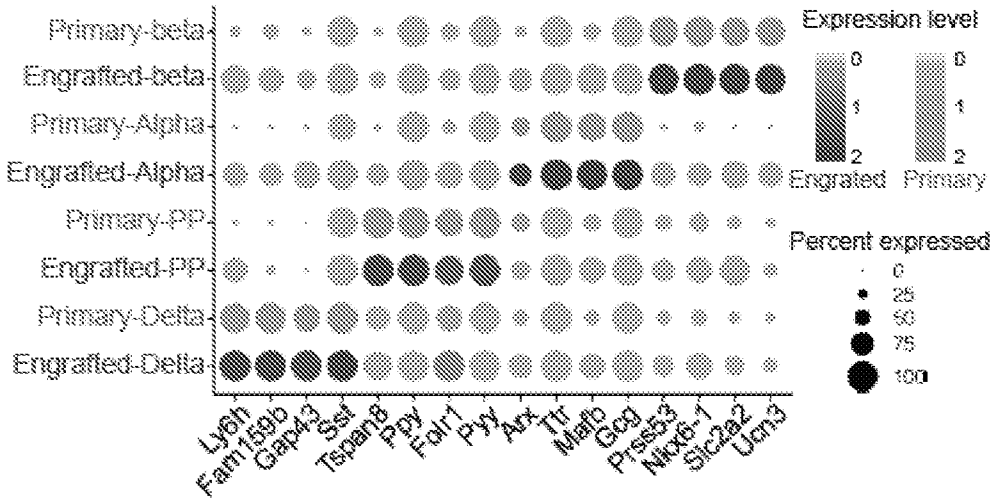

Primary-beta
Engrafted-beta
Primary-Alpha
Engrafted-Alpha
Primary-PP
Engrafted-PP
Primary-Delta
Engrafted-Delta
Lyl6h
Fam159b
Gap43
Ssl
Tspan8
Ppy
Foir1
Pyy
Arx
Ttr
Mafb
Gcg
Ptrss53
Nkx6-1
Slc2a2
Ucn3
Expression level
Engrated
Primary
Percent expressed
25
50
75
100

FIG. 7M

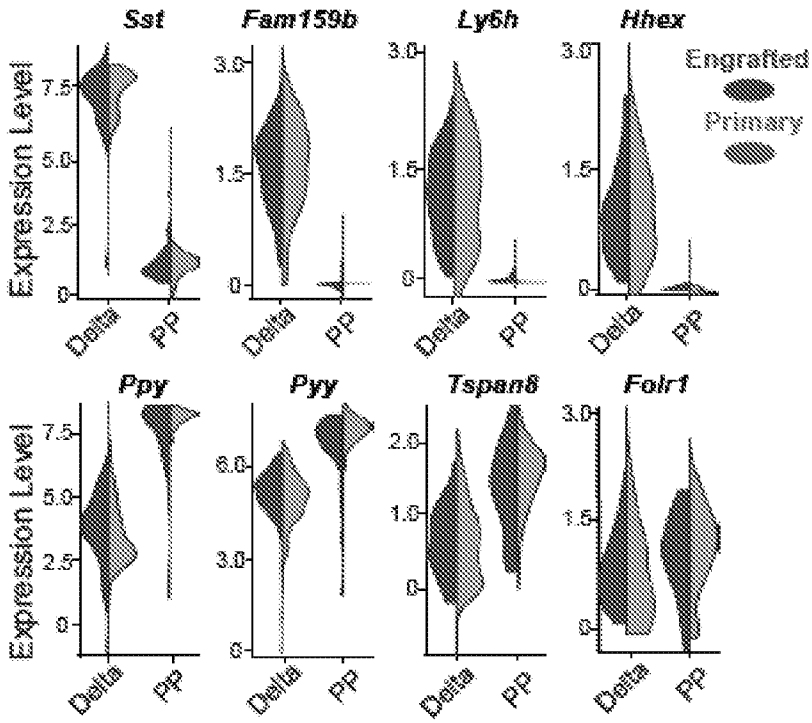


FIG. 7N

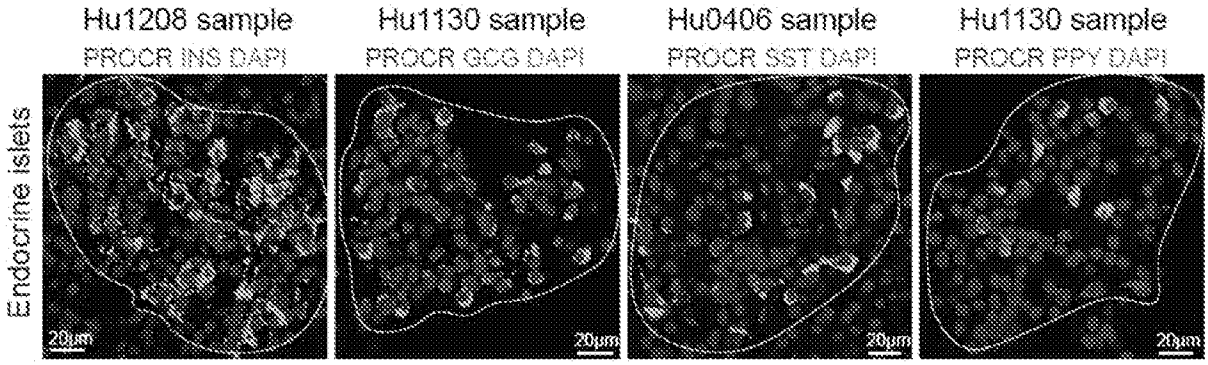


FIG. 8A

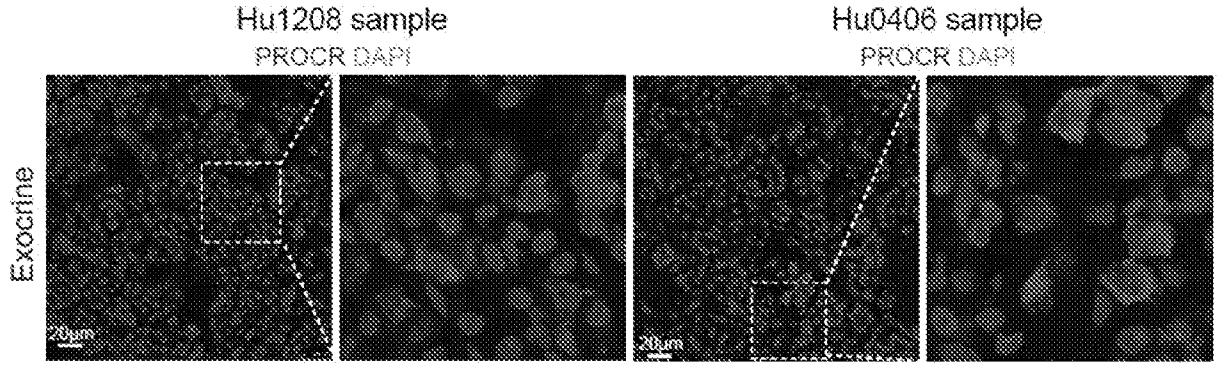


FIG. 8B

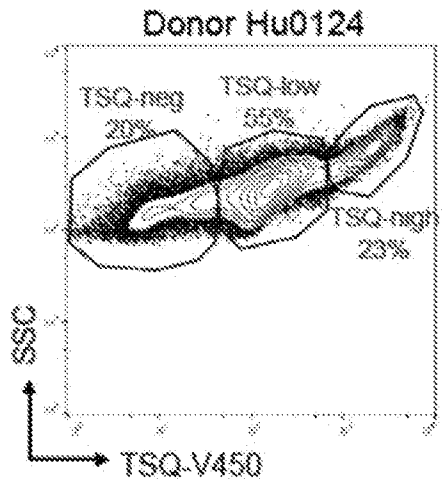


FIG. 9A

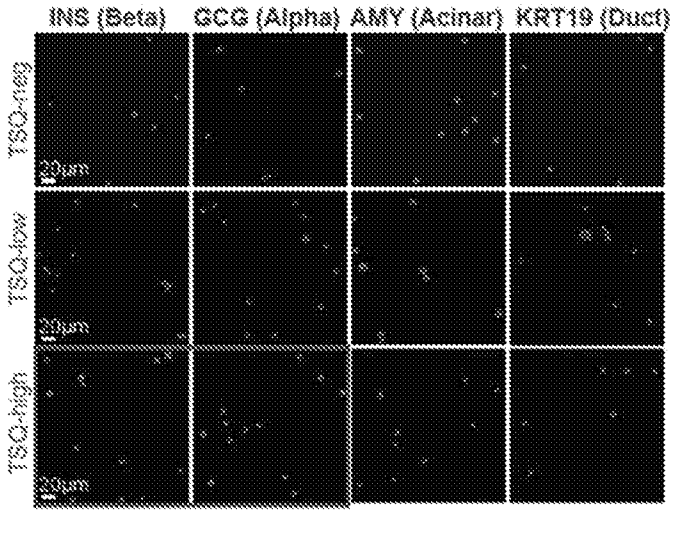


FIG. 9B

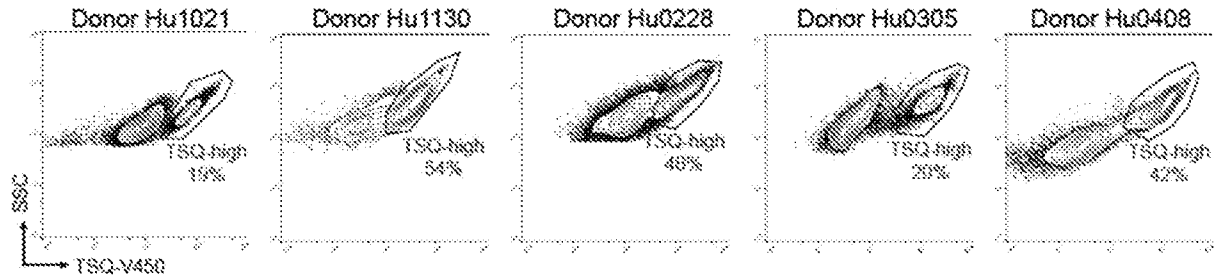


FIG. 9C

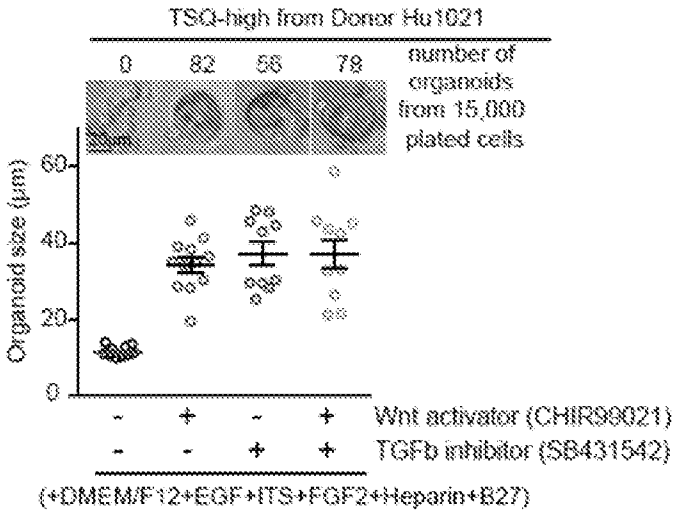


FIG. 10A

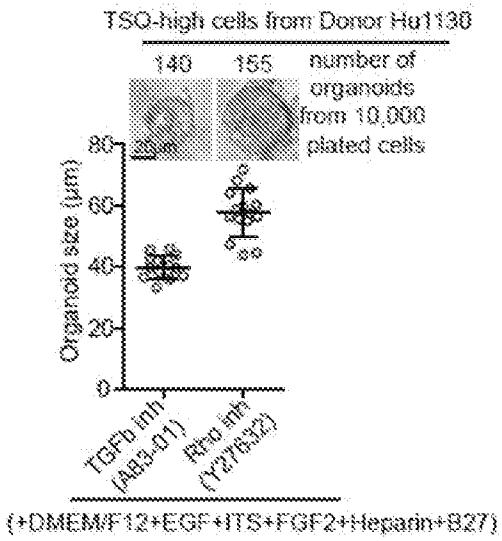


FIG. 10B

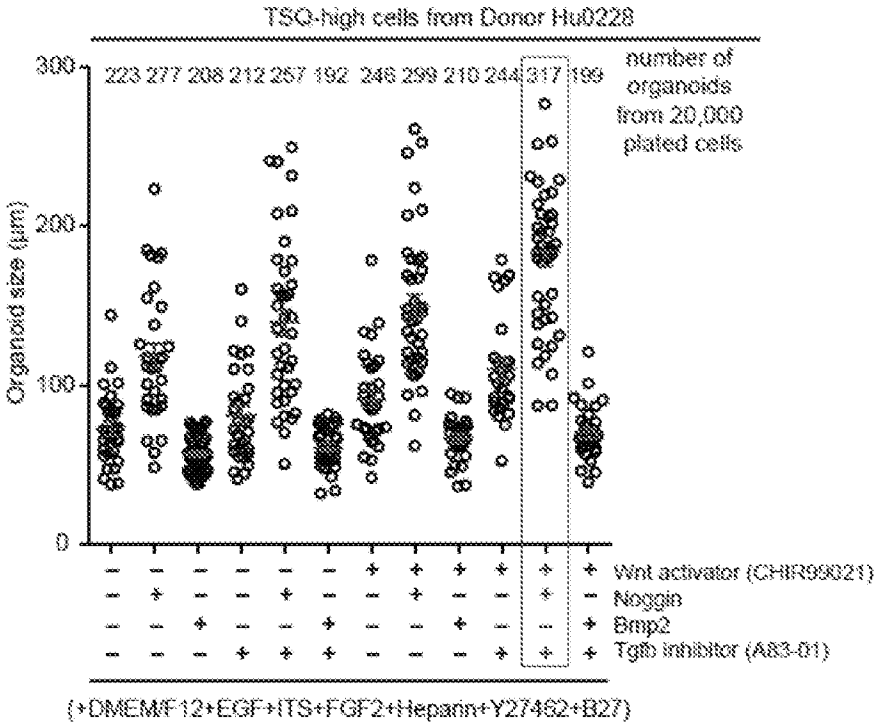


FIG. 10C

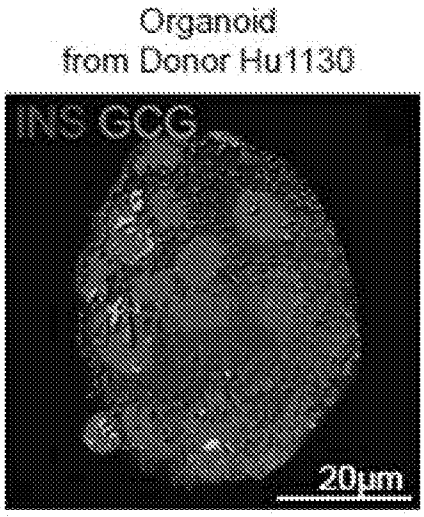


FIG. 10D

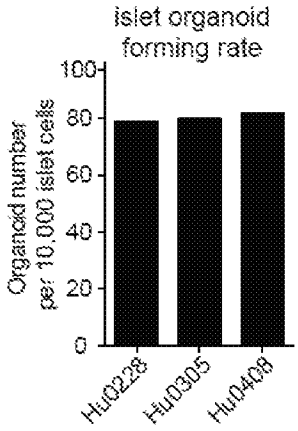


FIG. 11A

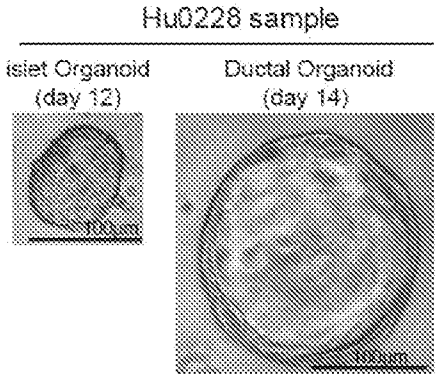


FIG. 11B

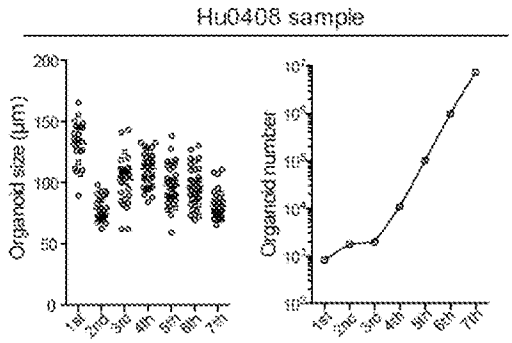


FIG. 11C

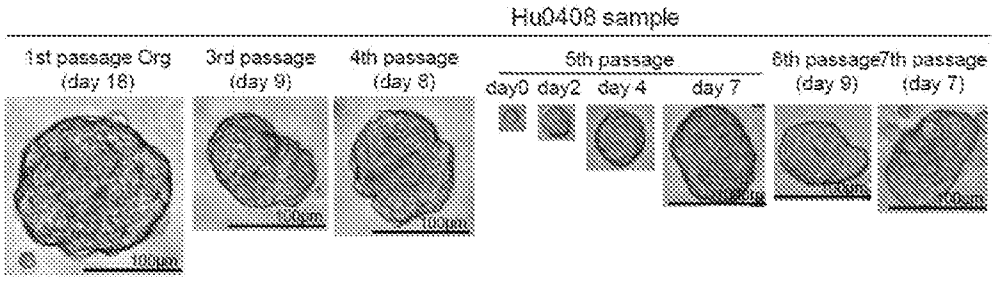


FIG. 11D

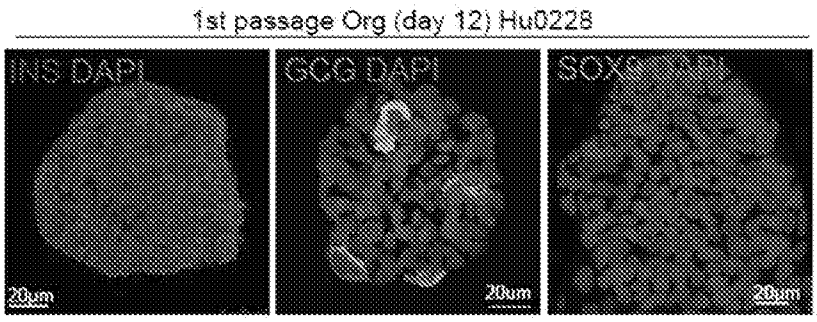


FIG. 12A

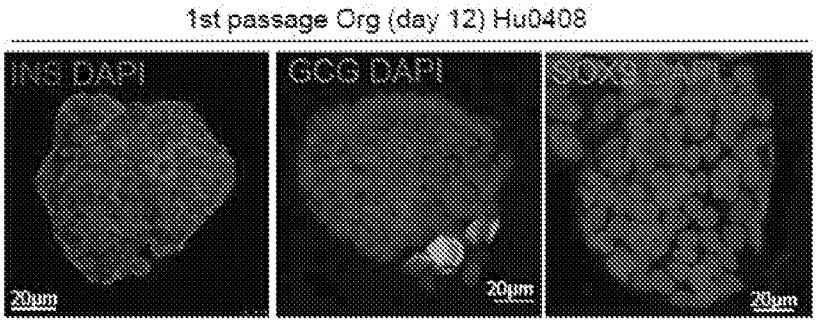


FIG. 12B

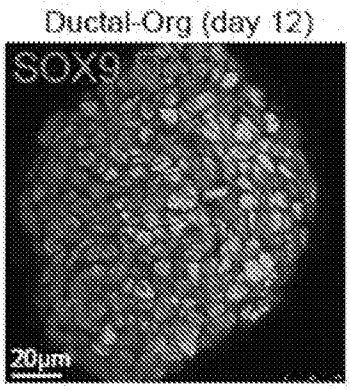


FIG. 12C

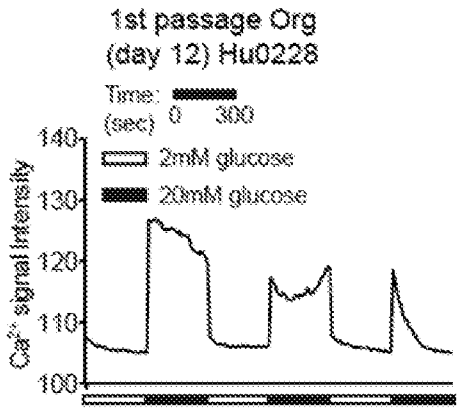


FIG. 12D

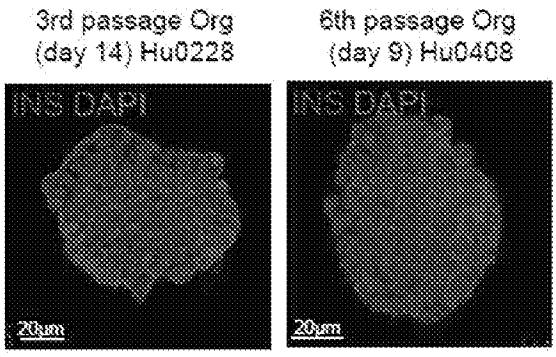


FIG. 12E

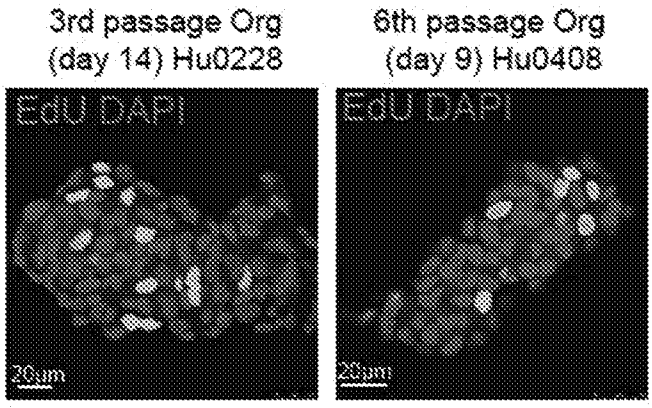


FIG. 13A

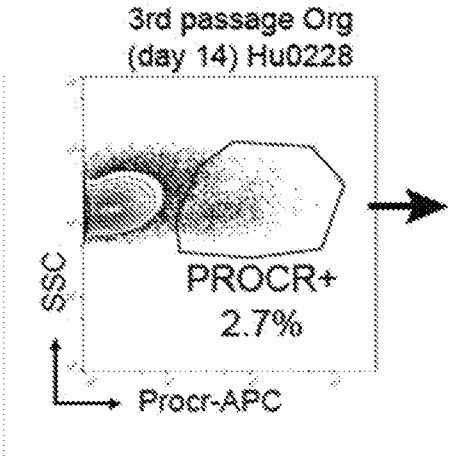


FIG. 13B

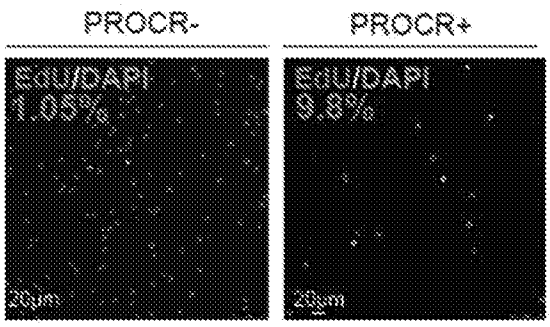


FIG. 13C

INTERNATIONAL SEARCH REPORT

International application No.
PCT/CN2019/106093

A. CLASSIFICATION OF SUBJECT MATTER

C12N 5/071(2010.01)i; C12N 5/07(2010.01)i; A61K 35/39(2015.01)i; A61K 9/50(2006.01)i

According to International Patent Classification (IPC) or to both national classification and IPC

B. FIELDS SEARCHED

Minimum documentation searched (classification system followed by classification symbols)

C12N; A61K

Documentation searched other than minimum documentation to the extent that such documents are included in the fields searched

Electronic data base consulted during the international search (name of data base and, where practicable, search terms used)

Data bases: CNABS,SIPOABS,DWPI,CNTXT,WOTXT,USTXT,CNKI,PUBMED,ISI_Web of Science,Baidu Scholar; Search terms: islet cells, islet cell, islet, pro-endocrine progenitor cells, endocrine progenitor cells, endothelial cells, endothelial cell, protein C receptor, Procr, medium, media, beta cells, beta-like cells, β cells,organoid

C. DOCUMENTS CONSIDERED TO BE RELEVANT

Category*	Citation of document, with indication, where appropriate, of the relevant passages	Relevant to claim No.
A	WO 2014059402 A1 (UNIV JOHNS HOPKINS) 17 April 2014 (2014-04-17) see claims 1 to 26	1-23
A	US 2016175363 A1 (HARVARD COLLEGE) 23 June 2016 (2016-06-23) see the whole document	1-23
A	WO 2017177163 A1 (UNIV CALIFORNIA) 12 October 2017 (2017-10-12) see the whole document	1-23
A	CN 102803475 A (国立大学法人京都大学) 28 November 2012 (2012-11-28) see the whole document	1-23
A	CN 107787363 A (哥本哈根大学) 09 March 2018 (2018-03-09) see the whole document	1-23
A	CN 104411815 A (大学健康网络) 11 March 2015 (2015-03-11) see the whole document	1-23

☑ Further documents are listed in the continuation of Box C. ☑ See patent family annex.

* Special categories of cited documents:
"A" document defining the general state of the art which is not considered to be of particular relevance
"E" earlier application or patent but published on or after the international filing date
"L" document which may throw doubts on priority claim(s) or which is cited to establish the publication date of another citation or other special reason (as specified)
"O" document referring to an oral disclosure, use, exhibition or other means
"P" document published prior to the international filing date but later than the priority date claimed
"T" later document published after the international filing date or priority date and not in conflict with the application but cited to understand the principle or theory underlying the invention
"X" document of particular relevance; the claimed invention cannot be considered novel or cannot be considered to involve an inventive step when the document is taken alone
"Y" document of particular relevance; the claimed invention cannot be considered to involve an inventive step when the document is combined with one or more other such documents, such combination being obvious to a person skilled in the art
"&" document member of the same patent family

Date of the actual completion of the international search	Date of mailing of the international search report
14 April 2020	**20 April 2020**
Name and mailing address of the ISA/CN **National Intellectual Property Administration, PRC** **6, Xitucheng Rd., Jimen Bridge, Haidian District, Beijing 100088** **China** Facsimile No. **(86-10)62019451**	Authorized officer **YU,Ting** Telephone No. **010-62411103**

INTERNATIONAL SEARCH REPORT

International application No.
PCT/CN2019/106093

C. DOCUMENTS CONSIDERED TO BE RELEVANT

Category*	Citation of document, with indication, where appropriate, of the relevant passages	Relevant to claim No.
A	Lena Wedeken et al. "Adult Murine Pancreatic Progenitors Require Epidermal Growth Factor and Nicotinamide for Self-Renewal and Differentiation in a Serum- and Conditioned Medium-Free Culture" *STEM CELLS AND DEVELOPMENT,* Vol. 26, No. 8, 17 January 2017 (2017-01-17), ISSN: 1547-3287, see the pages 599-607	1-23

INTERNATIONAL SEARCH REPORT

International application No.
PCT/CN2019/106093

Box No. I Nucleotide and/or amino acid sequence(s) (Continuation of item 1.c of the first sheet)

1. With regard to any nucleotide and/or amino acid sequence disclosed in the international application, the international search was carried out on the basis of a sequence listing:
   a. ☑ forming part of the international application as filed:
      ☑ in the form of an Annex C/ST.25 text file.
      ☐ on paper or in the form of an image file.
   b. ☐ furnished together with the international application under PCT Rule 13*ter*.1(a) for the purposes of international search only in the form of an Annex C/ST.25 text file.
   c. ☐ furnished subsequent to the international filing date for the purposes of international search only:
      ☐ in the form of an Annex C/ST.25 text file (Rule 13*ter*.1(a)).
      ☐ on paper or in the form of an image file (Rule 13*ter*.1(b) and Administrative Instructions, Section 713).

2. ☐ In addition, in the case that more than one version or copy of a sequence listing has been filed or furnished, the required statements that the information in the subsequent or additional copies is identical to that forming part of the application as filed or does not go beyond the application as filed, as appropriate, were furnished.

3. Additional comments:

INTERNATIONAL SEARCH REPORT

International application No.
PCT/CN2019/106093

Box No. II Observations where certain claims were found unsearchable (Continuation of item 2 of first sheet)

This international search report has not been established in respect of certain claims under Article 17(2)(a) for the following reasons:

1. ☑ Claims Nos.: **24**
because they relate to subject matter not required to be searched by this Authority, namely:

[1] The treatment methods of diseases of the human or animal body

2. ☐ Claims Nos.:
because they relate to parts of the international application that do not comply with the prescribed requirements to such an extent that no meaningful international search can be carried out, specifically:

3. ☐ Claims Nos.:
because they are dependent claims and are not drafted in accordance with the second and third sentences of Rule 6.4(a).

INTERNATIONAL SEARCH REPORT
Information on patent family members

International application No.
PCT/CN2019/106093

Patent document cited in search report	Publication date (day/month/year)	Patent family member(s)	Publication date (day/month/year)
WO 2014059402 A1	17 April 2014	US 2015265656 A1	24 September 2015
US 2016175363 A1	23 June 2016	WO 2016100921 A1	23 June 2016
		US 2018153941 A1	07 June 2018
WO 2017177163 A1	12 October 2017	EP 3440192 A1	13 February 2019
		US 2019177697 A1	13 June 2019
		EP 3440192 A4	23 October 2019
CN 102803475 A	28 November 2012	US 2013122586 A1	16 May 2013
		JP 2013521797 A	13 June 2013
		CN 102803475 B	22 April 2015
		US 8852934 B2	07 October 2014
		WO 2011114719 A1	22 September 2011
		EP 2547761 A1	23 January 2013
		EP 2547761 A4	04 December 2013
CN 107787363 A	09 March 2018	WO 2016170069 A1	27 October 2016
		CA 2983764 A1	27 October 2016
		US 2018127724 A1	10 May 2018
		US 10494608 B2	03 December 2019
		JP 2018512886 A	24 May 2018
		EP 3286300 A1	28 February 2018
CN 104411815 A	11 March 2015	AU 2013255031 A1	04 December 2014
		EP 3594323 A1	15 January 2020
		EP 2844739 A1	11 March 2015
		PT 2844739 T	01 October 2019
		HR P20191677 T1	13 December 2019
		JP 2015519048 A	09 July 2015
		PL 2844739 T3	31 December 2019
		EP 2844739 A4	02 December 2015
		HK 1208047 A1	19 February 2016
		AU 2013255031 B2	06 September 2018
		CN 104411815 B	28 November 2017
		CA 2871795 A1	07 November 2013
		DK 2844739 T3	30 September 2019
		JP 2018198620 A	20 December 2018
		CN 108004199 A	08 May 2018
		SI 2844739 T1	29 November 2019
		EP 2844739 B1	19 June 2019
		JP 6397397 B2	26 September 2018
		US 2015104430 A1	16 April 2015
		HU E046271 T2	28 February 2020
		LT 2844739 T	10 October 2019
		AU 2013255031 C1	06 December 2018
		IN 10053DEN2014 A	14 August 2015
		WO 2013163739 A1	07 November 2013